Electronic Supplementary Material (ESI) for Green Chemistry.
This journal is © The Royal Society of Chemistry 2019

Electronic Supplementary Information (ESI)

for

Towards Cleaner Polarclean: Efficient Synthesis and Extended Applications of the Polar Aprotic Solvent Methyl 5-(Dimethylamino)-2-methyl-5-oxopentanoate

Levente Cseri*[a] and Gyorgy Szekely*[a,b]

[a]School of Chemical Engineering and Analytical Science, University of Manchester, The Mill, Sackville Street, Manchester, M1 3BB, United Kingdom, E-mail: levente.cseri@manchester.ac.uk, gyorgy.szekely@manchester.ac.uk, Phone: +441613062662

[b]Advanced Membranes & Porous Materials Center, Physical Science Engineering Division (PSE), King Abdullah University of Science and Technology (KAUST), Thuwal 23955-6900, Saudi Arabia, E-mail: gyorgy.szekely@kaust.edu.sa, Phone: +966128082769

Table of Contents

1. Materials and methods

1.1. Materials

1.1.1. Reagents and solvents

RhodiaSolv® PolarClean (major component methyl 5-(dimethylamino)-2-methyl-5-oxopentanoate, **1**) can be purchased from Solvay. PolarClean solvent samples from different batches were denoted as PolarCleanX and PolarCleanY, respectively.

N,*N*-Dimethylacrylamide (DMAA; 99%, 500 ppm MEHQ), Methyl isobutyrate (MIB; 99%), 2-Methyltetrahydrofuran (MeTHF; anhydrous, ≥99.0%, 250 ppm BHT), Phenol (≥99%), Benzimidazole (98%), 1-*tert*-Butyl-4,4,4-tris(dimethylamino)-2,2-bis[tris(dimethylamino)-phosphoranylidenamino]-2λ^5,4λ^5-catenadi(phosphazene) (P_4-phosphazene; ~0.8 M sol. in hexane), 2-*tert*-Butylimino-2-diethylamino-1,3-dimethylperhydro-1,3,2-diazaphosphorine (BEMP; ≥98.0%), 7-Methyl-1,5,7-triazabicyclo[4.4.0]dec-5-ene (MTBD; 98%), γ-Valerolactone (GVL; 99%), Dihydrolevoglucosenone (Cyrene^{TM}; 99%), Propylene carbonate (PC; 99%) and Potassium hexachloroplatinate(IV) (K_2PtCl_6; 99.9% trace metals basis) were purchased from Sigma-Aldrich. *N*,*N*-Dimethylacetamide (DMAc; 99.5%, Extra Dry), Methyl Propionate (MeOProp; 99+%), Lithium diisopropylamide (LDA; 2M sol. in THF/*n*-heptane/ethylbenzene), Potassium *tert*-butoxide (KO*t*Bu; 98+%, pure), 1,8-Diazabicyclo[5.4.0]undec-7-ene (DBU, 98%), Isosorbide dimethyl ether (ISDME; 99%) and Cobalt(II) chloride hexahydrate ($CoCl_2{\cdot}6H_2O$; 98-102%) were purchased from Acros Organics. Methyl methacrylate (MMA; 99%, MEHQ stab.), Potassium carbonate (K_2CO_3; anhydrous, 99%) and 1,1,3,3-Tetramethylguanidine (TMG; 99%) were supplied by Alfa Aesar. Bis(4-fluorophenyl) sulfone (98%) was purchased from Fluorochem. All chemicals were used as received. Deionised (DI) water with a resistivity of 18.2 MΩ cm was obtained from a Millipore Direct-Q® 3UV system.

1.1.2. Polymers

Polysulfone pellets (PSf; approx. MW = 60 kg mol^{-1}) were purchased from Acros Organics. P84 polyimide powder (PI; ~200 mesh SG STD) was purchased from HP Polymer GmbH, Austria. Polyacrylnitrile powder (PAN; 50 µm particle size, MW = 85 kg mol^{-1}) was supplied by Goodfellow Cambridge Limited, UK. Poly(vinylidene fluoride) pellets (PVDF; Av. Mw~180 kg mol^{-1}) was purchased from Sigma-Aldrich. Poly(lactic acid) pellets (PLA; IngeoTM biopolymer 2003D) manufactured by NatureWorks LLC, USA were purchased from Innovative Pultrusion Sdn Bhd, Malaysia. Polyvinyl alcohol (PVA; fully hydrolysed, approx. MW=60kDa) was purchased from Merck.

Polybenzimidazole (PBI; 26 wt% sol. in DMAc) was purchased from PBI Performance Products, USA. The polymer was precipitated upon pouring the solution into cold DI water (10-fold in volume), filtered, washed with excessive amounts of water and dried under vacuum to obtain the PBI powder used for the solubility tests.

PIM-1 (MW 23 kg mol^{-1} by GPC) was prepared to the high temperature synthesis described in the literature.[1] PIM-COOH was synthesized from this PIM-1 by acidic hydrolysis as described elsewhere.[2]

1.1.3. Membranes

GMT-oNF-1 A4 size flat sheet membrane was purchased from Borsig Membrane Technology GmbH, Germany. NF030705 A4 size flat sheet membrane was supplied by SolSep BV, The Netherlands. Nadir® NP010 A4 size flat sheet membrane was purchased from Microdyn-Nadir GmbH, Germany. Duramem® 900 T1 type A4 size flat sheet membrane was produced by Evonik Resource Efficiency GmbH, Germany. The PBI membrane was prepared in-house as reported elsewhere.[3]

1.2. Synthetic methods

1.2.1. Methyl 5-(dimethylamino)-2-methyl-5-oxopentanoate via Route B (**1B**)

80 mL (160 mmol) of 2.0 M LDA solution in THF/heptane/ethylbenzene was added to 80 mL of dry MeTHF at −78 °C under Ar atmosphere via a rubber septum. 15.3 mL (152 mmol) dry DMAc was added dropwise to this solution over 5 minutes. The mixture was stirred at −78 °C for 1 hour followed by the dropwise addition of 13.2 g (144 mmol) MMA over 5 minutes. The reaction was stirred for 1.5 hours before it was quenched by the addition of a mixture of 40 mL of 4 M HCl and 20 mL of THF. The mixture was allowed to warm up to room temperature. The phases were separated, and the organic phase was washed with 70 mL brine. The combined aqueous phases were extracted with EtOAc (2 × 50mL). The organic phases were combined, the volatile components were drawn off using a rotavap and the product was purified by vacuum distillation (103 °C, 3.8 mbar) yielding **1B** as a transparent viscous liquid (7.2 g, 27%) which developed a yellow colouration over storage. GC-MS purity: 90.1%; DSC boiling point: 277.1 °C (1020 mbar). The spectroscopic properties of **1B** were consistent with 1C and commercial PolarClean samples.

1.2.2. Methyl 5-(dimethylamino)-2-methyl-5-oxopentanoate via Route C (**1C**)

MeOProp (45.82 g, 520 mmol) and DMAA (10.31 g, 104 mmol) were mixed in a dry round bottom flask under Ar atmosphere. The mixture was cooled down to 0–5 °C using an ice-water bath. Potassium *tert*-butoxide (5 mol%, 583 mg, 5.2 mmol) was added in small portions over 30 minutes. HPLC analysis 2.5 min after the addition was finished showed the total consumption of DMAA. Saturated oxalic acid solution (~1 M, 5 mL) was slowly added to quench the reaction. The reaction mixture was allowed to warm up to room temperature. The volatile components were evaporated, and the product was purified by vacuum distillation at 98 °C and 3.6 mbar to obtain **1C** as a transparent, viscous liquid (9.40 g, 48%). DSC boiling point: 281.5 °C (1020 mbar). ATR-FTIR ν_{max}/cm^{-1} 2937 (C–H), 1730 (OC=O), 1642 (NC=O), 1206 (C(O)–O), 1150 (C(O)–N); ^{1}H NMR (500 MHz, $CDCl_3$) δ 3.59 (s, 3H), 2.91 (s, 3H), 2.85 (s, 3H), 2.45 (h, *J* = 7.0 Hz, 1H), 2.32–2.17 (m, 2H), 1.91–1.81 (m, 1H), 1.77–1.68 (m, 1H), 1.10 (d, *J* = 7.0 Hz, 3H); ^{13}C NMR (126 MHz, $CDCl_3$) δ 176.7, 172.2, 51.5, 38.8, 37.1, 35.3, 30.8, 28.9, 17.3; (Assignment of ^{1}H and ^{13}C NMR spectra can be found in Table 8–9 of the main text); ^{15}N NMR (obtained from ^{15}N–^{1}H HMBC spectrum, 400 MHz, $CDCl_3$) δ 99.2; GC-MS purity: >99%; HRMS (ESI+/Orbitrap) *m/z*: calcd. for $[M+H]^+$ $C_9H_{18}NO_3$: 188.1281; found: 188.1280; D = −0.64 ppm.

1.2.3. Isolation of impurity 1,4-diphenylbutane (**5**)

The hydrocarbon impurities of **1B** were isolated as 1 mL of it was partitioned between 10 mL of water and 2 mL of *n*-hexane. The organic phase was separated, the volatile components were evaporated, and the residue was analysed by NMR spectroscopy.

1.2.4. Isolation of by-product 4-methoxycarbonyl-*N*,*N*,*N*',*N*',4-pentamethylpimelamide (**8**)

The vacuum distillation residue of **1C** was allowed to cool down to room temperature from the distillation temperature while it was continuously stirred. 20 mL diethyl ether was added and the solution was cooled down to 0–5 °C to induce crystallisation. The crystals were collected by filtration, washed with cold ether and dried under vacuum to yield **8** as a beige solid (3.62 g, 24%). ATR-FTIR ν_{max}/cm^{-1} 2942 (C–H), 1722 (OC=O), 1642 (NC=O); ^1H NMR (500 MHz, $CDCl_3$) δ 3.62 (s, 3H, OCH_3), 2.95 (s, 6H, N(CH_3)$_2$), 2.88 (s, 6H, N(CH_3)$_2$), 2.34–2.10 (m, 4H, C(O)CH_2), 1.96 (ddd, *J* = 14.0, 10.6, 5.9 Hz, 2H, CH_2CMe), 1.79 (ddd, *J* = 14.0, 10.4, 6.5 Hz, 2H, CH_2CMe), 1.14 (s, 3H, CCH_3); ^{13}C NMR (126 MHz, $CDCl_3$) δ 177.1 (*C*(O)O), 172.4 (*C*(O)N), 51.9 (OCH_3), 44.8 (*C*Me), 37.2 (N(CH_3)$_2$), 35.5 (N(CH_3)$_2$), 34.0 (CH_2CMe), 28.7 (C(O)CH_2), 21.4 (CCH_3); HRMS (ESI+/Orbitrap) *m/z*: calcd. for $[M+Na]^+$ $C_{14}H_{26}N_2O_4Na$: 309.1785; found: 309.1770; D = −4.78 ppm.

1.2.5. Optimisation of reaction excess and base catalyst for Route C

All experiments with KO*t*Bu and P_4-phosphazene shown in Table 3 in the main text were carried out as described in section 1.2.2 in the ESI. In the case of BEMP, MTBD, TMG and DBU, the base addition was followed by 48 hours of reflux at 95 °C. The reactions were monitored by HPLC.

1.2.6. Methyl 5-(dimethylamino)-2,2-dimethyl-5-oxopentanoate (**9**)

9 was synthesized using 10.0 g (97.9 mmol) DIM, 8.82 g (89.0 mmol) DMAA and 330 mg (2.94 mmol, 3 mol%) KO*t*Bu according to the procedure described in section 1.2.2. The vacuum distillation was performed at 120 °C and 3.6 mbar to yield **9** as a transparent viscous liquid (13.94 g, 78%). The 1.38 g pre-distillate collected at 60–100 °C and 3.5 mbar contains **9** with ≥95% purity which may be recycled in a subsequent vacuum distillation batch or used as it is (Sum yield: 15.32 g, 86%). DSC boiling point: 283.4 °C (1020 mbar). ATR-FTIR ν_{max}/cm^{-1} 2952 (C–H), 1726 (OC=O), 1640 (NC=O), 1194 (C(O)–O), 1130 (C(O)–N); ^1H NMR (400 MHz, $CDCl_3$) δ 3.63 (s, 3H, OCH_3), 2.97 (s, 3H, N(CH_3)$_2$), 2.90 (s, 3H, N(CH_3)$_2$), 2.42 – 2.11 (m, 2H, C(O)CH_2), 1.98 – 1.67 (m, 2H, CH_2C(Me)$_2$), 1.17 (s, 6H, C(CH_3)$_2$); ^{13}C NMR (101 MHz, $CDCl_3$) δ 178.1 (*C*(O)O), 172.6 (*C*(O)N), 51.9 (OCH_3), 41.9 (*C*(Me)$_2$), 37.3 (N(CH_3)$_2$), 35.7 (CH_2C(Me)$_2$), 35.5 (N(CH_3)$_2$), 29.3 (C(O)CH_2), 25.3 (C(CH_3)$_2$); ^{15}N NMR (obtained from ^{15}N–^1H HMBC spectrum, 400 MHz, $CDCl_3$) δ 99.1; GC-MS purity: >99%; HRMS (ESI+/Orbitrap) *m/z*: calcd. for $[M+H]^+$ $C_{10}H_{20}NO_3$: 202.1438; found: 202.1432; D = −2.82 ppm.

1.2.7. Synthesis of bis(4-phenoxyphenyl) sulfone (**10**) in S_NAr test reaction

254 mg (1.0 mmol) of bis(4-phenoxyphenyl) sulfone, 207 mg (2.2 mmol) phenol and 304 mg (2.2 mmol) of K_2CO_3 were mixed in 2 mL of solvent. The reaction was carried out for 6 hours at 160 °C while stirring continuously. In case of Cyrene, the solution turned into a black charred mass. The reaction mixture was allowed to cool down to room temperature. 10 mL DI water solution was added and the precipitated product was collected by filtration and washed with 25 mL cold water, 25 mL of boiling water and 25 mL of cold water again to obtain **10** as white solid. In case of Cyrene and PC, no solid precipitated after the water addition; therefore the mixture was extracted with 25 mL of toluene. The organic phase was washed with water, saturated NH_4Cl and brine (25 mL each), dried over $MgSO_4$ and evaporated. The crude product was purified by preparative HPLC to obtain **10** as a white solid. The spectroscopic properties of **10** were consistent with the literature.[4] ^1H NMR (400 MHz, $CDCl_3$) δ 7.87 (d, *J* = 8.9 Hz, 4H), 7.49 – 7.35 (m, 4H), 7.22 (t, *J* = 7.5 Hz, 2H), 7.04 (d, *J* = 8.2 Hz, 4H), 7.01 (d, *J* = 8.9 Hz, 4H).

1.2.8. Solvent recovery after S_NAr reaction

The reaction described in section 1.2.7 was carried out on a 1.5 times larger scale using 3 mL (3.13 g) of **1C** as solvent. After the filtration of the product, the solvent was recovered from the mother liquor containing 3 mL of water and 10 mL of DI water. Two recovery methods, namely vacuum distillation and extraction was considered. The high purity (>99%) of the recovered solvent in both cases indicates the potential of these methods. On the other hand, the relatively low recoveries (13–62%) can be attributed to the small scale and non-optimised conditions.

Recovery by vacuum distillation: 3.6 mL of 1 M oxalic acid was added to the aqueous mother liquor to neutralise the excess K_2CO_3. Water was drawn off using a rotavap and **1C** was recovered from the mixture by vacuum distillation. Recovery: 1.93 g (62%); GC-MS purity: >99%.

Recovery by extraction: The aqueous mother liquor was washed with 10 mL toluene. The pH was set to 3–4 using 4 mL of 1 M HCl and the aqueous phase was washed with 2×10 mL toluene. The organic phases were discarded. The pH of the aqueous phase was set to 11–12 using 2 mL of NaOH and it was extracted with 3×10 mL of EtOAc. The organic phase was dried over $MgSO_4$ and the volatile components were drawn off using a rotavap leaving **1C** behind. Recovery: 0.42 g (13%); GC-MS purity: >99%.

1.2.9. Synthesis of bis(4-benzimidazol-1-ylphenyl) sulfone (**11**) in S_NAr test reaction

254 mg (1.0 mmol) of bis(4-phenoxyphenyl) sulfone, 260 mg (2.2 mmol) benzimidazole and 304 mg (2.2 mmol) of K_2CO_3 were mixed in 2 mL of solvent. The reaction was carried out for 4 hours at 140 °C while stirring continuously. In case of Cyrene, the solution turned into a black charred mass. The reaction mixture was allowed to cool down to room temperature. 20 mL 0.1 M NaOH solution was added and the precipitated product was collected by filtration and washed with 20 mL cold water, 20 mL of boiling water and 20 mL of cold water again to obtain **11** as white solid. In case of Cyrene and PC, no solid precipitated after the addition of NaOH solution; therefore the yield was calculated based on the HPLC analysis of the reaction mixture. The spectroscopic properties of **11** were in line with the literature.[5] ^1H NMR (400 MHz, $CDCl_3$) δ 8.22 (d, J = 8.6 Hz, 4H), 8.14 (s, 2H), 7.92 – 7.84 (m, 2H), 7.74 (d, J = 8.6 Hz, 4H), 7.61 – 7.52 (m, 2H), 7.41 – 7.33 (m, 4H).

2. Green analysis

2.1. Key process performance indicators

The key process performance indicators, complexity and ideality were obtained as follows:

$$\text{Complexity} = \Sigma\,\text{Construction steps} \tag{S1}$$

$$\text{Ideality} = \frac{\text{Complexity}}{\Sigma\,\text{Steps}} \cdot 100\% \tag{S2}$$

The definitions for complexity and ideality were adopted from Roschangar *et al.*[6] All synthetic steps were classified either as construction steps or concession steps. Construction steps are chemical transformations that form skeletal C–C, C–X, C–H, and X–H bonds (X = hetero atom), which are eventually present in the product. Concession steps are all "non-constructive" reactions and do not form skeletal bonds, for example carbonyl activation steps.[6] The starting materials have been defined as chemicals that contribute to the final product structure and which are available from a major reputable company with a catalogue cost less than US $100/mol.

2.2. Atom economy

The atom economy (AE) of a step or a synthetic route was calculated as follows:

$$\text{AE} = \frac{MW_{\text{product}}}{\sum n \cdot MW_{\text{reagents}}} \cdot 100\% \tag{S3}$$

where *MW* is molecular weight and *n* is the stoichiometric number of a reagent. The atom economy shows the proportion of the sum mass of all reagents that would be incorporated into the final product if the use of exact stoichiometric quantities and a chemical yield of 100% were assumed. Therefore, the AE provides information on the inherent sustainability of a chemical synthesis. The overall or cumulated AE (ΣAE) was calculated by taking all reagents and starting materials from all synthetic steps in that route into account. Scheme S1 summarizes the atom economies calculated for the synthesis of methyl 5-(dimethylamino)-2-methyl-5-oxopentanoate (**1**) via different synthetic routes.

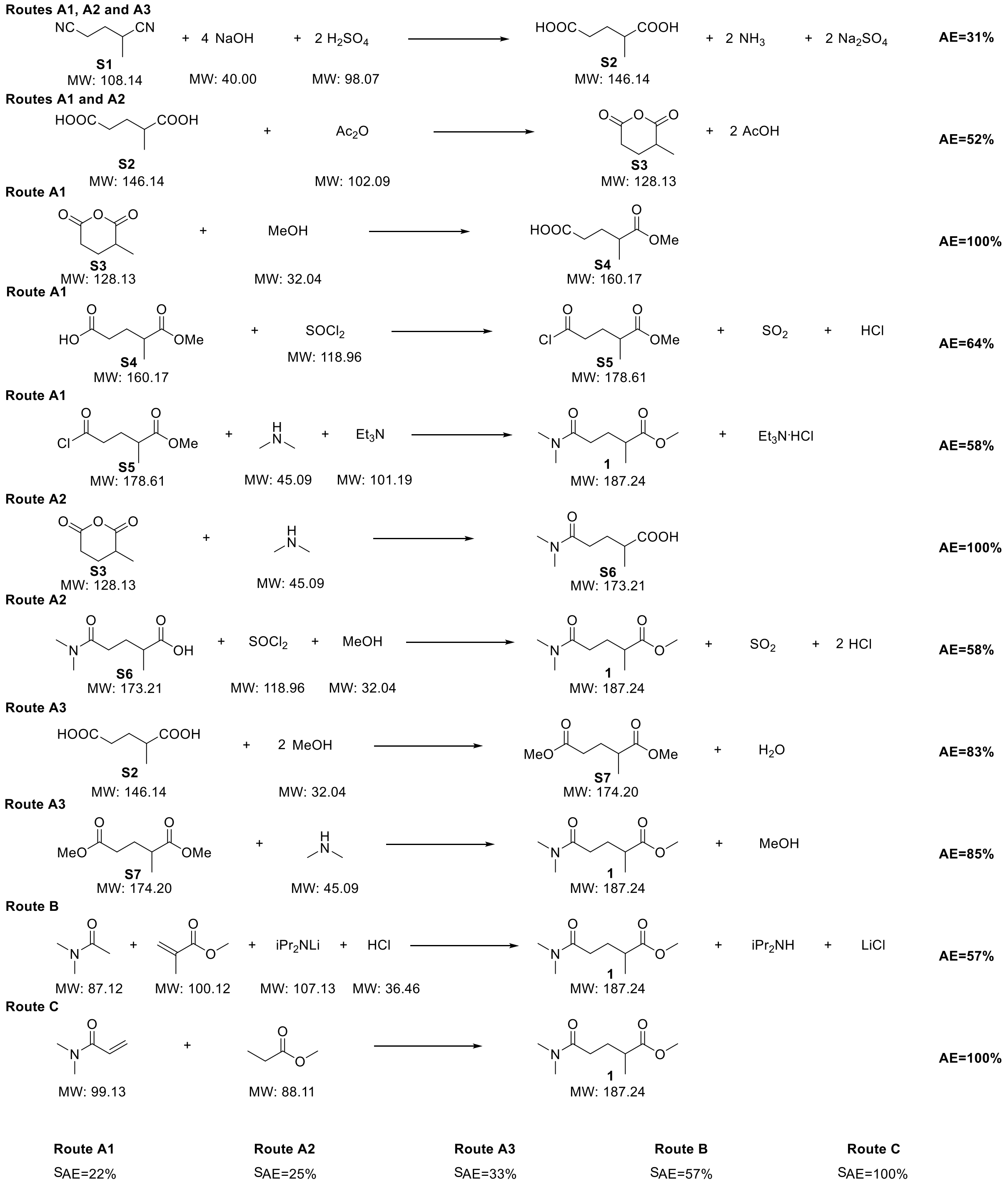

Scheme S1. Atom economies calculated for the synthesis of methyl 5-(dimethylamino)-2-methyl-5-oxopentanoate (**1**).

2.3. Complete *E* factor

Complete *E* factor (cEF) was calculated according to the formula established by Sheldon *et al.*[7]:

$$\mathrm{cEF} = \frac{\sum m_{\text{raw materials}} + \sum m_{\text{reagents}} + \sum m_{\text{solvents}} + m_{\text{water}} - m_{\text{product}}}{m_{\text{product}}} \qquad \text{(S4)}$$

where *m* and *Σm* denote the mass and cumulated mass of the corresponding compounds involved in the synthetic procedure.

The cEF provides an indication of the waste generation associated by the production of a chemical. This value is usually below 0.1 kg waste per kg product in the oil refinery, 1–5 kg kg^{-1} for bulk chemicals and 5–50 kg kg^{-1} for fine chemicals.[7] Table S1–6 show the contributors to the cEF values normalised to 1 kg of PolarClean produced via different routes. For the patented routes the data was obtained from the corresponding patents.[8,9]

Table S1 Chemicals needed for the synthesis of 1 kg of PolarClean via Route A1 and theoretical Carbon Intensity (CI) originating from their perfect combustion. The isolated intermediates produced and used within the synthesis which do not contribute to the waste generation or CI are indicated with blue. MTBE: Methyl *tert*-butyl ether.

Chemicals used	Step	Mass / kg	Molar mass / g mol^{-1}	Molar amount / mol	Molar C content / mol mol^{-1}	C content / mol	CI / kg kg^{-1}	GHS Hazard pictograms
S1	1	1.23	108.14	11.4	6	68.2	3.00	☠
NaOH	1	0.96	40.00	23.9	0	0.0	0.00	🧪
cc H_2SO_4	1	1.19	98.07	12.2	0	0.0	0.00	🧪
H_2O	1	6.32	18.02	351.0	0	0.0	0.00	–
MTBE	1	5.05	88.15	57.3	5	286.5	12.61	! 🔥
S2	2	1.61	146.14	11.0	6	66.1	2.91	!
Ac_2O	2	2.66	102.09	26.1	4	104.4	4.60	🔥 ☠ 🧪
S3	3	1.30	128.13	10.1	6	60.7	2.67	?
MeOH	3	6.24	32.04	194.7	1	194.7	8.57	🔥 ☠ ⚕
S4	4	1.38	160.17	8.6	7	60.3	2.65	?
$SOCl_2$	4	2.30	118.96	19.3	0	0.0	0.00	☠ 🧪
S5	5	1.70	178.61	9.5	7	66.5	2.93	?
Me_2NH	5	0.85	45.08	18.9	2	37.9	1.67	! 🔥 🧪
Et_3N	5	1.19	101.19	11.8	6	70.7	3.11	🔥 ☠ 🧪
Toluene	5	10.14	92.14	110.1	7	770.4	33.90	! 🔥
Chemical produced	Step	Mass / kg	Molar mass / g mol^{-1}	Molar amount / mol	Molar C content / mol mol^{-1}	C content / mol	CI / kg kg^{-1}	GHS Hazard pictograms
S2	1	1.61	146.14	11.0	6	66.1	−2.91	!
S3	2	1.30	128.13	10.1	6	60.7	−2.67	?
S4	3	1.38	160.17	8.6	7	60.3	−2.65	?
S5	4	1.70	178.61	9.5	7	66.5	−2.93	?
1	5	1.00	187.24	5.3	9	48.1	−2.12	!

Table S2 Chemicals needed for the synthesis of 1 kg of PolarClean via Route A2 and theoretical Carbon Intensity (CI) originating from their perfect combustion. The isolated intermediates produced and used within the synthesis that do not contribute to the waste generation or CI are indicated with blue. MTBE: Methyl *tert*-butyl ether.

Chemicals used	Step	Mass / kg	Molar mass / g mol^{-1}	Molar amount / mol	Molar C content / mol mol^{-1}	C content / mol	CI / kg kg^{-1}	GHS Hazard pictograms
S1	1	0.94	108.14	8.7	6	52.1	2.29	☠
NaOH	1	0.73	40.00	18.3	0	0.0	0.00	🧪
H_2SO_4	1	0.91	98.07	9.3	0	0.0	0.00	🧪
H_2O	1	4.83	18.02	268.2	0	0.0	0.00	–
MTBE	1	3.86	88.15	43.8	5	218.9	9.64	❗ 🔥
S2	2	1.74	146.14	11.9	6	71.3	3.14	❗
Ac_2O	2	2.87	102.09	28.1	4	112.5	4.95	🔥 ☠ 🧪
S3	3	0.99	128.13	7.7	6	46.4	2.04	❓
Me_2NH	3	1.10	45.08	24.5	2	48.9	2.15	❗ 🔥 🧪
H_2O	3	2.24	18.02	124.0	0	0.0	0.00	–
S6	4	1.38	173.21	8.0	8	63.7	2.81	❓
$SOCl_2$	4	2.26	118.96	19.0	0	0.0	0.00	☠ 🧪
MeOH	4	10.93	32.04	341.1	1	341.1	15.01	🔥 ☠ ⚕

Chemical produced	Step	Mass / kg	Molar mass / g mol^{-1}	Molar amount / mol	Molar C content / mol mol^{-1}	C content / mol	CI / kg kg^{-1}	GHS Hazard pictograms
S2	1	1.74	146.14	11.9	6	71.3	−3.14	❗
S3	2	0.99	128.13	7.7	6	46.4	−2.04	❓
S6	3	1.38	173.21	8.0	8	63.7	−2.81	❓
1	4	1.00	187.24	5.3	9	48.1	−2.12	❗

Table S3 Chemicals needed for the synthesis of 1 kg of PolarClean via Route A3 and theoretical Carbon Intensity (CI) originating from their perfect combustion. The isolated intermediates produced and used within the synthesis that do not contribute to the waste generation or CI are indicated with blue. MTBE: Methyl *tert*-butyl ether.

Chemicals used	Step	Mass / kg	Molar mass / g mol^{-1}	Molar amount / mol	Molar C content / mol mol^{-1}	C content / mol	CI / kg kg^{-1}	GHS Hazard pictograms
S1	1	0.69	108.14	6.4	6	38.4	1.69	☠
NaOH	1	0.54	40.00	13.5	0	0.0	0.00	⚗
H_2SO_4	1	0.67	98.07	6.9	0	0.0	0.00	⚗
H_2O	1	3.57	18.02	198.0	0	0.0	0.00	–
MTBE	1	2.85	88.15	32.3	5	161.6	7.11	❗ 🔥
S2	2	0.91	146.14	6.2	6	37.3	1.64	❗
MeOH	2	7.11	32.04	221.9	1	221.9	9.76	🔥 ☠ ⚕
Amberlyst 36[a]	2	0.74	N/A	N/A	N/A	N/A	N/A	❗
S7	3	1.01	128.13	7.9	8	62.9	2.77	–
Me_2NH	3	0.32	45.08	7.1	2	14.2	0.63	❗ 🔥
NaOMe	3	0.01	54.02	0.3	1	0.3	0.01	❗ ☠ ⚗
MeOH	3	0.29	32.04	9.1	1	9.1	0.40	⚕
H_2SO_4	3	0.01	98.07	0.1	0	0.0	0.00	⚗
Chemical produced	Step	Mass / kg	Molar mass / g mol^{-1}	Molar amount / mol	Molar C content / mol mol^{-1}	C content / mol	CI / kg kg^{-1}	GHS Hazard pictograms
S2	1	0.91	146.14	6.2	6	37.3	−1.64	❗
S7	2	1.01	128.13	7.9	8	62.9	−2.77	–
1	3	1.00	187.24	5.3	9	48.1	−2.12	❗

[a] The acidic resin catalyst was assumed to be recycled and therefore disregarded from waste generation or CI.

Table S4 Chemicals needed for the synthesis of 1 kg of **1B** via Route B and theoretical Carbon Intensity (CI) originating from their perfect combustion. The isolated intermediates produced and used within the synthesis that do not contribute to the waste generation or CI are indicated with blue. THF: Tetrahydrofuran.

Chemicals used	Mass / kg	Molar mass / g mol^{-1}	Molar amount / mol	Molar C content / mol mol^{-1}	C content / mol	CI / kg kg^{-1}	GHS Hazard pictograms
DMAc	1.83	87.1	21.04	4	84.2	3.70	
MMA	2.00	100.1	19.98	5	99.9	4.40	
MeTHF	9.49	86.1	110.17	5	550.9	24.24	
LDA	2.38	107.1	22.17	6	133.0	5.85	
THF[a]	6.62	72.1	91.78	4	367.1	16.16	
1M HCl solution	5.56	–	–	0	0.0	0.00	
EtOAc	13.89	88.1	157.63	4	630.5	27.75	
H_2O	6.94	18.0	385.37	0	0.0	0.00	–
sat. $NaHCO_3$ solution	6.94	84.0	7.94	1	7.9	0.35	–
Brine	6.94	–	–	0	0.0	0.00	–
Chemical produced	**Mass / kg**	**Molar mass / g mol^{-1}**	**Molar amount / mol**	**Molar C content / mol mol^{-1}**	**C content / mol**	**CI / kg kg^{-1}**	**GHS Hazard pictograms**
1	1.00	187.24	5.3	9	48.1	−2.12	

[a]Since its exact composition is unknown, the solvent of LDA, THF/*n*-heptane/ethylbenzene mixture was assessed as pure THF.

Table S5 Chemicals needed for the synthesis of 1 kg of **1C** via Route C and theoretical Carbon Intensity (CI) originating from their perfect combustion.

Chemicals used	Mass / kg	Molar mass / g mol^{-1}	Molar amount / mol	Molar C content / mol mol^{-1}	C content / mol	CI / kg kg^{-1}	GHS Hazard pictograms
MeOProp	4.87	88.11	55.3	4	221.3	9.74	
DMAA	1.10	99.13	11.1	5	55.3	2.43	
KO*t*Bu	0.06	112.21	0.5	4	2.2	0.10	
$(COOH)_2$	0.05	90.03	0.6	2	1.1	0.05	
H_2O	0.48	18.02	26.7	0	0.0	0.00	–
Chemical produced	**Mass / kg**	**Molar mass / g mol^{-1}**	**Molar amount / mol**	**Molar C content / mol mol^{-1}**	**C content / mol**	**CI / kg kg^{-1}**	**GHS Hazard pictograms**
1	1.00	187.24	5.3	9	48.1	−2.12	

Table S6 Chemicals needed for the synthesis of 1 kg of **1C** via Route C and theoretical Carbon Intensity (CI) originating from their perfect combustion. In this scenario, **8** is isolated and utilised as a profitable by-product of the synthesis.

Chemicals used	Mass / kg	Molar mass / g mol^{-1}	Molar amount / mol	Molar C content / mol mol^{-1}	C content / mol	CI / kg kg^{-1}	GHS Hazard pictograms
MeOProp	4.87	88.11	55.3	4	221.3	9.74	❗ 🔥
DMAA	1.10	99.13	11.1	5	55.3	2.43	☠ 🧪
KO*t*Bu	0.06	112.21	0.5	4	2.2	0.10	🔥 🧪
$(COOH)_2$	0.05	90.03	0.6	2	1.1	0.05	❗ 🧪
H_2O	0.48	18.02	26.7	0	0.0	0.00	–
Et_2O	1.52	74.12	20.5	4	81.9	3.60	❗ 🔥
Chemical produced	Mass / kg	Molar mass / g mol^{-1}	Molar amount / mol	Molar C content / mol mol^{-1}	C content / mol	CI / kg kg^{-1}	GHS Hazard pictograms
1	1.00	187.24	5.3	9	48.1	−2.12	❗
8	0.39	286.37	1.3	14	18.8	−0.83	❓

Table S7 Complete *E* factor (cEF) of different synthetic routes leading to **1** and theoretical Carbon Intensity (CI) originating from the perfect combustion of chemical waste produced.

Route	cEF / -	CI_{chem} / kg kg^{-1}
A1	25.8	65.3
A2	23.5	31.9
A3	13.5	17.5
B	61.6	83.6
C	5.6	10.2
C^{a}	4.8	9.3

^{a}With the utilisation of by-product **8.**

2.4. Carbon intensity

Carbon Intensity (CI) is the mass emission of CO_2 associated with the production of unit mass of product (Eq S5).

$$\mathrm{CI} = \frac{m_{\mathrm{CO_2 emission}}}{m_{\mathrm{product}}} \tag{S5}$$

In this context, three contributors to the total CI were considered, namely chemical waste (CI_{chem}), energy consumption (CI_{en}) and cooling water consumption (CI_{cw}), as shown in Eq S6.

$$\mathrm{CI} = \mathrm{CI_{chem}} + \mathrm{CI_{en}} + \mathrm{CI_{cw}} \tag{S6}$$

Four activities were taken into account for the energy consumption, namely stirring, heating, chilling and applying vacuum (Eq S7).

$$\mathrm{CI_{en}} = \mathrm{CI_{stirring}} + \mathrm{CI_{heating}} + \mathrm{CI_{chilling}} + \mathrm{CI_{vacuum}} \tag{S7}$$

The CI values, energy or cooling water consumption are not reported for the patented synthetic routes; therefore they need to be calculated from the existing data. The same set of assumptions were established for the patented routes (A1, A2, A3) and the routes reported in this work (B, C) for comparable results. Syntheses of 100 g **1** (laboratory scale) was considered via the different synthetic routes. Most steps (8 out of 9) in the patented syntheses are reported on a 10^1-10^2 g scale, similarly to the syntheses in this work. Thus, this small change of scale is not likely to cause any significant change in process parameters, such as yield or reaction time.

Each synthesis was broken down into subsequent process steps, namely reactions, extractions, filtrations, atmospheric distillations and vacuum distillations. The process steps were associated with cooling water consumption and/or energy consuming activities, namely, heating, stirring, chilling and using vacuum. The energy consumptions were estimated based on the catalogue power consumption of laboratory scale equipment and the duration of the activity. IKA C-MAG HS7 hot plate with a power consumption of 1000 W was used for the estimation of heating energy. The power consumption of the same hot plate is 15 W for stirring. Lauda Alpha RA 12 thermostat with a power consumption of 1800 W was considered for the estimation of chilling of the reaction vessel. Although the lower temperature limit of this laboratory scale chiller is −25 °C, the same power consumption value was used to estimate the energy used in the lithiation in Route B for simplicity, which in fact was carried out at −78 °C (acetone–dry ice bath). KNF N 920 KT.29.18 vacuum pump with a power consumption of 135 W was considered for the estimation.

Table S8 Power consumption of the laboratory scale equipment considered for the calculation of CI for the different synthetic routes.

Equipment	Model	Power consumption / W
Cooling thermostat	Lauda Alpha RA 12	1800
Hot plate	IKA C-MAG HS7	1000
Vacuum pump	KNF N 920 KT.29.18	135
Magnetic stirrer	IKA C-MAG HS7	15

The durations of reaction steps are well reported but the duration of other process steps, such as vacuum distillation, is not known for the patented synthetic steps. Therefore, standard process durations were assumed based on the experimental observations for Route B and C. The duration of stirring needed for each extraction step was 6 minutes. The time needed to distil off 100 g of low-boiling solvents at atmospheric pressure was 20 minutes. The duration of the vacuum distillation (Vac. dist.) of 100 g of product (or high-boiling intermediate) was 2 hours. The filtration of 1 L slurry required the use of vacuum for 0.5 hours.

Table S9 Standard duration of process steps based on experimental observations.

Process step	Duration / h
One step of extraction	0.1
Atmospheric distillation of 100 g low-boiling solvent	0.33
Filtration of 1 L slurry	0.5
Vac. dist. of 100 g high-boiling liquid	2

While a closed-loop chiller was assumed to be used for the cooling or chilling of the reaction vessel, in reflux condensers and distillation apparatus, the use of running tap water was considered for cooling. The flow rate of tap water was assumed to be 2.5 L hr^{-1} as reported elsewhere.[10]

The conversion of the energy and cooling water consumption to CI was done based on 2018 UK government emission conversion factors.[11]

Table S10 2018 UK government emission conversion factors.[11]

Contributor	Conversion factor
Electricity generated	0.28307 kg CO_2 eq. kWh^{-1}
Electricity transmitted & distributed	0.02413 kg CO_2 eq. kWh^{-1}
Electricity used	0.30720 kg CO_2 eq. kWh^{-1}
Tap water used	0.344 kg CO_2 eq. m^{-3}

Table S11 Process steps contributing to the CI_{en} and CI_{cw} of the 100 g scale synthesis of **1** via Route A1.

Process step	Duration / h				
	Vacuum	Stirring	Heating	Chiller	Water-cooling
Reaction I	0	8	8	0	8
Extraction I	0	0.3	0	0	0
Distillation I	0	1.67	1.67	0	1.67
Reaction II	0	7	7	0	7
Vac. dist. I	6	6	6	0	6
Vac. dist. II	2	2	2	0	2
Reaction III	3	3	3	0	3
Distillation II	0	2	2	0	2
Vac. dist. III	2	2	2	0	2
Reaction IV	0	1	1	0	1
Distillation III	0	0.33	0.33	0	0.33
Reaction V	0	16	0	2	0
Filtration I	0.5	0	0	0	0
Distillation IV	0	3.33	3.33	0	3.33
Vac. dist. IV	2	2	2	0	2
	Vacuum	Stirring	Heating	Chiller	Water-cooling
Total time / h	15.50	54.63	38.33	2.00	38.33
Total energy / kWh	2.09	0.82	38.33	3.60	–
Total volume / m^3	–	–	–	–	5.75
CI / kg kg^{-1}	6.4	2.5	117.8	11.1	19.8

Table S12 Process steps contributing to the CI_{en} and CI_{cw} of the 100 g scale synthesis of **1** via Route A2.

Process step	Duration / h				
	Vacuum	Stirring	Heating	Chiller	Water-cooling
Reaction I	0	8	8	0	8
Extraction I	0	0.3	0	0	0
Distillation I	0	1.67	1.67	0	1.67
Reaction II	0	7	7	0	7
Vac. dist. I	6	6	6	0	6
Vac. dist. II	2	2	2	0	2
Reaction III	0	24	0	2	0
Distillation II	0	1	1	0	1
Vac. dist. III	2	2	2	0	2
Reaction IV	0	6	0	0	6
Distillation III	0	4	4	0	4
Vac. dist. IV	2	2	0	0	2
	Vacuum	Stirring	Heating	Chiller	Water-cooling
Total time / h	12.00	63.97	31.67	2.00	39.67
Total energy / kWh	1.62	0.96	31.67	3.60	–
Total volume / m^3	–	–	–	–	5.95
CI / kg kg^{-1}	5.0	2.9	97.3	11.1	20.5

Table S13 Process steps contributing to the CI_{en} and CI_{cw} of the 100 g scale synthesis of **1** via Route A3.

Process step	Duration / h				
	Vacuum	Stirring	Heating	Chiller	Water-cooling
Reaction I	0	8	8	0	8
Extraction I	0	0.3	0	0	0
Distillation I	0	1.67	1.67	0	1.67
Reaction II	0	6	6	0	6
Distillation II	0	2.33	2.33	0	2.33
Vac. dist. I	2	2	2	0	2
Reaction III	0	6	0	2	0
Distillation II	0	0.33	0.33	0	0.33
Filtration I	0.1	0	0	0	0
Vac. dist. II	2	2	2	0	2
	Vacuum	Stirring	Heating	Chiller	Water-cooling
Total time / h	4.10	28.63	22.33	2.00	22.33
Total energy / kWh	0.55	0.43	22.33	3.60	–
Total volume / m^3	–	–	–	–	3.35
CI / kg kg^{-1}	1.7	1.3	68.6	11.1	11.5

Table S14 Process steps contributing to the CI_{en} and CI_{cw} of the 100 g scale synthesis of **1** via Route B.

Process step			Duration / h		
	Vacuum	Stirring	Heating	Chiller	Water-cooling
Reaction I	0	3	0	3	0
Extraction I	0	0.5	0	0	0
Distillation I	0	10	10	0	10
Vac. dist. I	2	2	2	0	2
	Vacuum	Stirring	Heating	Chiller	Water-cooling
Total time / h	2.00	15.50	12.00	3.00	12.00
Total energy / kWh	0.27	0.23	12.00	5.40	–
Total volume / m^3	–	–	–	–	1.80
CI / kg kg^{-1}	0.8	0.7	36.9	16.6	6.2

Table S15 Process steps contributing to the CI_{en} and CI_{cw} of the 100 g scale synthesis of **1** via Route C.

Process step			Duration / h		
	Vacuum	Stirring	Heating	Chiller	Water-cooling
Reaction I	0	1	0	1	0
Distillation I	0	1.33	1.33	0	1.33
Vac. dist. I	2	2	2	0	2
	Vacuum	Stirring	Heating	Chiller	Water-cooling
Total time / h	2.00	4.33	3.33	1.00	3.33
Total energy / kWh	0.27	0.07	3.33	1.80	–
Total volume / m^3	–	–	–	–	0.50
CI / kg kg^{-1}	0.8	0.2	10.2	5.5	1.7

Table S16 Process steps contributing to the CI_{en} and CI_{cw} of the 100 g scale synthesis of **1** via Route C. In this scenario, **8** is isolated and utilised as a profitable by-product of the synthesis.

Process step			Duration / h		
	Vacuum	Stirring	Heating	Chiller	Water-cooling
Reaction I	0	1	0	1	0
Distillation I	0	1.33	1.33	0	1.33
Vac. dist. I	2	2	2	0	2
Crystal. I	0	0.5	0	0.5	0
Filtration I	0.5	0	0	0	0
	Vacuum	Stirring	Heating	Chiller	Water-cooling
Total time / h	2.50	4.83	3.33	1.50	3.33
Total energy / kWh	0.34	0.07	3.33	2.70	–
Total volume / m^3	–	–	–	–	0.50
CI / kg kg^{-1}	0.7	0.2	7.4	6.0	1.2

The CI associated with the chemical waste was obtained using the assumption that all the organic waste is disposed of via incineration. During this process, ideal combustion was assumed meaning that total carbon content of the chemicals was converted to CO_2. Other possible climate-relevant gas emissions have been disregarded in the calculation based on their significantly lower amounts in waste incineration plants.[12] Therefore, $CI_{chemicals}$ was calculated using Eq. S8.

$$\mathrm{CI}_{\mathrm{chem}} = \frac{\left(\sum n_{\mathrm{C,raw\ materials}} + \sum n_{\mathrm{C,reagents}} + \sum n_{\mathrm{C,solvents}} - n_{\mathrm{C,product}}\right) \cdot M_{\mathrm{CO_2}}}{m_{\mathrm{product}}} \qquad \text{(S8)}$$

Where $n_{C,raw\ materials}$, $n_{C,raw}$ materials, $n_{C,raw}$ materials and $n_{C,product}$ are the amount of carbon in the raw materials, reagents, solvents and product in the synthesis, respectively; M_{CO_2} is the molar weight of CO_2; and $m_{product}$ is the mass of product (100 g). The contributors to CI_{chem} are summarised in Table S1–6.

The contribution of different sources to the total CI for the different synthetic routes is summarised in Table S17.

Table S17 Breakdown of the different contributors to the overall estimated CI of the synthetic routes leading to **1**. All data is shown in kg kg^{-1} with the percentage values in brackets. CI_{en} is written is blue to emphasise that it is not an independent contributor but the sum of the first four rows.

Route	A1	A2	A3	B	C	C[a]
CI_{vacuum} [%]	6.4 [2.9]	5.0 [3.0]	1.7 [1.5]	0.8 [0.6]	0.8 [2.9]	0.7 [3.0]
$CI_{stirring}$ [%]	2.5 [1.1]	2.9 [1.7]	1.3 [1.2]	0.7 [0.5]	0.2 [0.7]	0.2 [0.6]
$CI_{heating}$ [%]	117.8 [52.8]	97.3 [57.7]	68.6 [61.4]	36.9 [25.5]	10.2 [35.6]	7.4 [29.7]
$CI_{chilling}$ [%]	11.1 [5.0]	11.1 [6.6]	11.1 [9.9]	16.6 [11.5]	5.5 [19.3]	6.0 [24.1]
CI_{en} [%]	137.8 [61.8]	116.3 [68.9]	82.7 [74.0]	55.0 [38.0]	16.8 [58.5]	14.2 [57.4]
CI_{cw} [%]	19.8 [8.9]	20.5 [12.1]	11.5 [10.3]	6.2 [4.3]	1.7 [6.0]	1.2 [5.0]
CI_{chem} [%]	65.3 [29.3]	31.9 [18.9]	17.5 [15.7]	83.6 [57.7]	10.2 [35.5]	9.3 [37.6]
TOTAL CI	**222**	**169**	**112**	**145**	**29**	**25**

[a]With the utilisation of by-product **8.**

3. Life cycle trees of starting materials

Table 1 of the main text shows the synthons and synthetic equivalents which were identified as building blocks for the synthesis of **1**. The sustainability aspects of the production of **1** from these starting materials have been thoroughly analysed and discussed in the main text and in Section 2 of the ESI. However, the synthesEs of these starting materials from basic building are also relevant to get a full picture of the chemical transformations involved in the total synthesis of **1**.

The starting materials as identified in Section 2.1 are 2-methylglutarate (**S1**), methanol and dimethylamine (DMA) for route A1–3; DMAc and MMA for route B; MeOProp and DMAA for route C. Fig. S1 shows the conventional industrially relevant life cycle tree of these starting materials.[13] It is worth noting that for the production of some chemicals, more than one industrially applied, high volume production methods exist. The following materials have been defined as basic building blocks: NH_3, O_2, CO, syngas and saturated hydrocarbons (C_xH_{2x+2}) present in natural gas or petroleum. Fig. S2 shows the bio-based life cycle tree of the starting materials.[14] In this case, chemicals with well-established direct production from biomass by fermentation or gasification are also considered as basic building blocks. Table S18 summarizes the number of steps required to obtain the starting materials of different routes.

Table S18 Number of steps required to obtain the starting materials of different synthetic routes leading to **1**.

	Number of steps to starting materials	
Route	Conventional	Bio-based
A	5	4
B	8	5
C	8	5

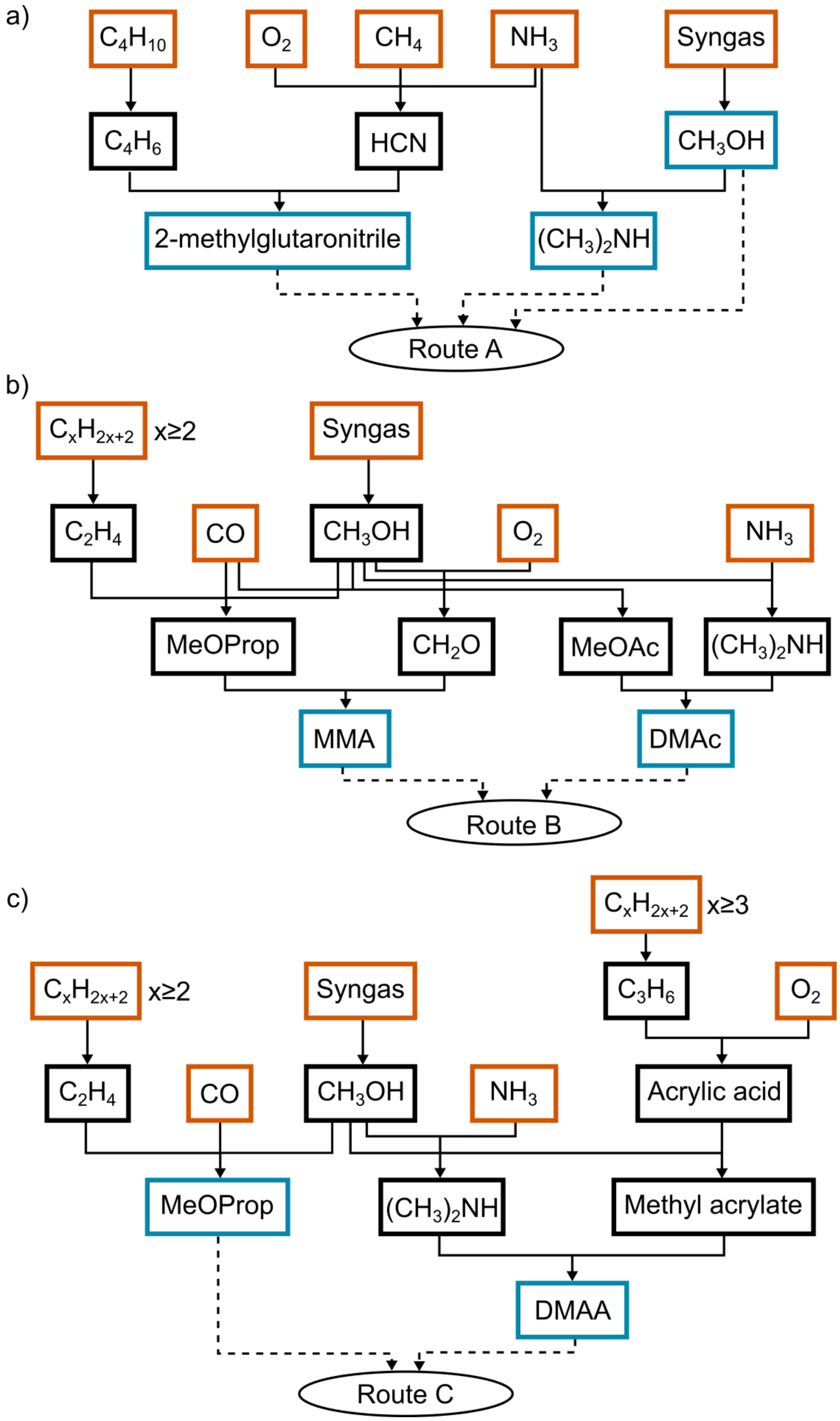

Fig. S1 Conventional industrially relevant life cycle tree of starting materials used in the different synthetic routes of **1**. The basic building blocks are indicated with orange and the starting materials of the different routes with blue frame.

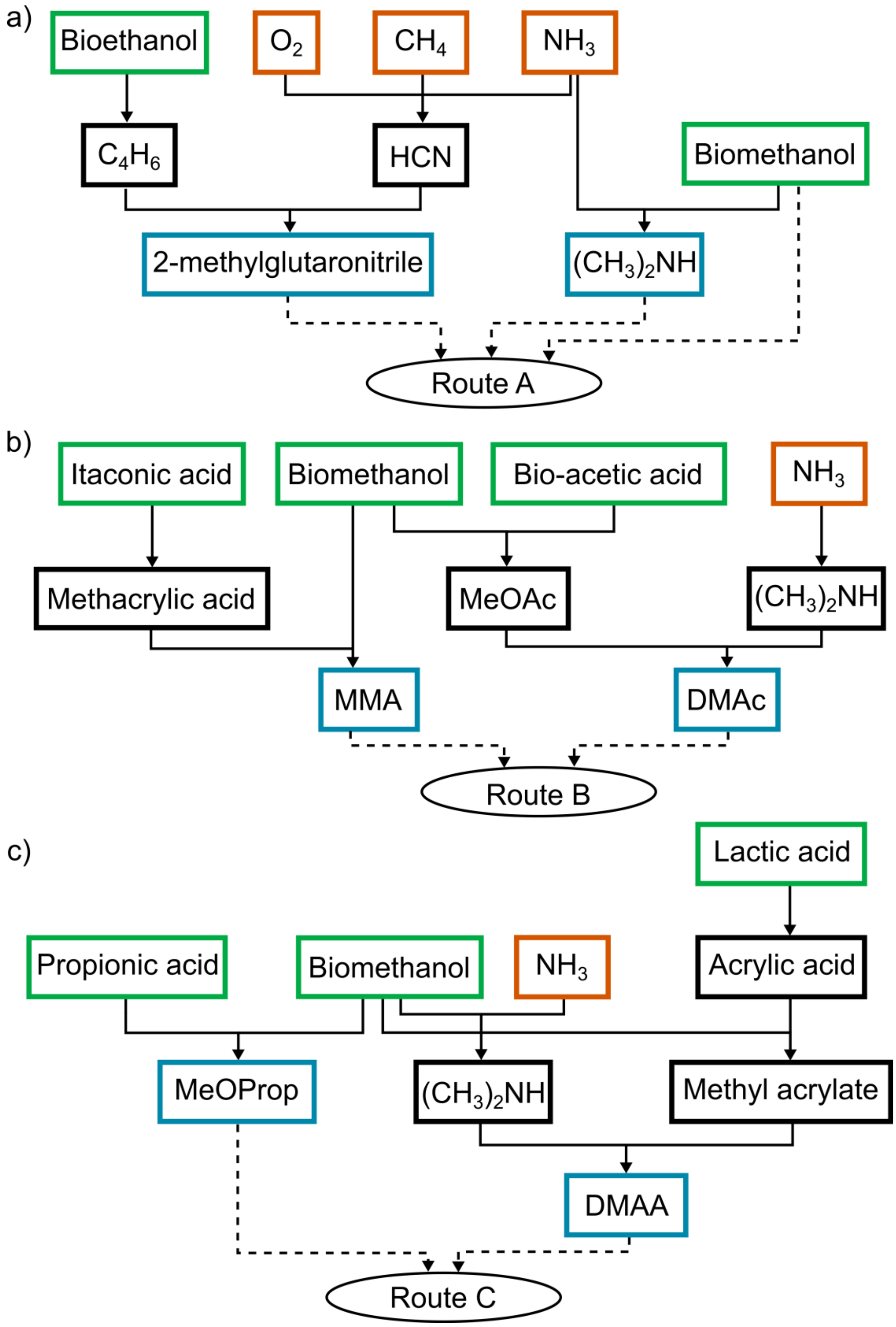

Fig. S2 Bio-based life cycle tree of starting materials used in the different synthetic routes of **1**. The basic building blocks are indicated with orange, the bio-based building blocks with green and the starting materials of the different routes with blue frame.

4. Polymer solubility and membrane stability

Polymer solubility tests have been performed by adding 285 mg solvent to 15 mg polymer (5 wt%) in a screw-cap vial. The closed vial was placed in an incubator shaker at 50 °C and 400 rpm for 24 hours, after which the solubility was evaluated. In the membrane solvent resistance tests, rectangular membrane pieces (0.5 cm × 0.5 cm) were soaked in 0.75 mL of solvent in closed screw-cap vials for 72 hours while shaking in an incubator shaker at 25 °C with 400 rpm.

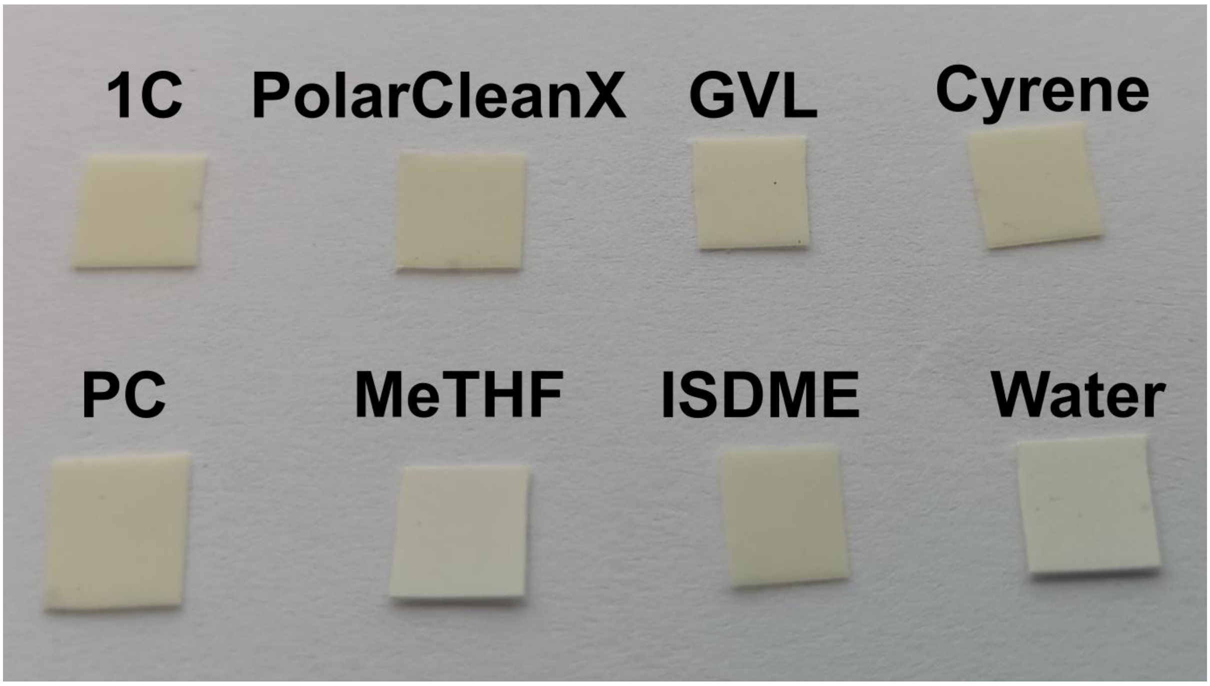

Fig. S3 Photograph of 0.5 cm × 0.5 cm GMT-oNF-1 pieces membrane soaked in different solvents. All membranes showed good structural integrity after the stability test. The shade of the membranes from MeTHF and water is somewhat brighter due to the relatively fast drying.

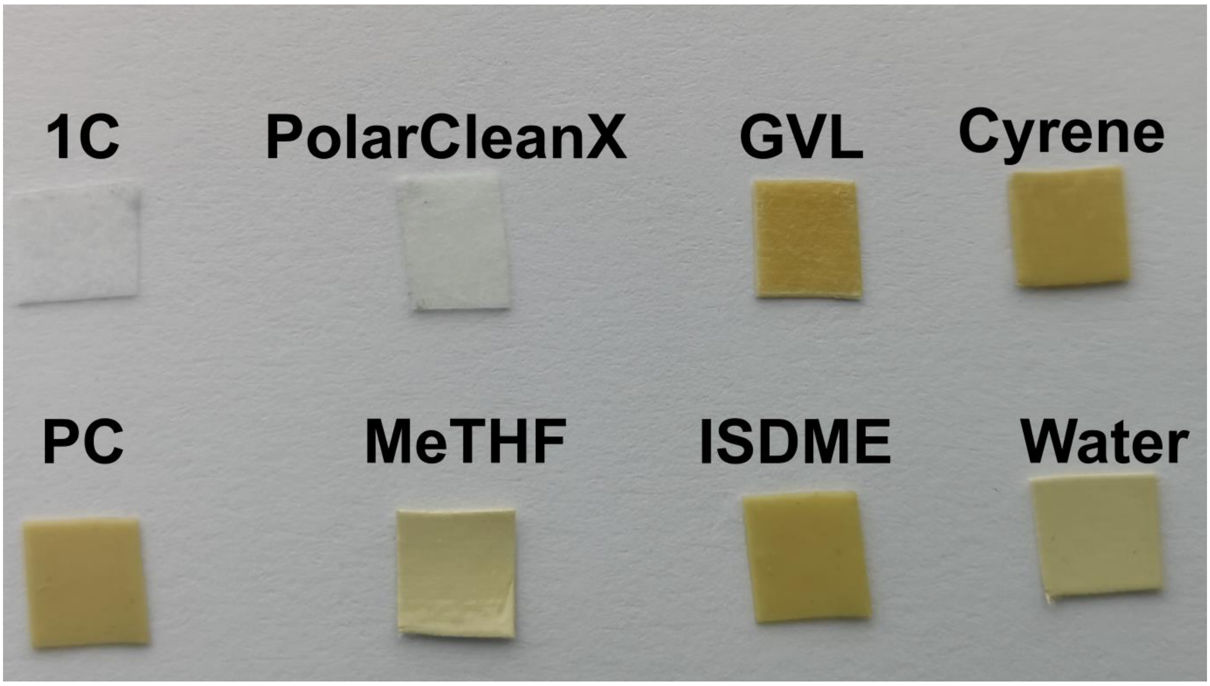

Fig. S4 Photograph of 0.5 cm × 0.5 cm NF030705 membrane pieces soaked in different solvents. In **1C** and PolarCleanX, the membrane layer completely disappeared leaving only the support behind. The other pieces showed good structural integrity after the stability test. The shade of the membranes from MeTHF and water is somewhat brighter due to the relatively fast drying.

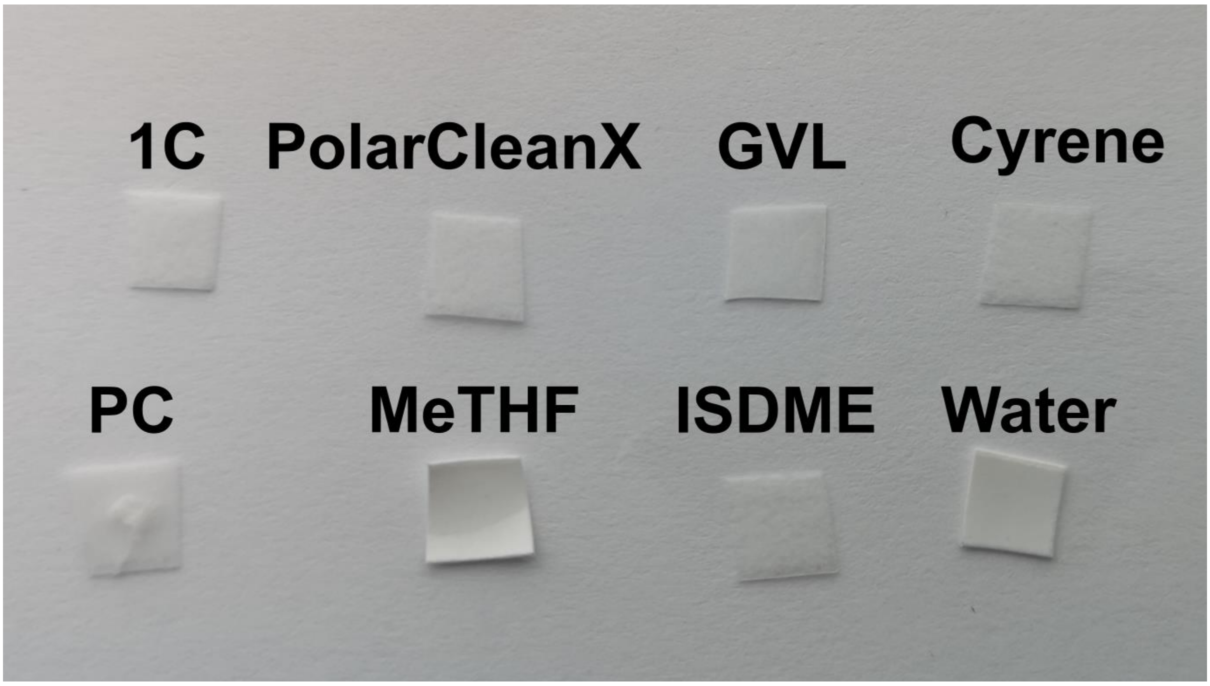

Fig. S5 Photograph of 0.5 cm × 0.5 cm Nadir NP010 membrane pieces soaked in different solvents. In **1C**, PolarCleanX, GVL, Cyrene and ISDME the membrane layer completely disappeared leaving only the support behind. In PC, the membrane layer shrank significantly and became detached from the support. Pieces in MeTHF and water showed good structural integrity after the stability test.

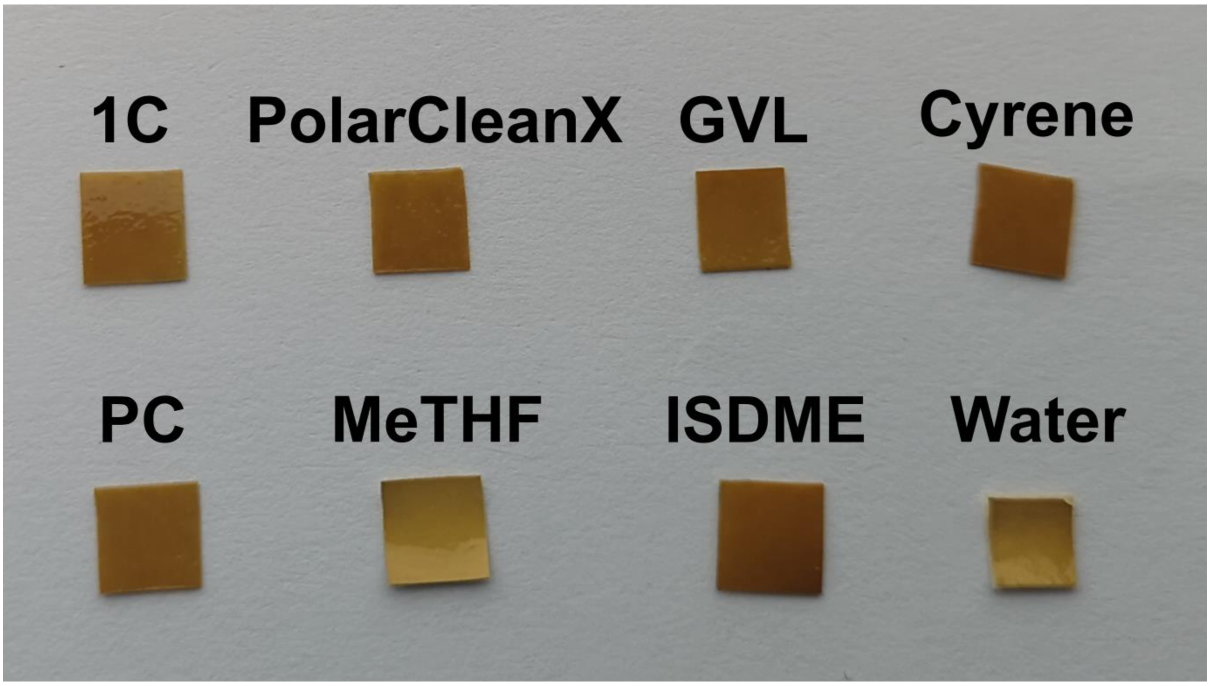

Fig. S6 Photograph of 0.5 cm × 0.5 cm Duramem 900 membrane pieces soaked in different solvents. All membranes showed good structural integrity after the stability test. The shade of the membranes from MeTHF and water is somewhat brighter due to the relatively fast drying.

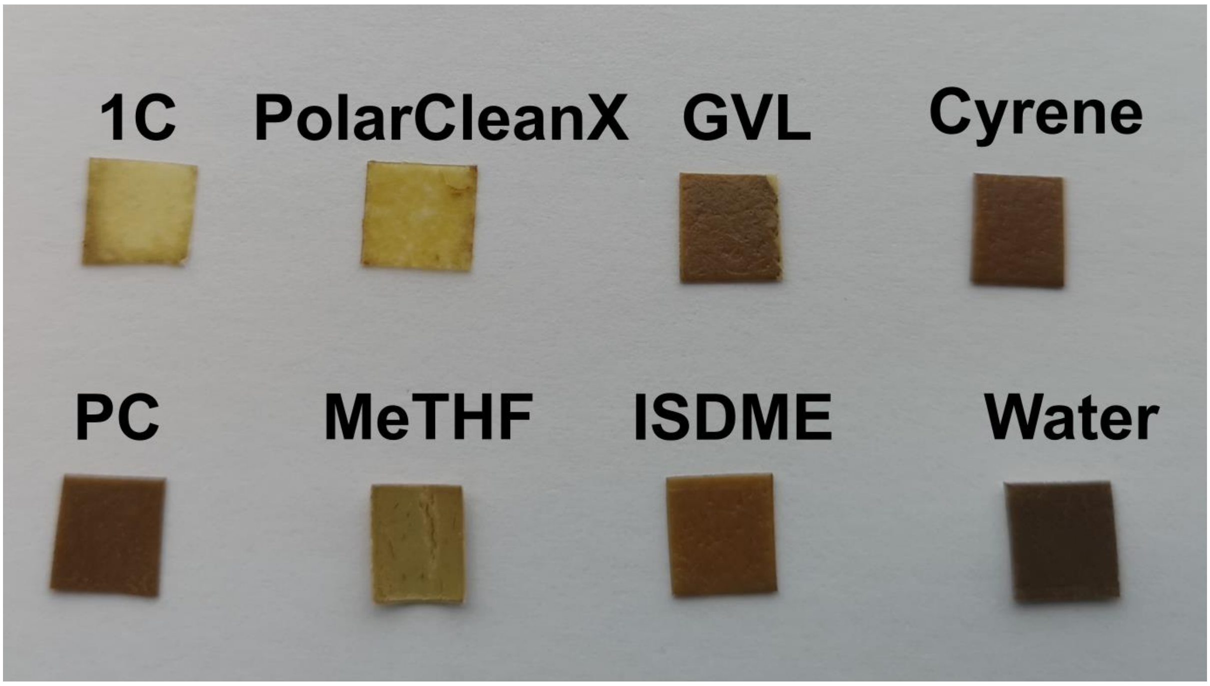

Fig. S7 Photograph of 0.5 cm × 0.5 cm in-house prepared PBI membrane pieces soaked in different solvents. In **1C** and PolarCleanX, the majority of membrane layer became dissolved or detached from the support. The other pieces showed good structural integrity after the stability test. The membrane from MeTHF developed cracks and a brighter colour after the removal from the solvent due to the fast drying.

5. Solvent miscibility

Solvent miscibility was tested by mixing 50 µL of **1B**, **1C** or PolarCleanX with 50 µL solvent in an HPLC vial at room temperature. Results are summarised in Table S19.

Table S19 Solvent miscibility chart of **1B**, **1C** and PolarCleanX with traditional and green solvents. The symbol ✓ indicates miscibility while ✗ indicates the presence of two immiscible liquid phases. **1B** formed an emulsion with water indicated by ***Em***.

	1B	**1C**	PolarCleanX
Acetic acid	✓	✓	✓
Acetone	✓	✓	✓
Acetonitrile	✓	✓	✓
Anisole	✓	✓	✓
Butyl acetate	✓	✓	✓
1-Butyl-3-methylimidazolium acetate	✓	✓	✓
Chloroform	✓	✓	✓
Cyclohexane	✗	✗	✗
Cyclohexanone	✓	✓	✓
Cyclopentyl methyl ether	✓	✓	✓
Cymene	✓	✓	✓
Cyrene	✓	✓	✓
Dimethyl carbonate	✓	✓	✓
N,*N*-Dimethylformamide	✓	✓	✓
2,5-Dimethyltetrahydrofuran	✓	✓	✓
Dimethyl sulfoxide	✓	✓	✓
Ethyl acetate	✓	✓	✓
Ethyl lactate	✓	✓	✓
Glycerol	✓	✓	✓
Heptane	✗	✗	✗
1,1,1,3,3,3-Hexafluoro-2-propanol	✓	✓	✓
Hexane	✗	✗	✗
Isopropyl alcohol	✓	✓	✓
Isosorbide dimethyl ether	✓	✓	✓
Methanol	✓	✓	✓
2-Methyltetrahydrofuran	✓	✓	✓

Pinacolone	✓	✓	✓
Propylene carbonate	✓	✓	✓
Pyridine	✓	✓	✓
Tetrahydrofuran	✓	✓	✓
Toluene	✓	✓	✓
Trifluoroacetic acid	✓	✓	✓
γ-Valerolactone	✓	✓	✓
Water	***Em***	✓	✓

6. Dielectric constant measurements

The dielectric constant (also known as the relative permittivity, ε_r) of **1** was calculated using fits to electrochemical impedance spectroscopy (EIS) data for **1** relative to solvents with known dielectric constant values.[15,16,17,18] The solvent was introduced into a custom EIS cell consisting of two 40 mm^2 parallel-plate aluminium electrodes separated by 11 mm. Data were acquired using a Compactstat potentiostat (Ivium Technologies, Netherlands) from 100kHz to 10Hz at seven points per decade, a voltage amplitude of 10 mV and no dc bias. IviumSoft (release: 2.801) was used to fit the EIS data to an R(RC)equivalent circuit. Measurements were done in quadruplicate. Fig. S8 plots the measured capacitance of **1** on the linear regression line determined for the eight standards. The dielectric constant of **1** showed some variation depending on the composition. ε_r of PolarCleanX, PolarCleanY and **1C** was determined to be 29.9 ± 1.2, 25.3 ± 1.0 and 28.3 ± 3.5, respectively. The uncertainty of the estimate is the 95% confidence limit derived from the propagated error of the repeated measurements and the standard error of the regression.

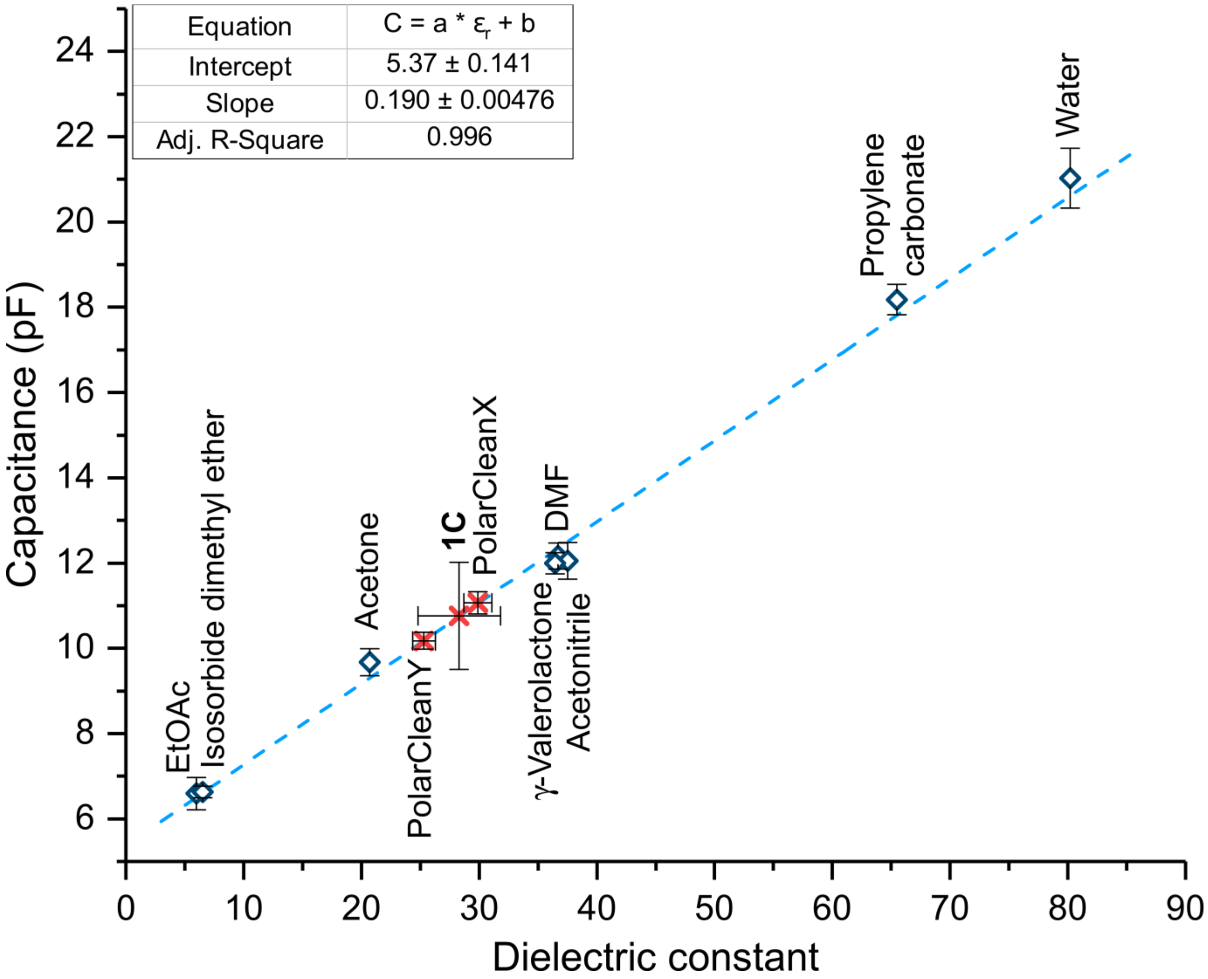

Fig. S8 Determination of the dielectric constant of PolarCleanX, PolarCleanY and **1C** from capacitance measurements using a calibration curve obtained with solvents with known dielectric constant.

7. Colour measurements

Colour measurements were performed according to ASTM D1209 Standard Test Method.[19] Pt-Co colour standards with 1, 5, 10, 50, 100, 250 and 500 Pt-Co colour units were used to obtain the calibration curve shown in Fig. S9. UV-Vis spectra were recorded on a Shimadzu UV2700 instrument in the wavelength region of 830–340 nm with 5 nm intervals and 10 mm path length. DI water was applied as a reference. Yellowness indices (YI) were obtained according to ASTM E313 Standard Practice.[20] Negative values may be obtained when the measured liquid is more transparent in the spectral window of measurement than the water reference. To avoid extrapolation, Pt-Co colours outside the range of calibration were reported as <1 or >500. Results are summarised in Table S20 and Fig. S10.

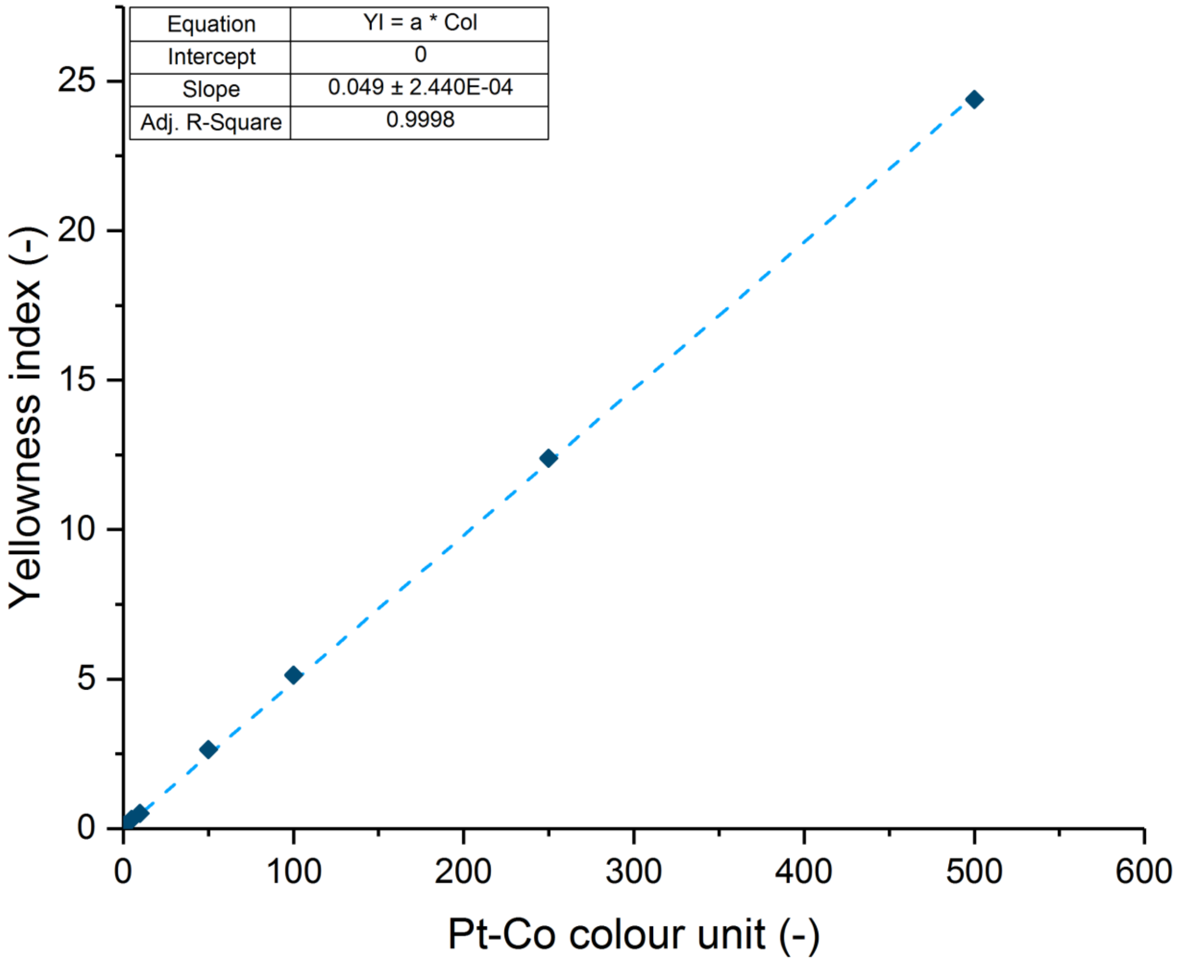

Fig. S9 Calibration curve showing the Yellowness Index (YI) as a function of Pt-Co colour unit. The vertical intercept was set to 0.

Table S20 Yellowness indices (YI) and Pt-Co colour units of commercial and novel green solvents.

Solvent	YI	YI Error	Pt-Co colour	Pt-Co colour Error
PolarCleanX	11.44	0.01	233.28	1.17
PolarCleanY	9.97	0.02	203.22	1.09
1B	31.10	0.02	>500	-
1C	1.08	0.00	22.04	0.15
9	0.97	0.02	19.69	0.50
GVL	-0.08	0.01	<1	-
Cyrene	11.19	0.04	228.21	1.39
MeTHF	-0.13	0.01	<1	-
PC	-0.15	0.03	<1	-
ISDME	-0.10	0.00	<1	-

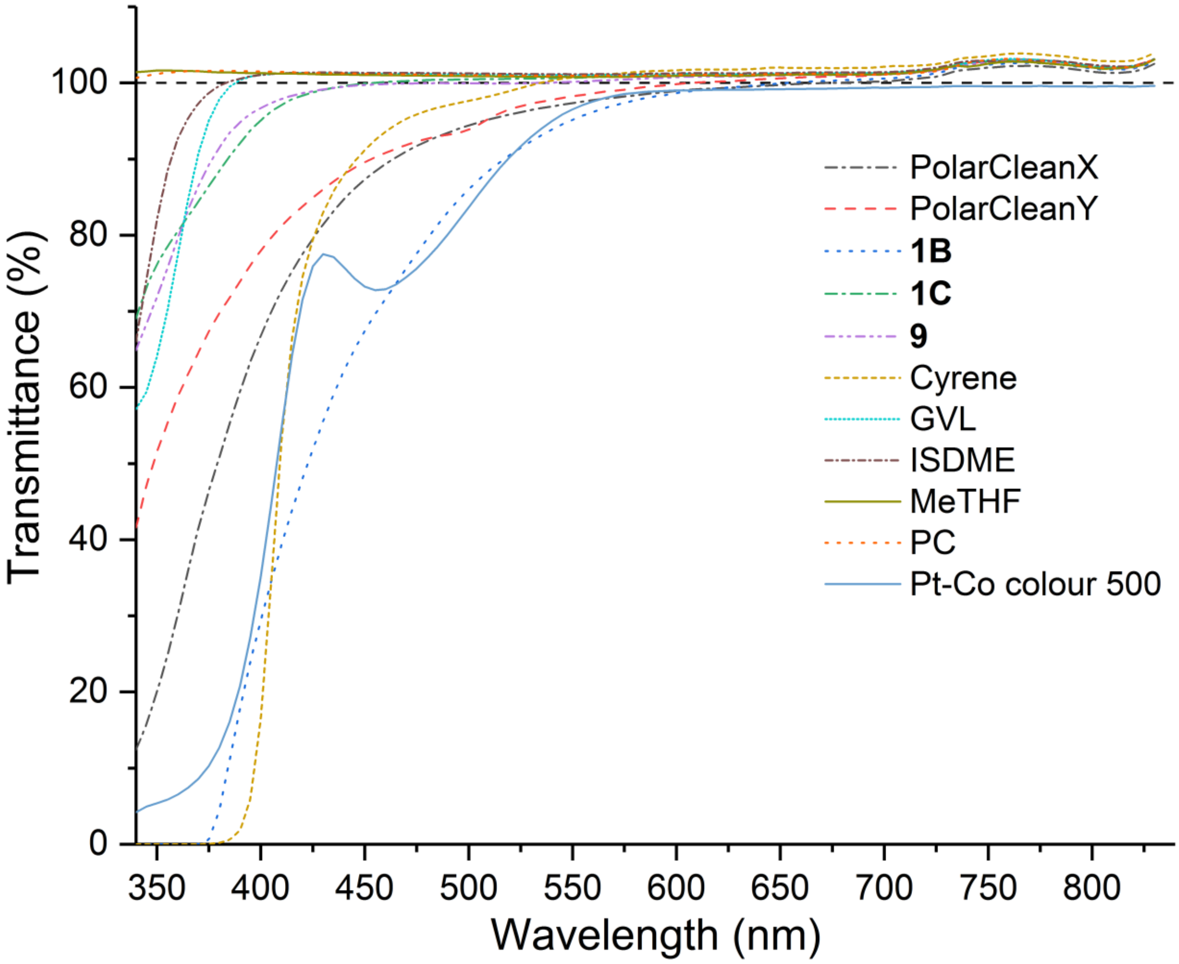

Fig. S10 UV-Vis transmittance spectra of green polar aprotic solvents and standard solution with Pt-Co colour of 500.

8. Boiling point measurements with DSC

Differential scanning calorimetry (DSC) was used to accurately determine the boiling points from minimal amounts of samples.[21] 5 μL liquid samples in Tzero aluminium hermetic pans with 75 μm pinholes in the lids were run in a DSC 2500 instrument (all from TA Instruments). A single ramp method between 40–320 °C with a gradient of 10 °C min^{-1} was used. The boiling of the sample was indicated as a negative peak in the DSC curve. The boiling point was obtained as the onset point of this peak. All measurements were performed under N_2 flow at atmospheric pressure (765.3 Hgmm, 1020 mbar). Duplicated runs from the same liquid indicated an error of ± 0.2 °C. Reference run with DI water showed a boiling point of 100.2 °C (1020 mbar).

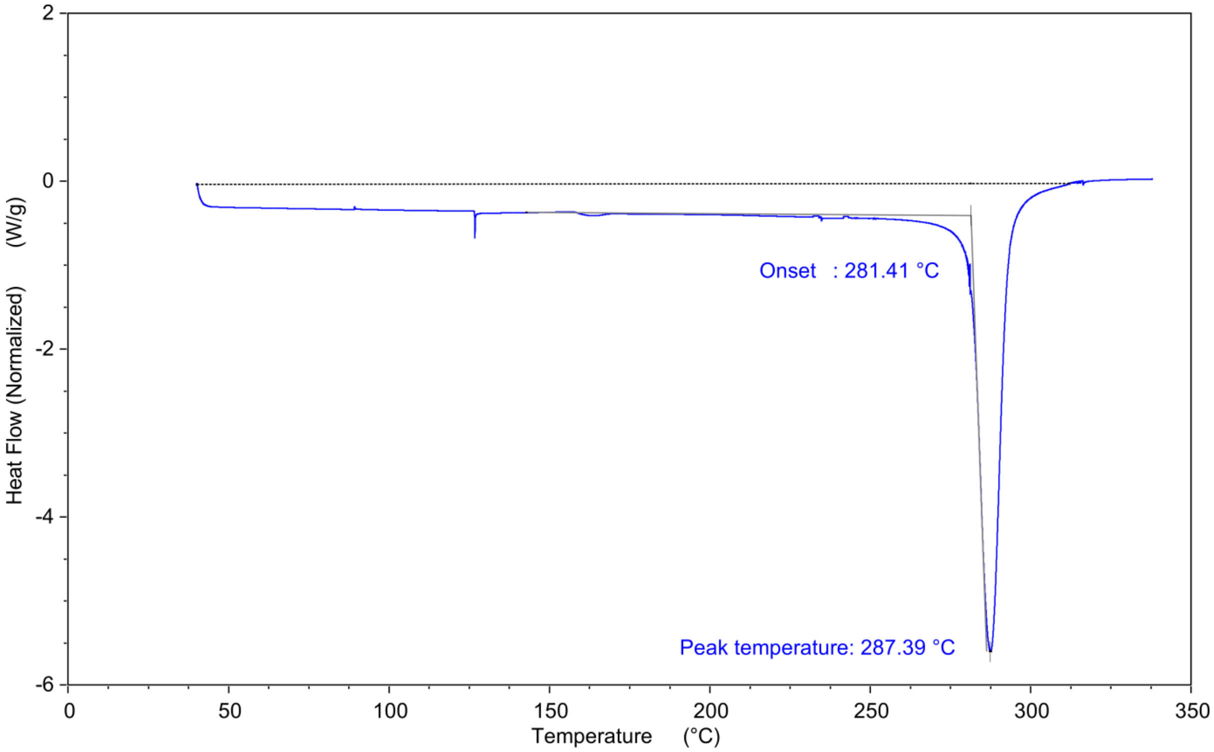

Fig. S11 DSC curve of PolarCleanX showing the boiling with an onset temperature of 281.4 °C.

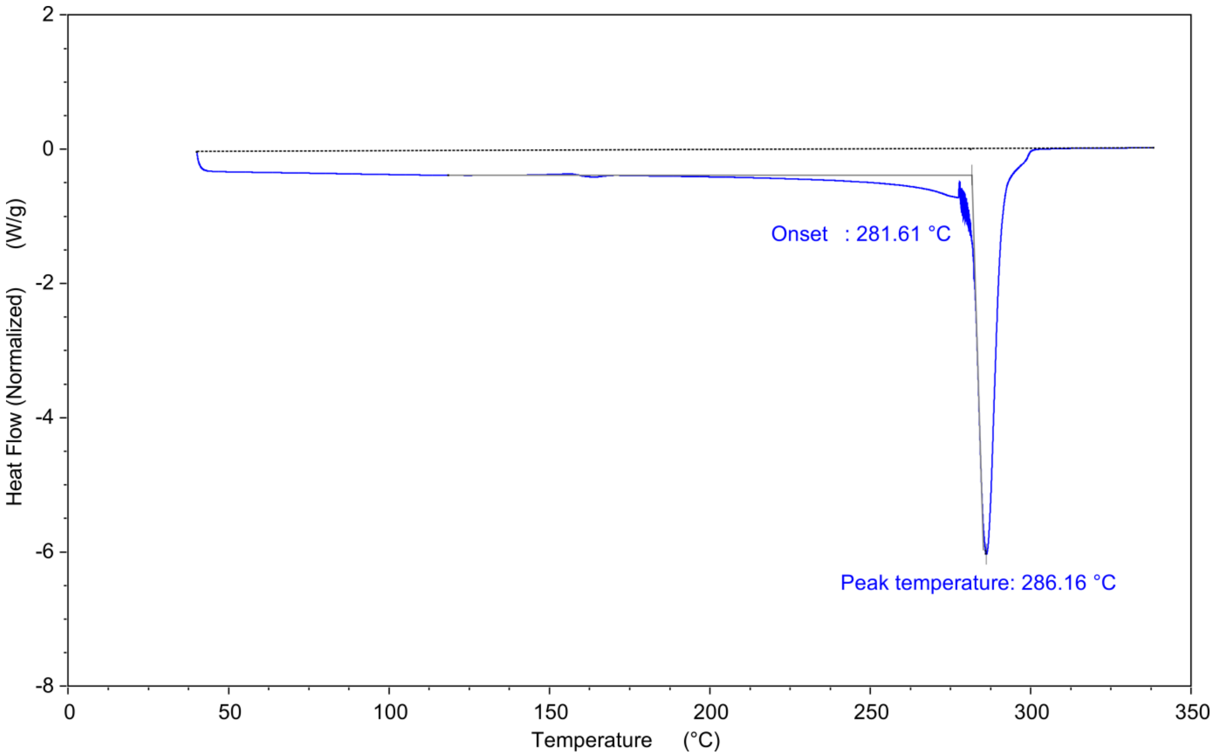

Fig. S12 DSC curve of PolarCleanY showing the boiling with an onset temperature of 281.6 °C.

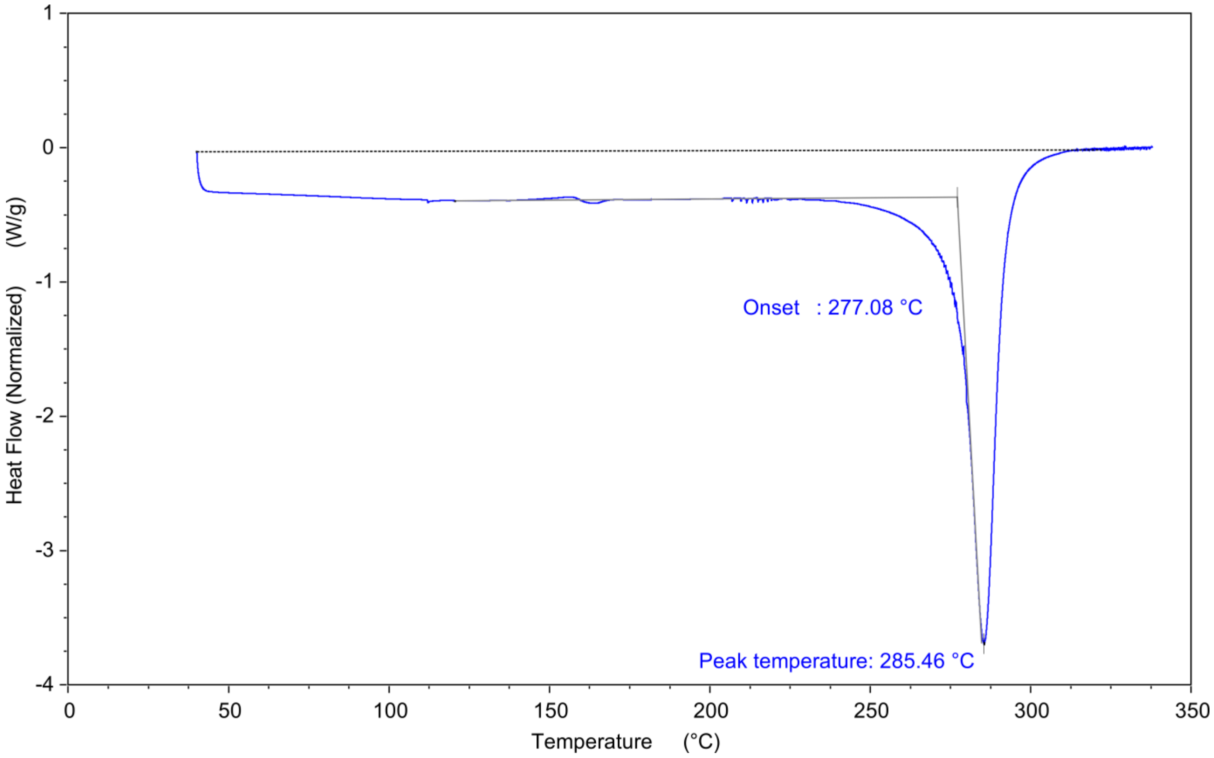

Fig. S13 DSC curve of **1B** showing the boiling with an onset temperature of 277.1 °C.

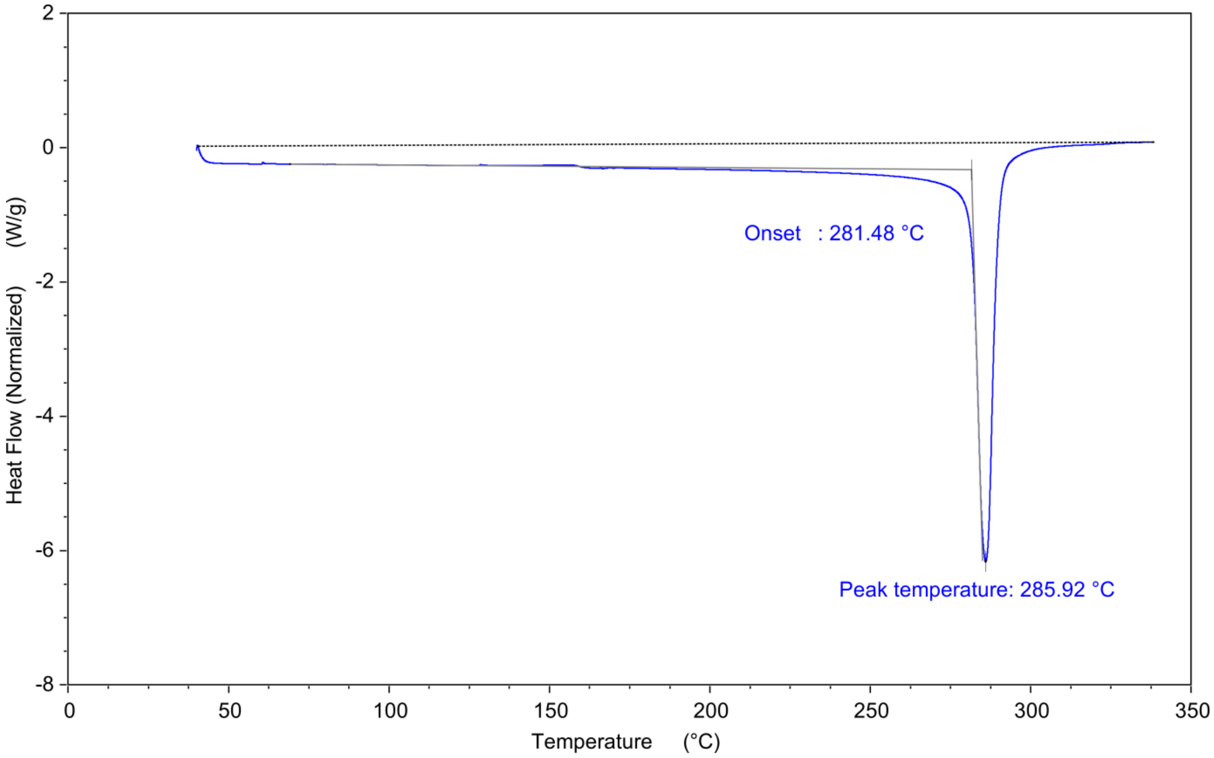

Fig. S14 DSC curve of **1C** showing the boiling with an onset temperature of 281.5 °C.

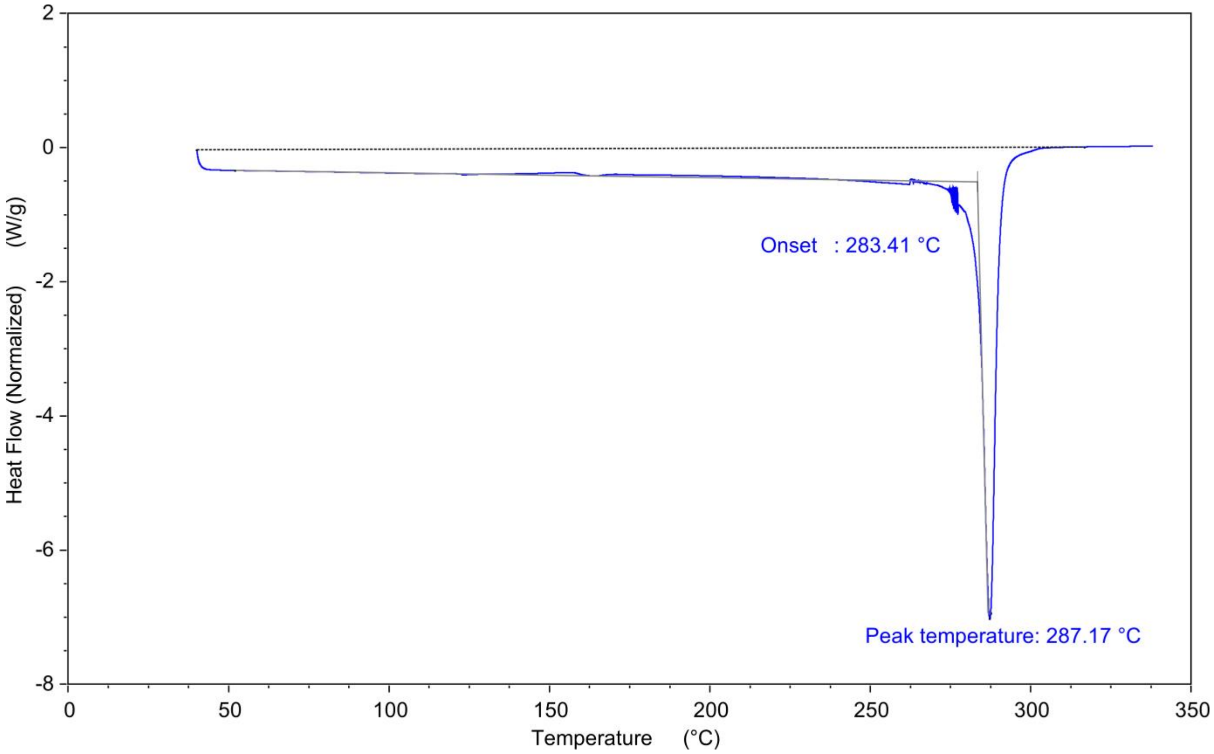

Fig. S15 DSC curve of **9** showing the boiling with an onset temperature of 283.4 °C.

9. Screening of residual peaks in different NMR solvents

1 µL of **1C** was dissolved in either 0.6 mL (CD_3OD, DMSO-*d*$_6$) or 0.75 mL ($CDCl_3$, CD_3CN, Acetone-*d*$_6$, D_2O, THF-*d*$_8$, benzene-*d*$_6$, toluene-*d*$_6$, TFA) of NMR solvent. The spectra were recorded on a Bruker Avance III 400 MHz instrument using 128 and 1024 scans for ^1H and ^{13}C spectra, respectively. The solvent peaks of the NMR solvents were used as chemical shift references. Spectra were processed using the MestRe Nova software. The spectra are summarized in Fig. S16–17.

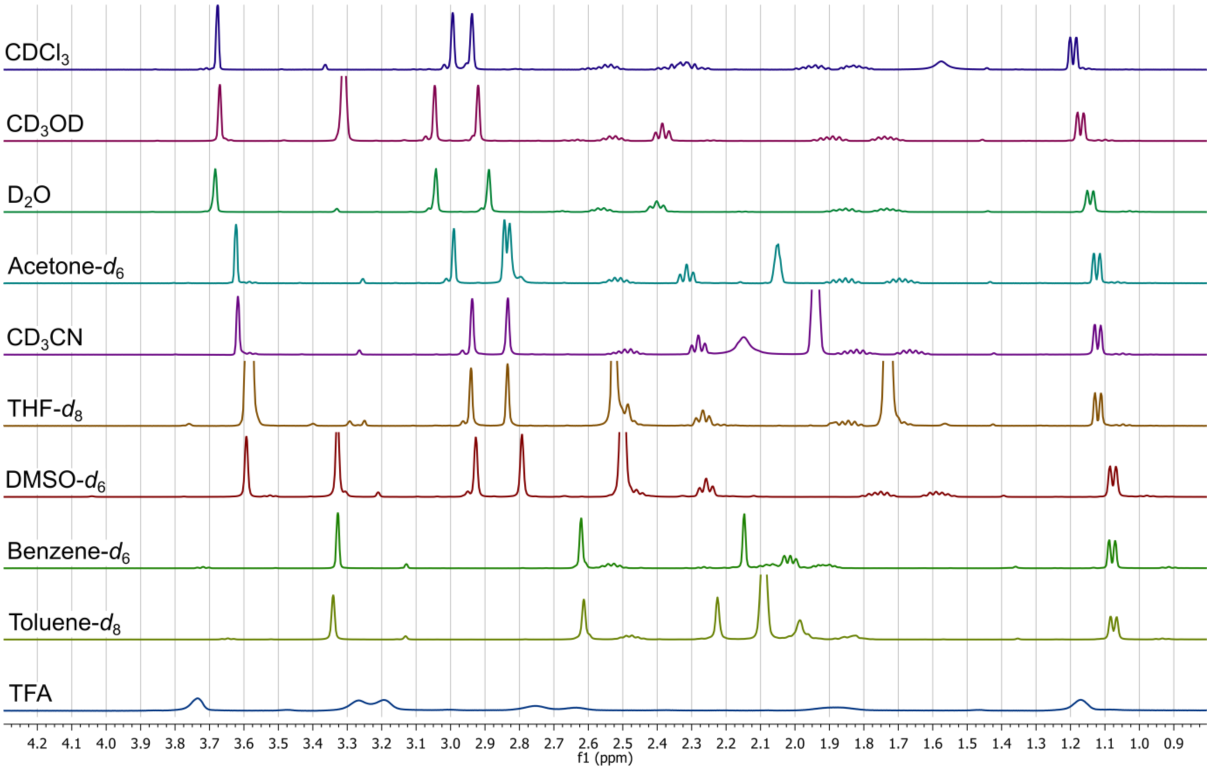

Fig. S16 Stacked ^1H NMR (400 MHz) spectra of **1C** in common NMR solvents.

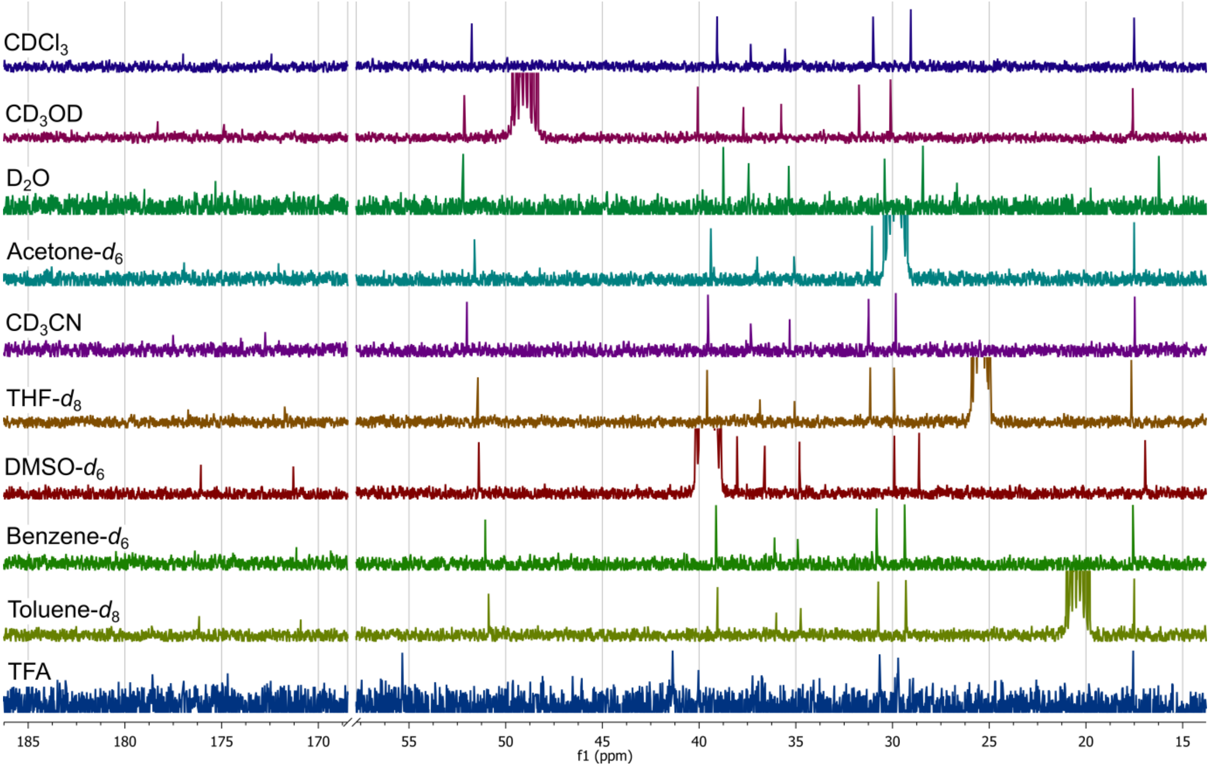

Fig. S17 Stacked ^{13}C NMR (400MHz) spectra of **1C** in common NMR solvents.

10. NMR spectroscopy

Individual NMR spectra were recorded either on a Bruker Avance III 400 MHz instrument or a B500 Bruker Avance II+ 500 MHz instrument as specified for each spectrum using 128 and 1024 scans for ^{1}H and ^{13}C spectra, respectively. Spectra were processed using the MestRe Nova software.

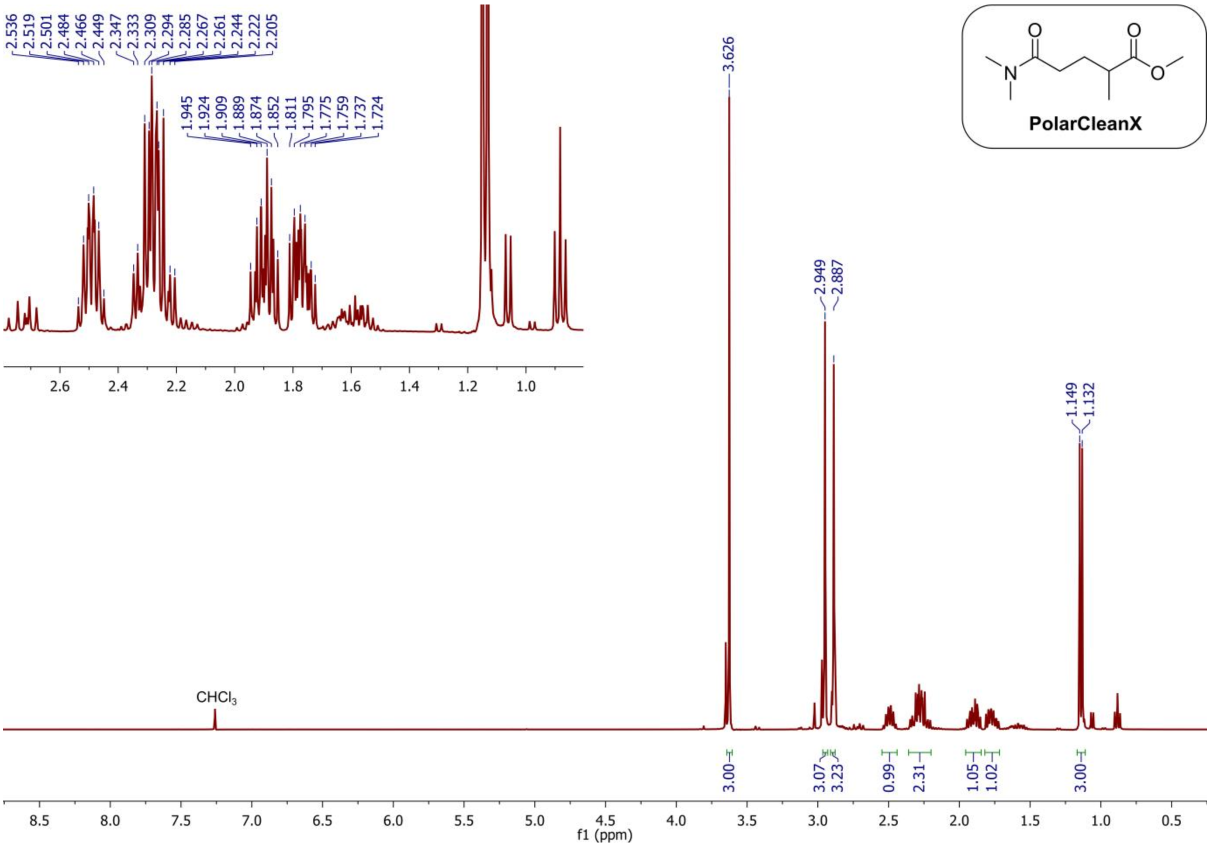

Fig. S18 ^{1}H NMR spectrum (400 MHz) of PolarCleanX with the structure of the main component in insert.

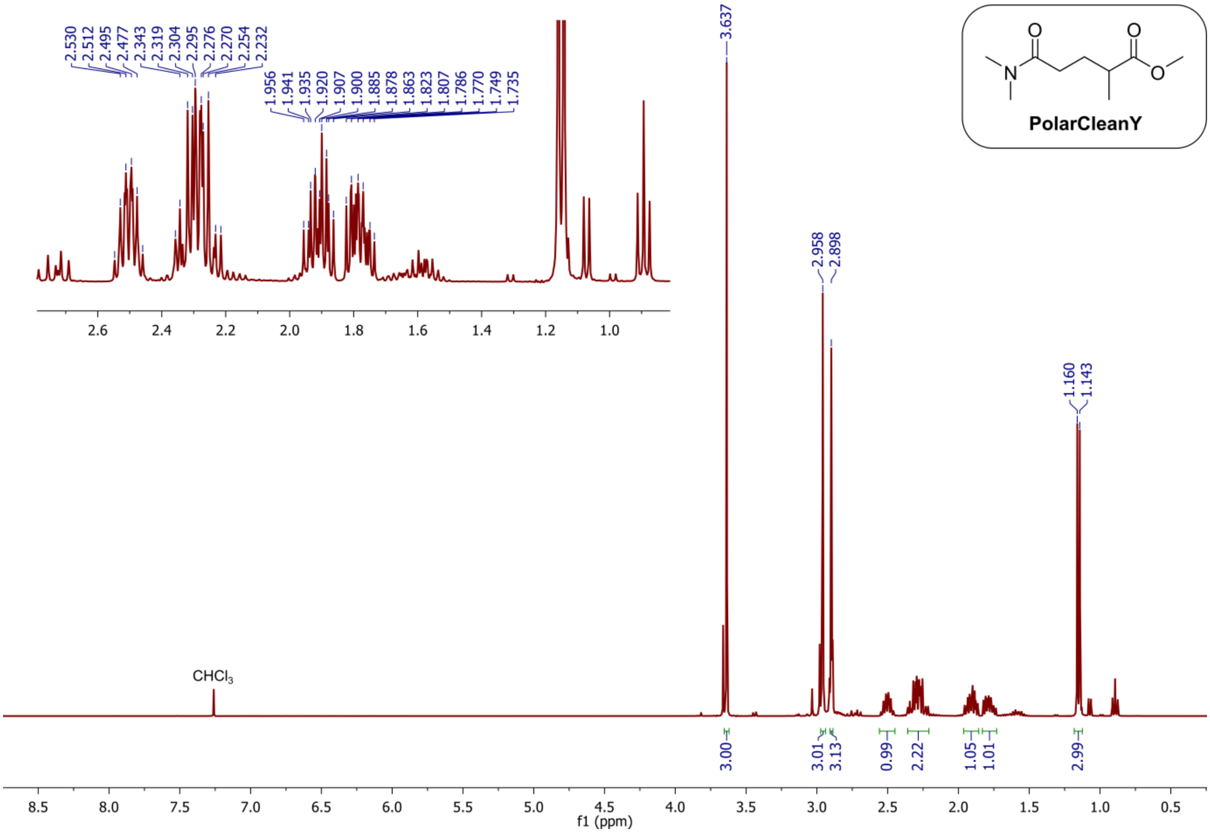

Fig. S19 ^{1}H NMR spectrum (400 MHz) of PolarCleanY with the structure of the main component in insert.

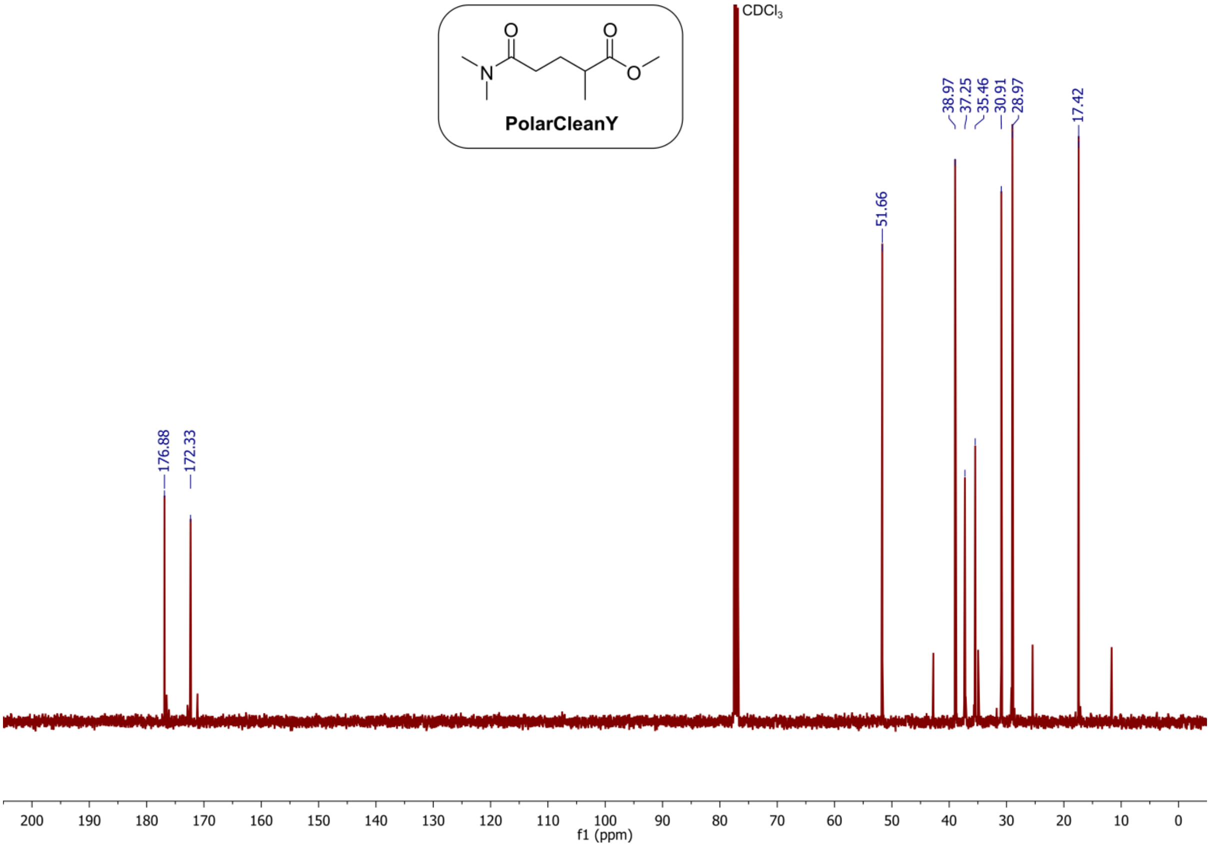

Fig. S20 ^{13}C NMR spectrum (101 MHz) of PolarCleanY with the structure of the main component in insert.

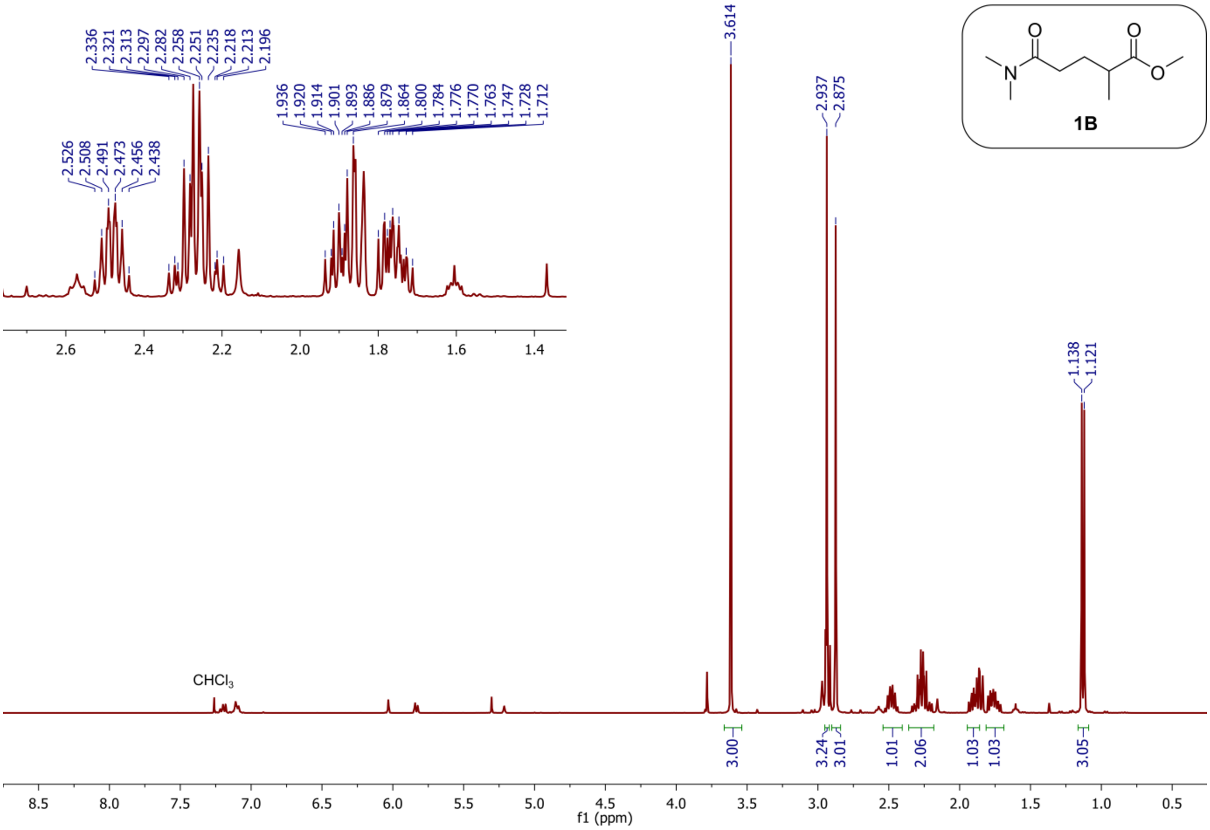

Fig. S21 ^{1}H NMR spectrum (400 MHz) of **1B** with the structure of the main component in insert.

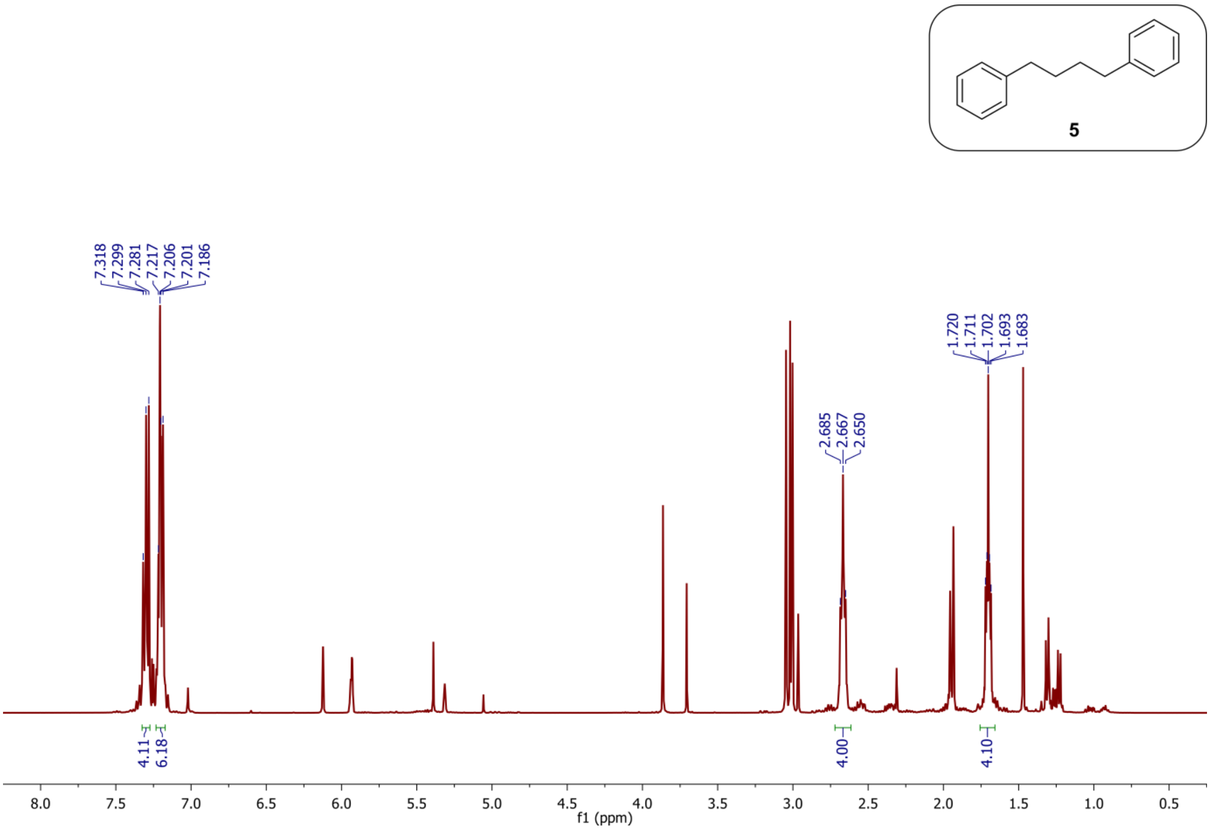

Fig. S22 ^{1}H NMR (400 MHz) spectrum of the impurities of **1B** obtained by extraction with *n*-hexane with the structure of the main impurity (**5**) in insert.

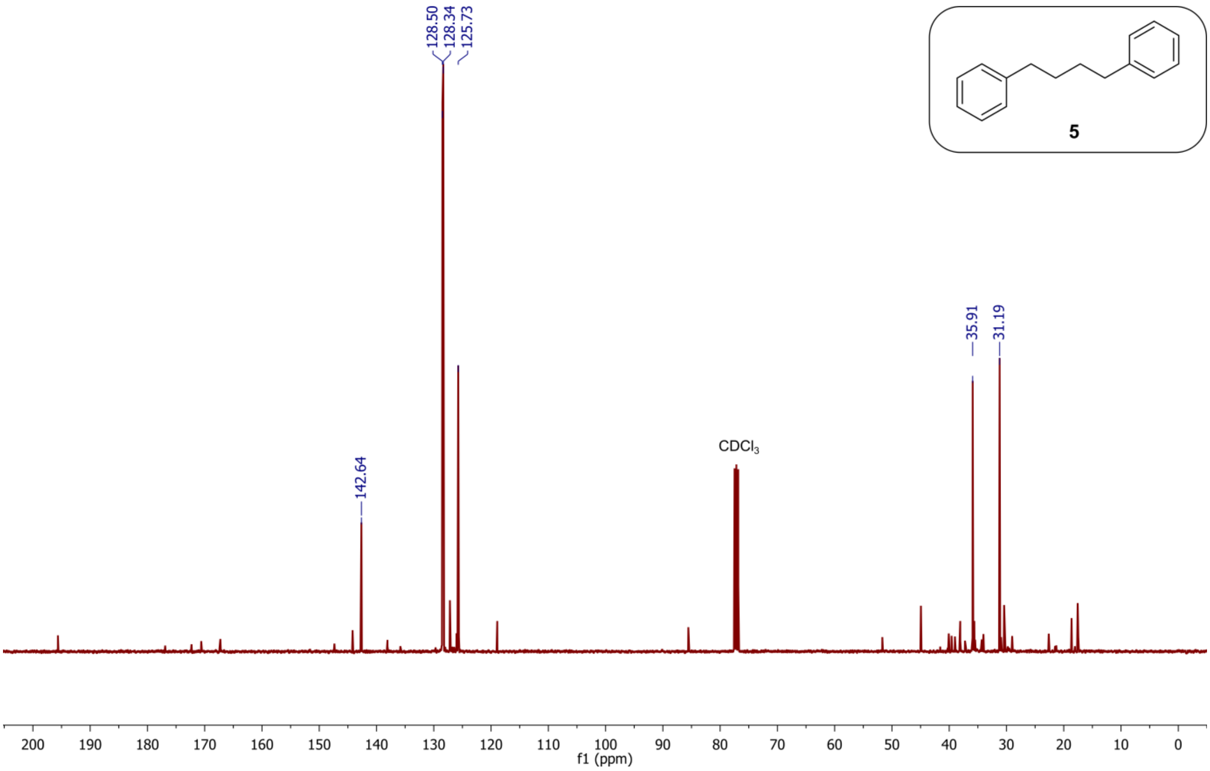

Fig. S23 ^{13}C NMR (101 MHz) spectrum of the impurities of **1B** obtained by extraction with *n*-hexane with the structure of the main impurity (**5**) in insert.

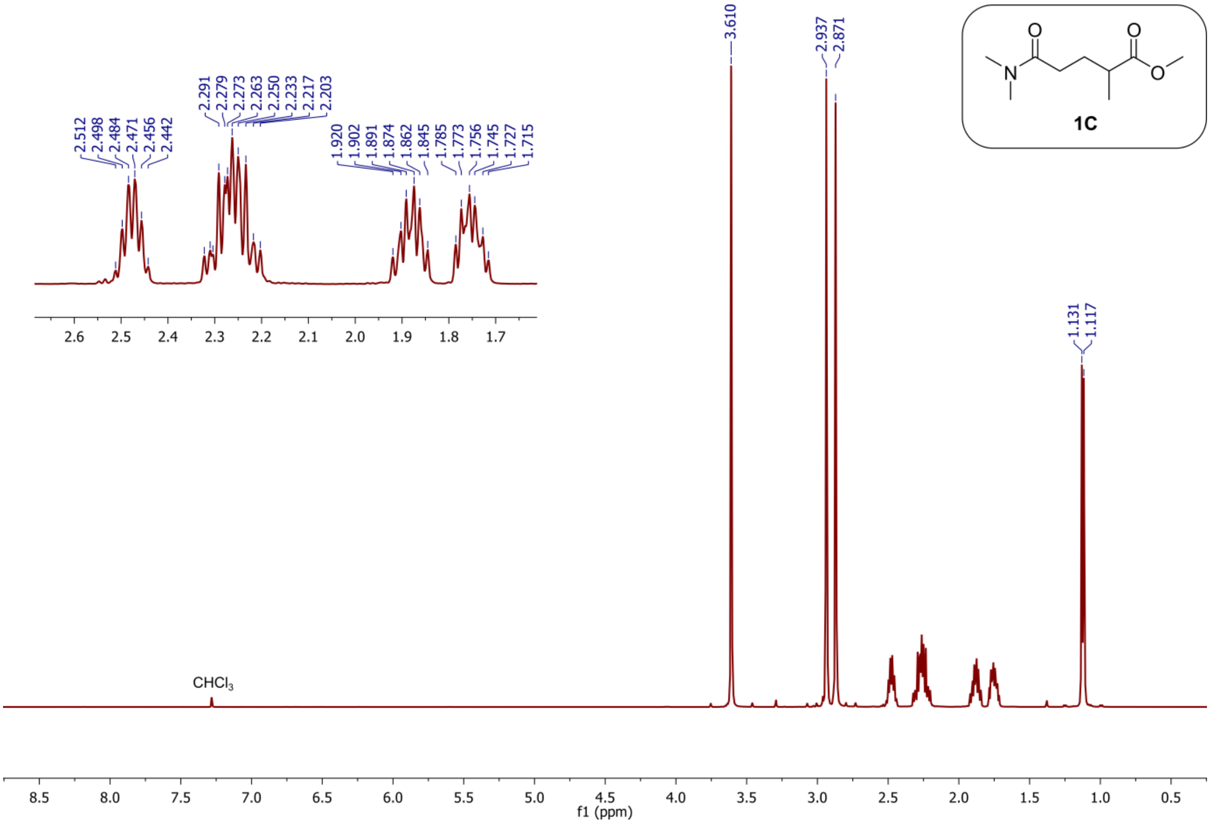

Fig. S24 ^{1}H NMR (500 MHz) spectrum of **1C** with the structure in insert.

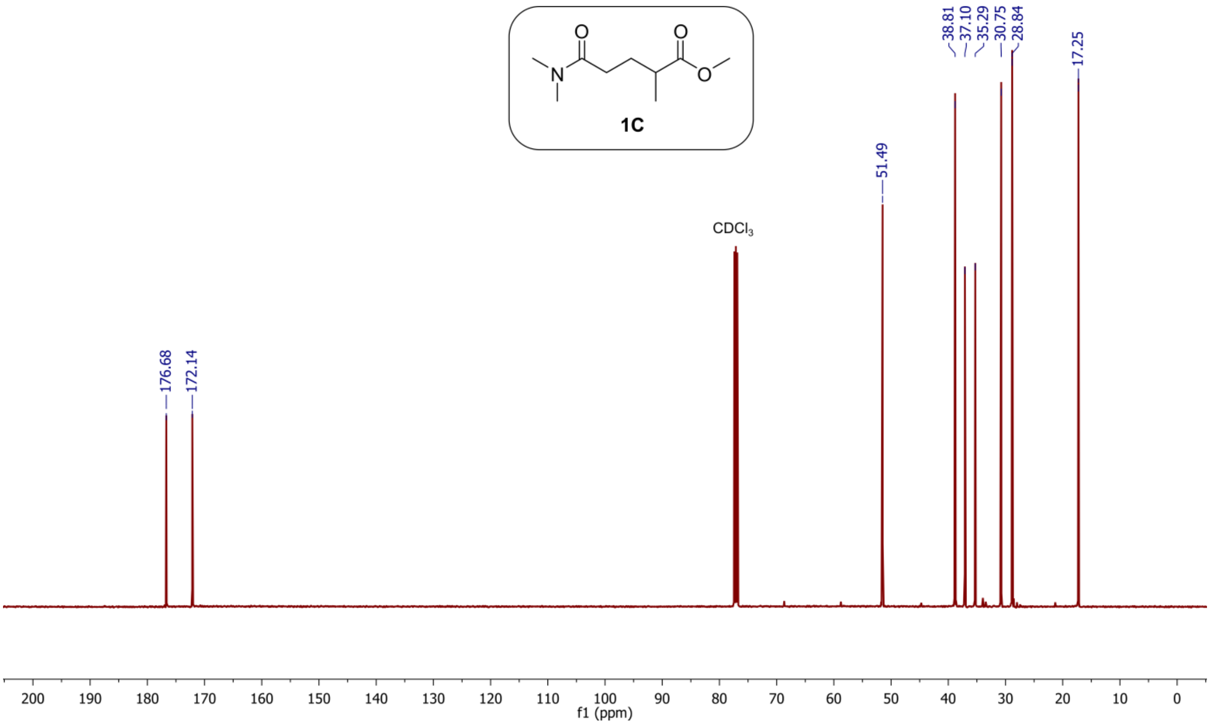

Fig. S25 ^{13}C NMR (126 MHz) spectrum of **1C** with the structure in insert.

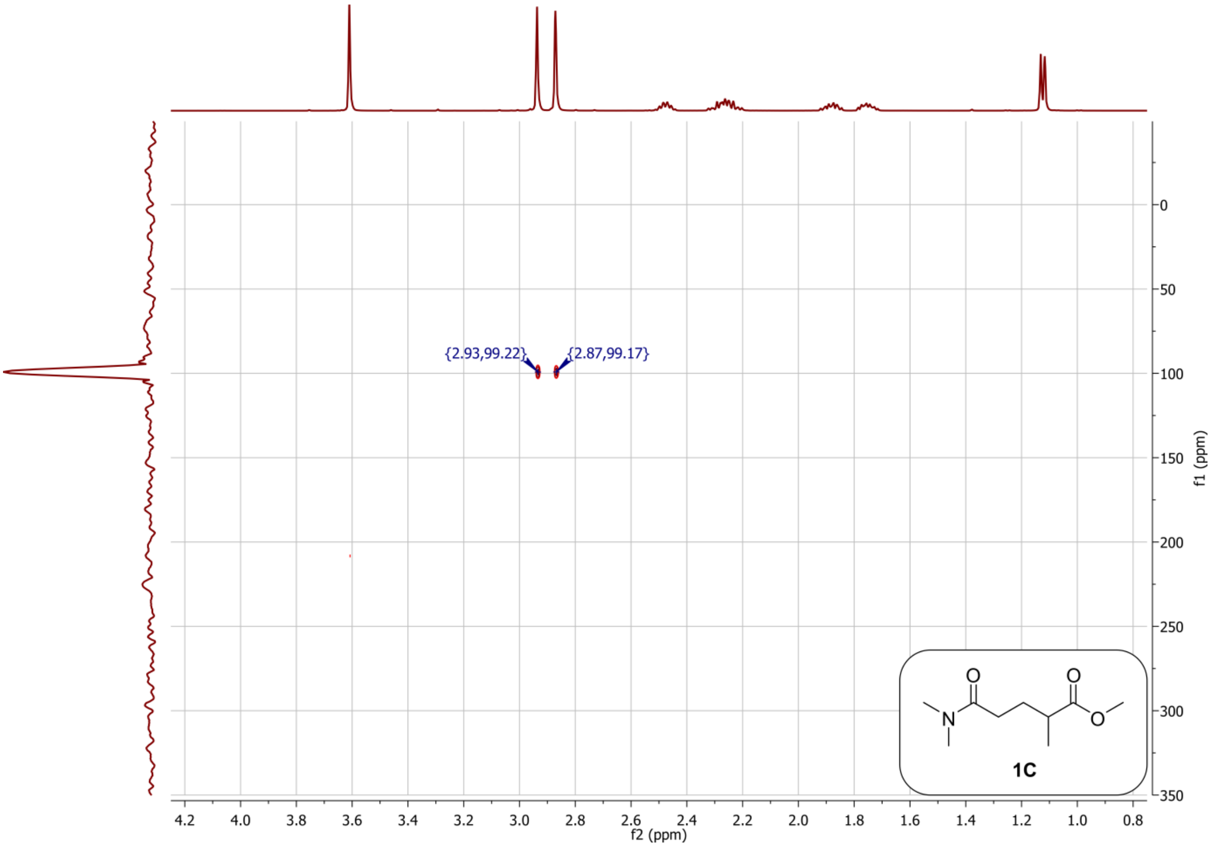

Fig. S26 ^{1}H–^{15}N HMBC (400 MHz) spectrum of **1C** with the structure in insert.

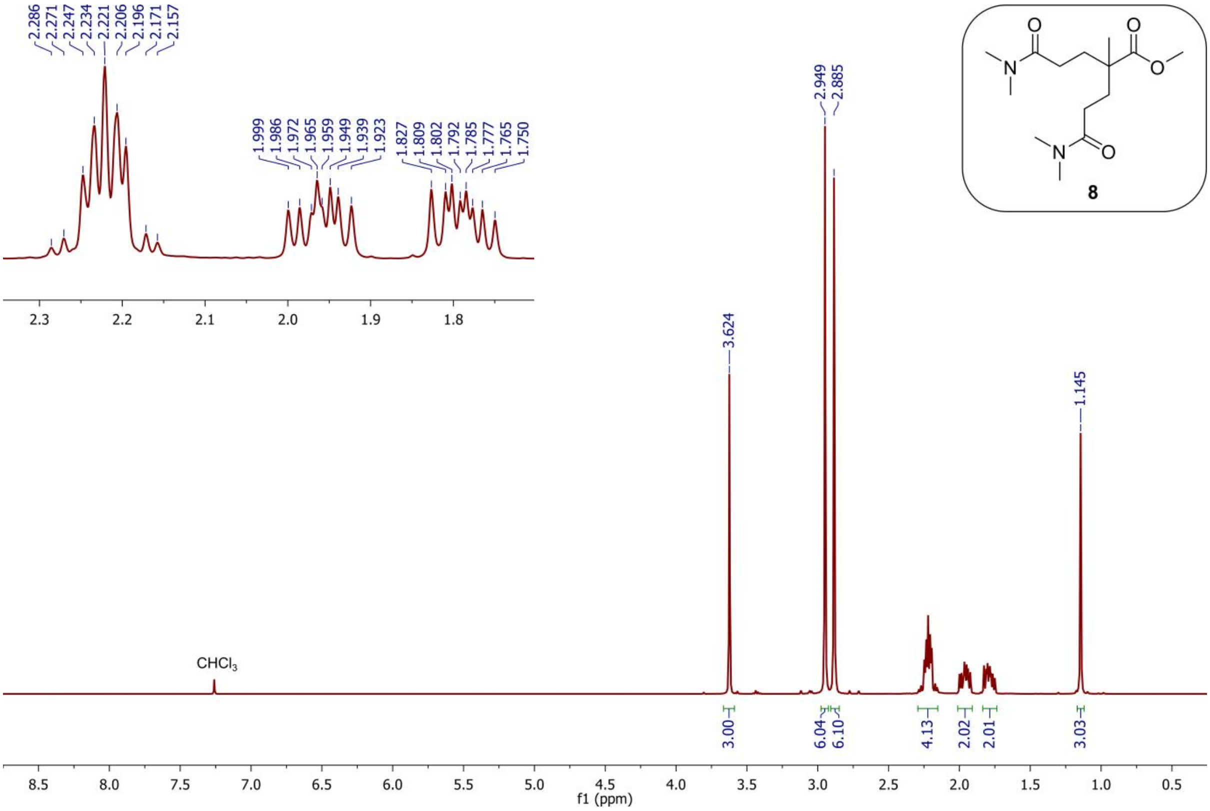

Fig. S27 ^{1}H NMR (400 MHz) spectrum of **8** with the structure in insert.

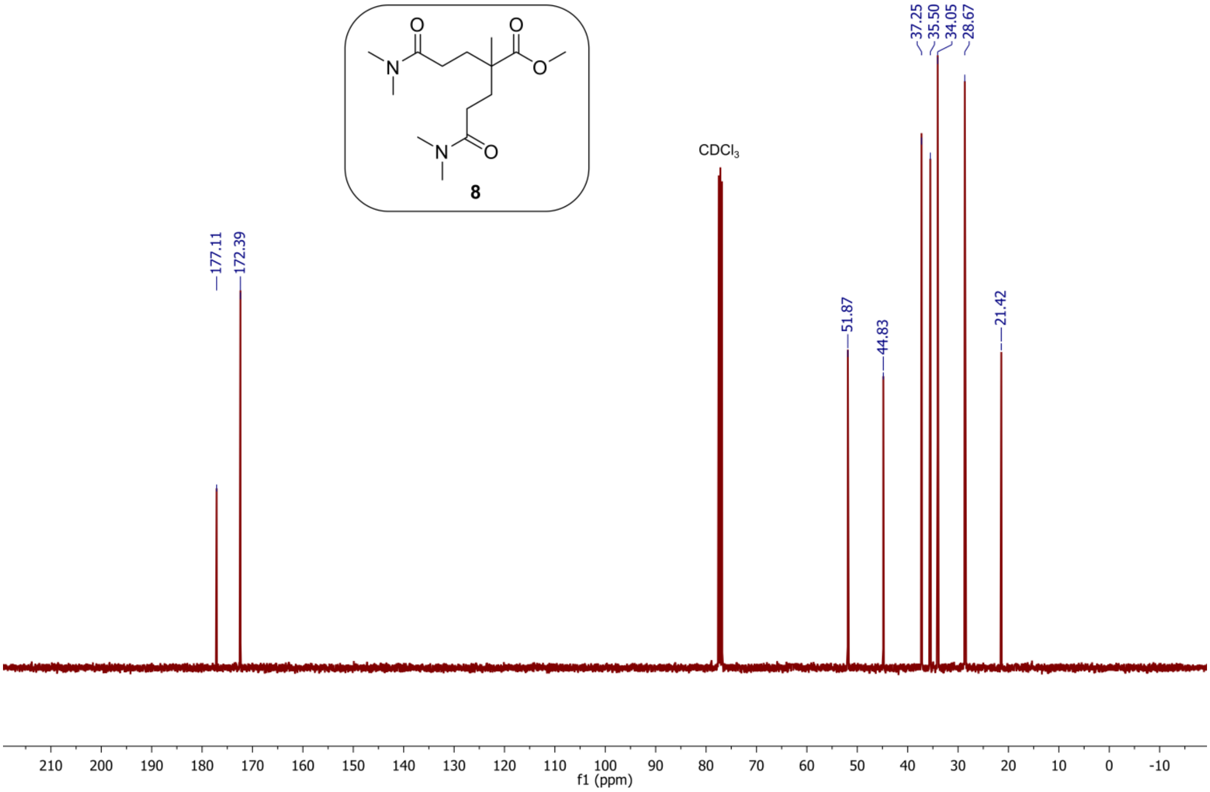

Fig. S28 ^{13}C NMR (101 MHz) spectrum of **8** with the structure in insert.

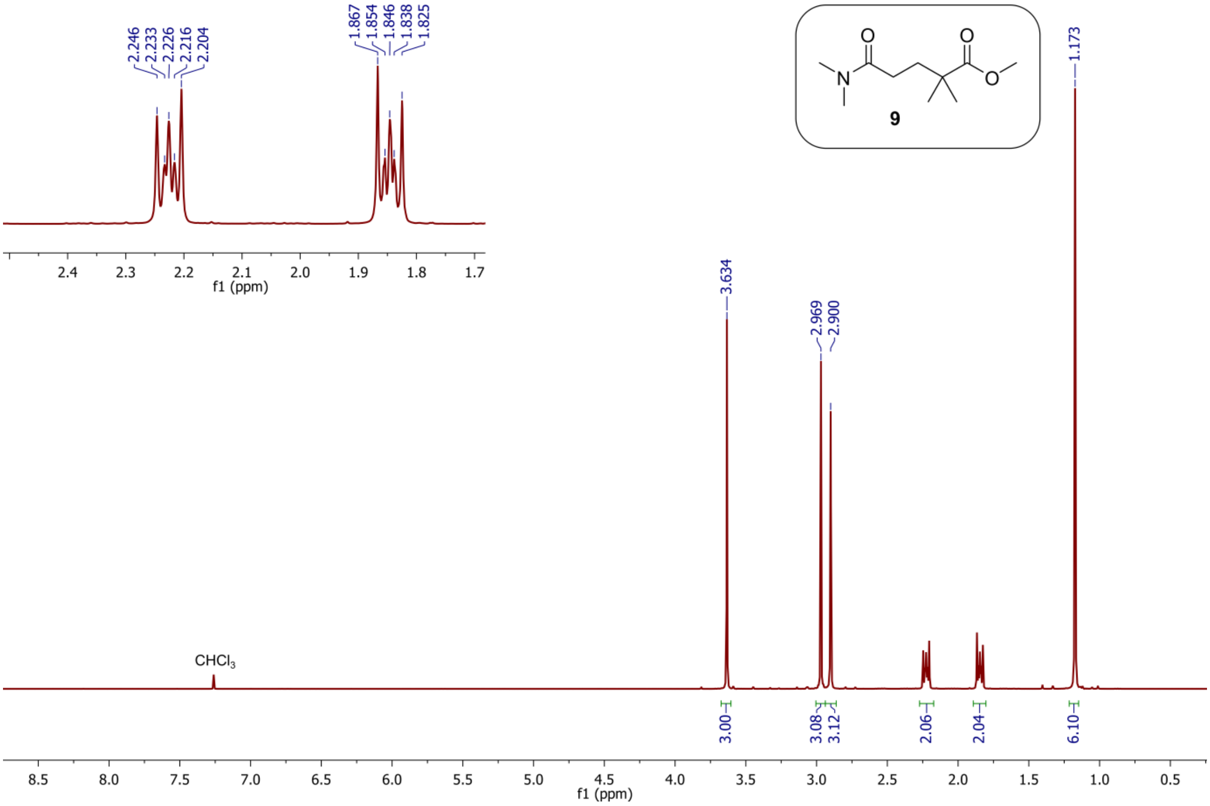

Fig. S29 ^{1}H NMR (400 MHz) spectrum of **9** with the structure in insert.

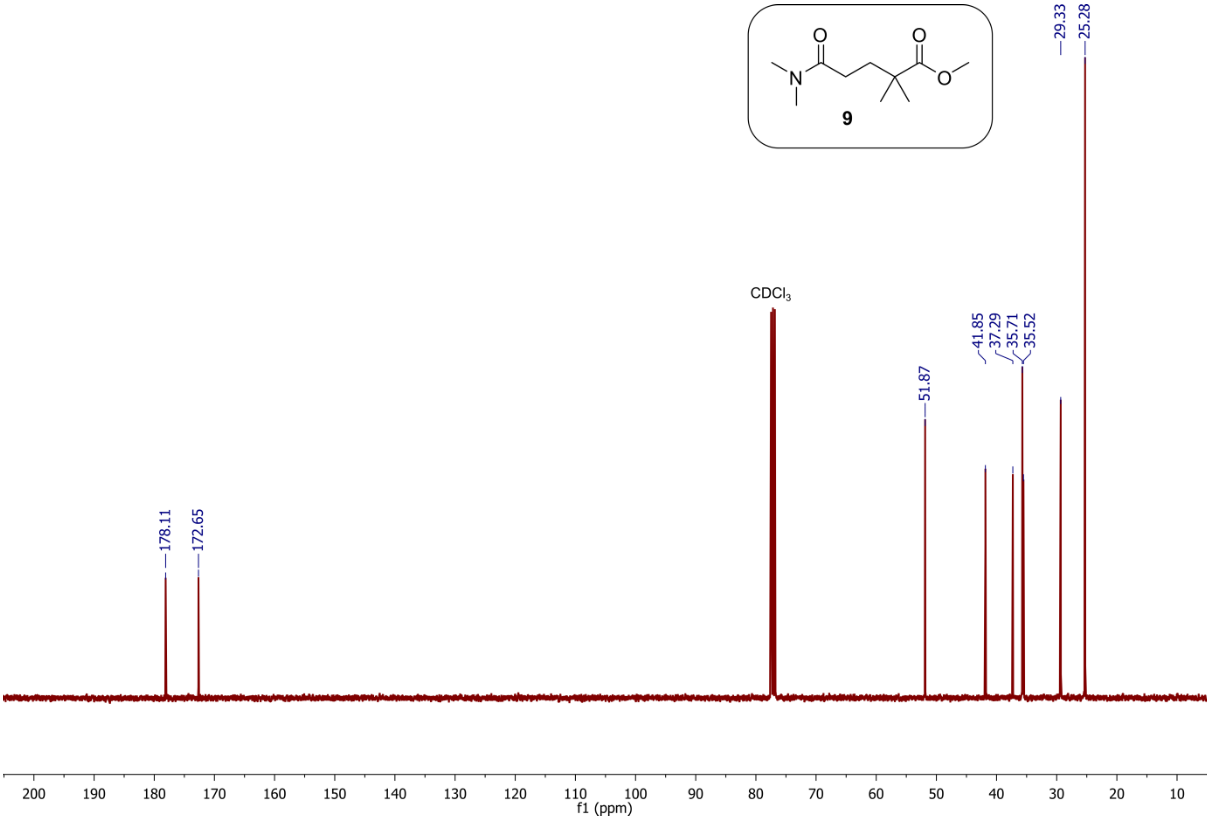

Fig. S30 ^{13}C NMR (101 MHz) spectrum of **9** with the structure in insert.

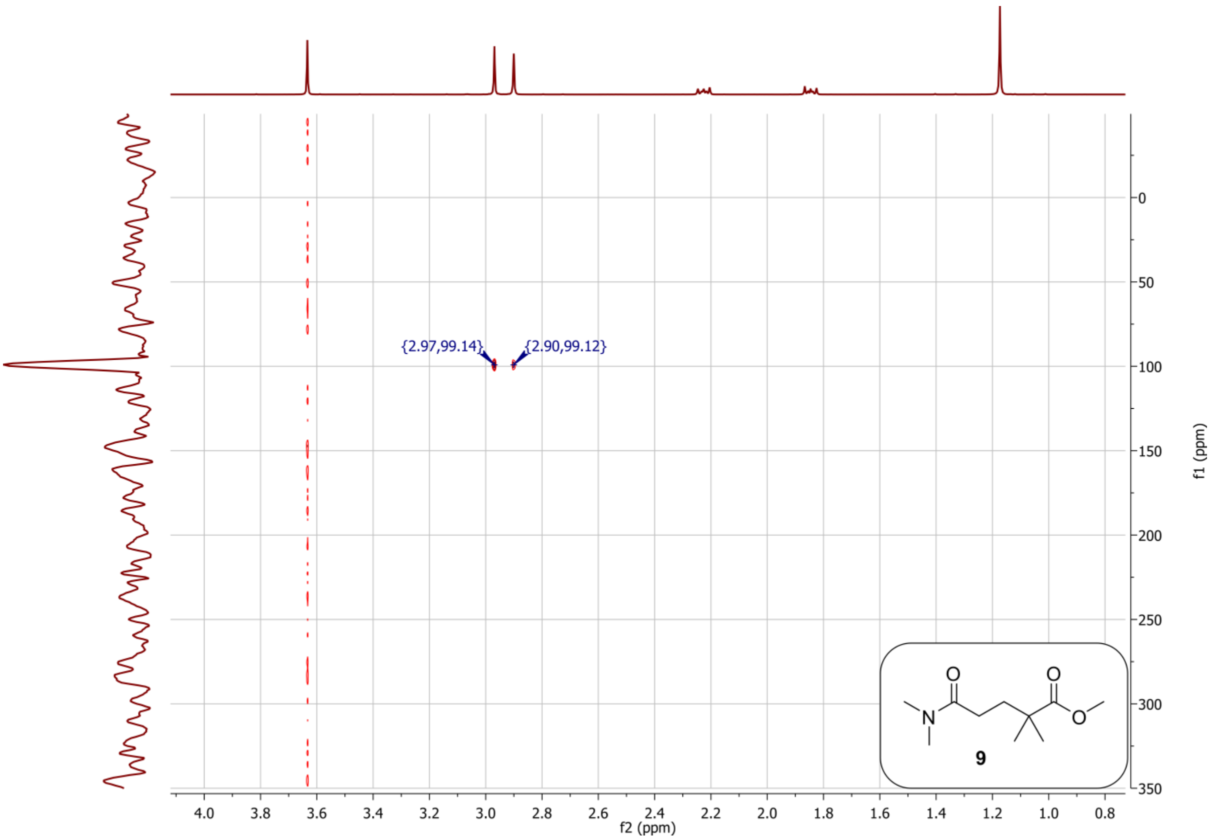

Fig. S31 ^{1}H–^{15}N HMBC (400 MHz) spectrum of **1C** with the structure in insert.

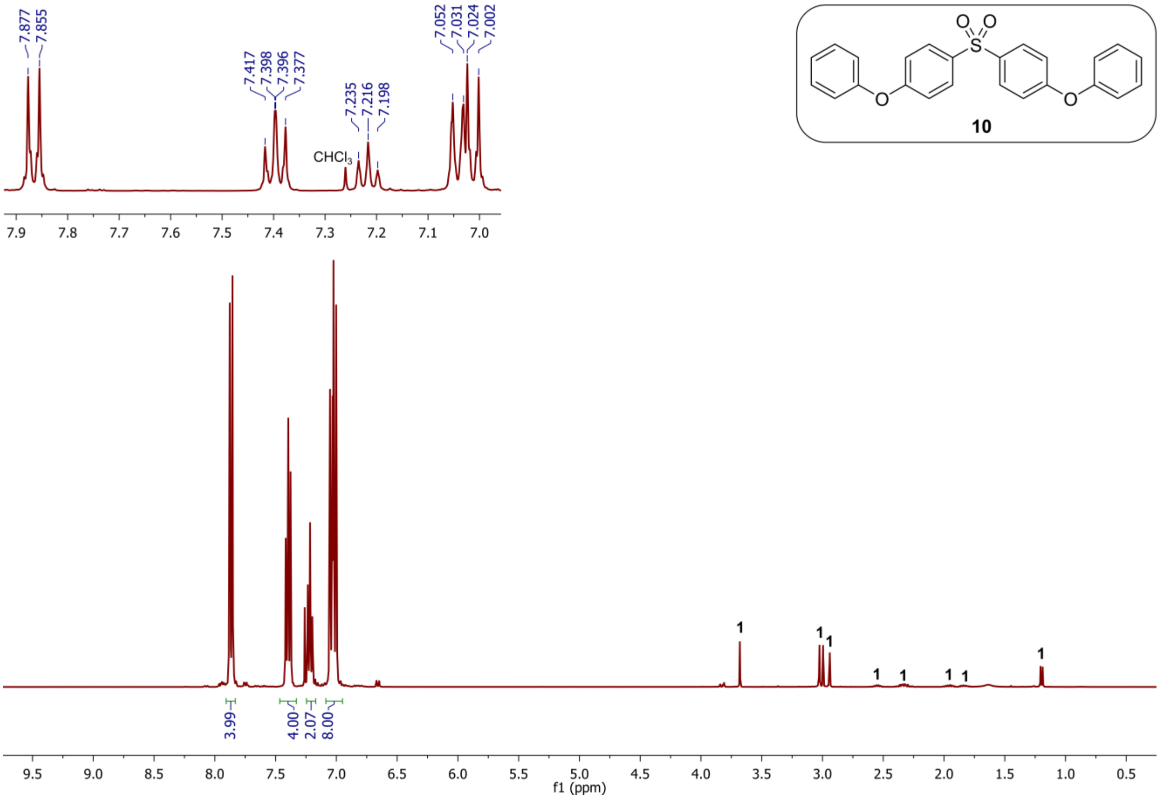

Fig. S32 ^{1}H NMR (400 MHz) spectrum of **10** with the structure in insert. The spectrum shows some residual peaks originating from the solvent used as reaction media. The sample was produced in the test reaction described in Table 6 Entry 1. The spectrum is consistent with the literature.[22]

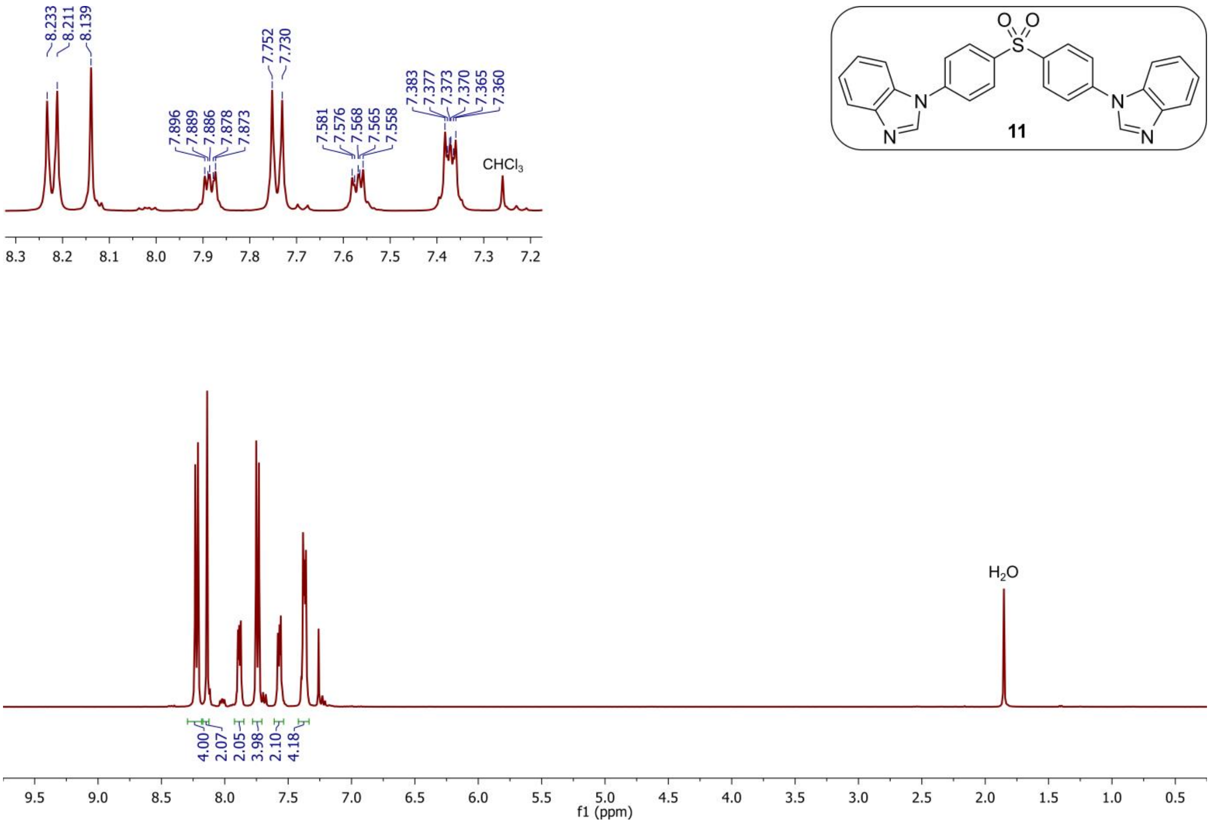

Fig. S33 ^{1}H NMR (400 MHz) spectrum of **11** with the structure in insert. The sample was produced in the test reaction described in Table 7 Entry 3. The spectrum is consistent with the literature.[5]

11. Gas chromatography

For GC-MS analysis, the 6890GC/5973MS (Agilent) instrument was used. A sample of 1 µl was injected into the GC column HP-5ms 30 m × 0.25 mm, with helium gas flux of 1 ml min^{-1}, injection split 20:1 at 300 °C. Heating was from 50 °C (3 min) with a heating rate of 25 °C min^{-1} up to 300 °C (5 min). MS analysis parameters were EI 70 eV, ionization scan 50–650 g mol^{-1}, scan time of 3–18 min and temperatures of ion source and transfer line were 230 °C and 320 °C, respectively.

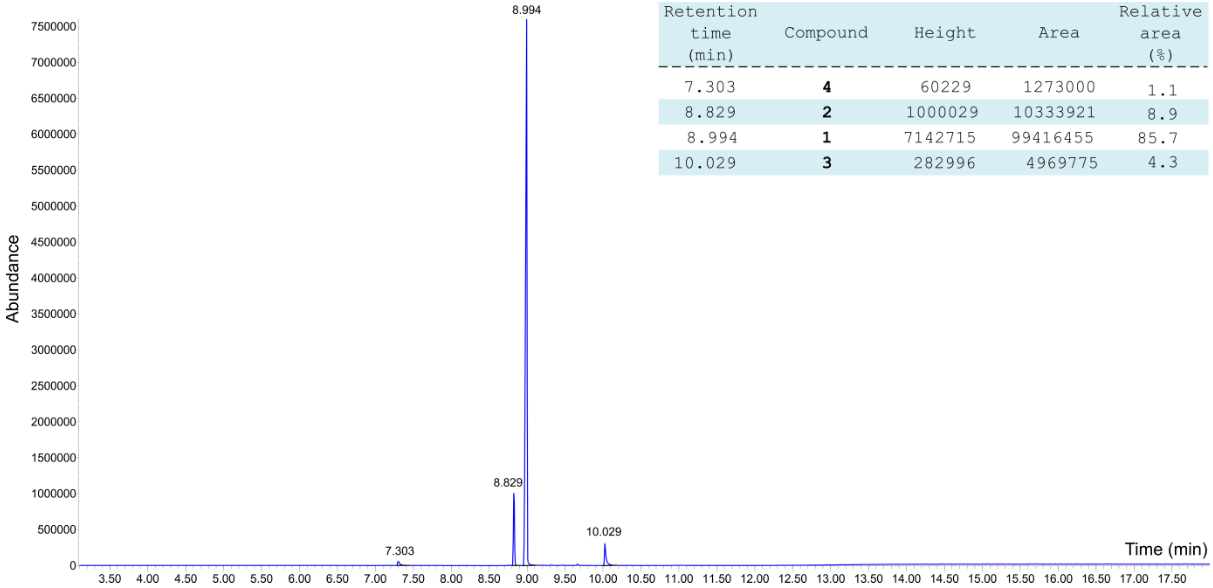

Retention time (min)	Compound	Height	Area	Relative area (%)
7.303	**4**	60229	1273000	1.1
8.829	**2**	1000029	10333921	8.9
8.994	**1**	7142715	99416455	85.7
10.029	**3**	282996	4969775	4.3

Fig. S34 GC-MS chromatogram of PolarCleanX with a table of components in insert. MS spectra corresponding to the individual compounds can be found in section 12.

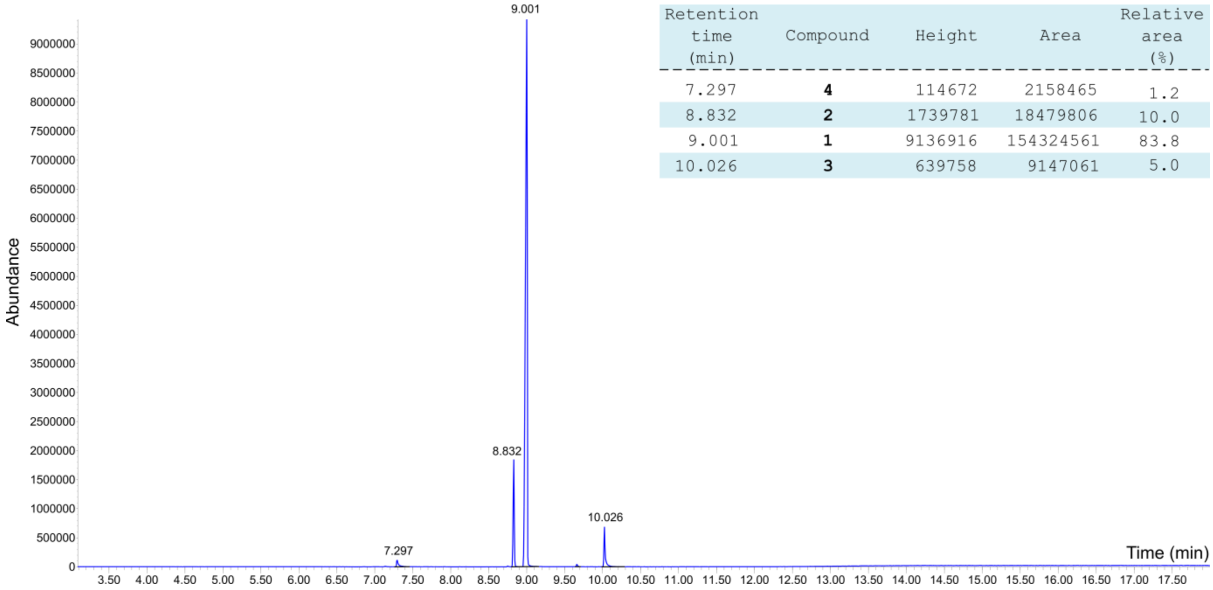

Retention time (min)	Compound	Height	Area	Relative area (%)
7.297	**4**	114672	2158465	1.2
8.832	**2**	1739781	18479806	10.0
9.001	**1**	9136916	154324561	83.8
10.026	**3**	639758	9147061	5.0

Fig. S35 GC-MS chromatogram of PolarCleanY with a table of components in insert. MS spectra corresponding to the individual compounds can be found in section 12.

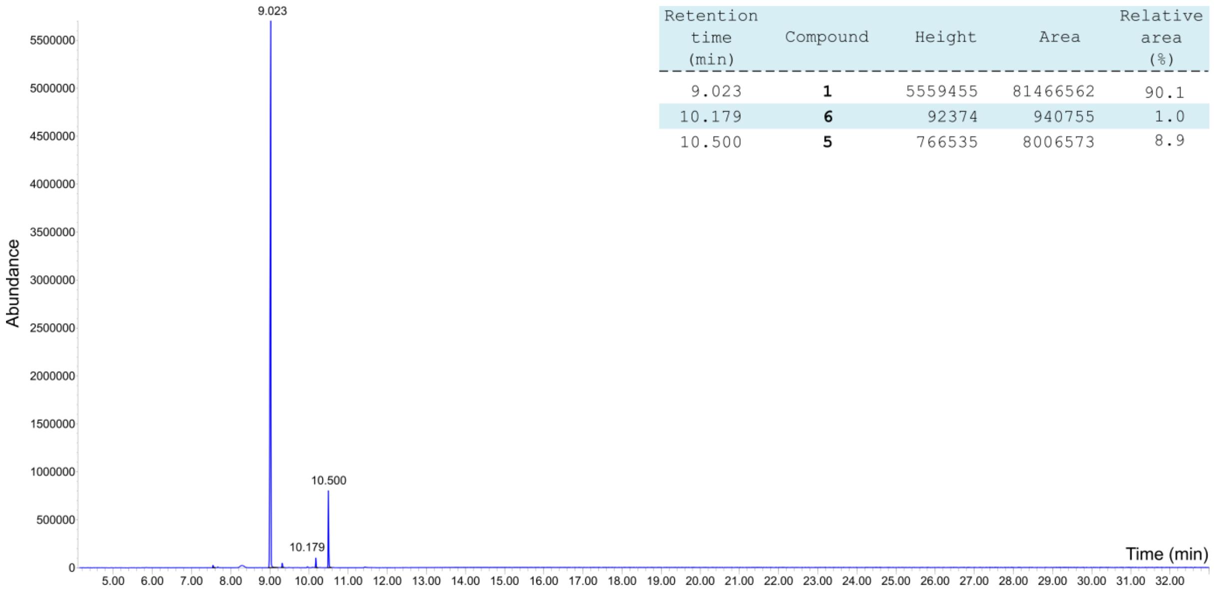

Retention time (min)	Compound	Height	Area	Relative area (%)
9.023	**1**	5559455	81466562	90.1
10.179	**6**	92374	940755	1.0
10.500	**5**	766535	8006573	8.9

Fig. S36 GC-MS chromatogram of **1B** with a table of components in insert. MS spectra corresponding to the individual compounds can be found in section 12.

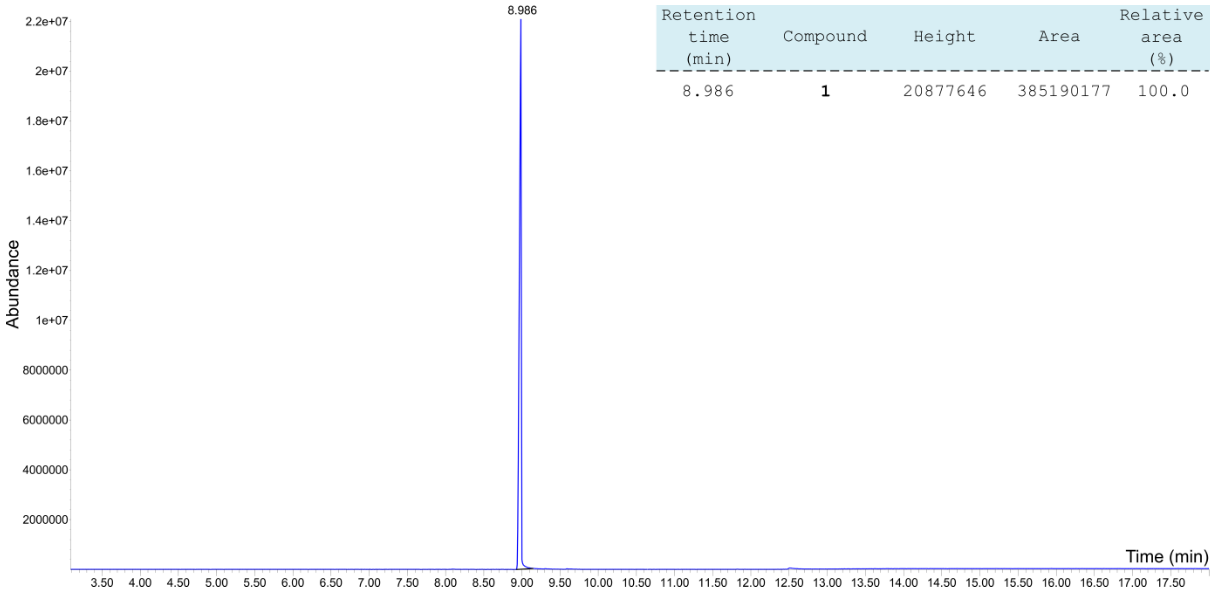

Retention time (min)	Compound	Height	Area	Relative area (%)
8.986	**1**	20877646	385190177	100.0

Fig. S37 GC-MS chromatogram of **1C** with a table of components in insert. MS spectrum corresponding to the individual compound can be found in section 12.

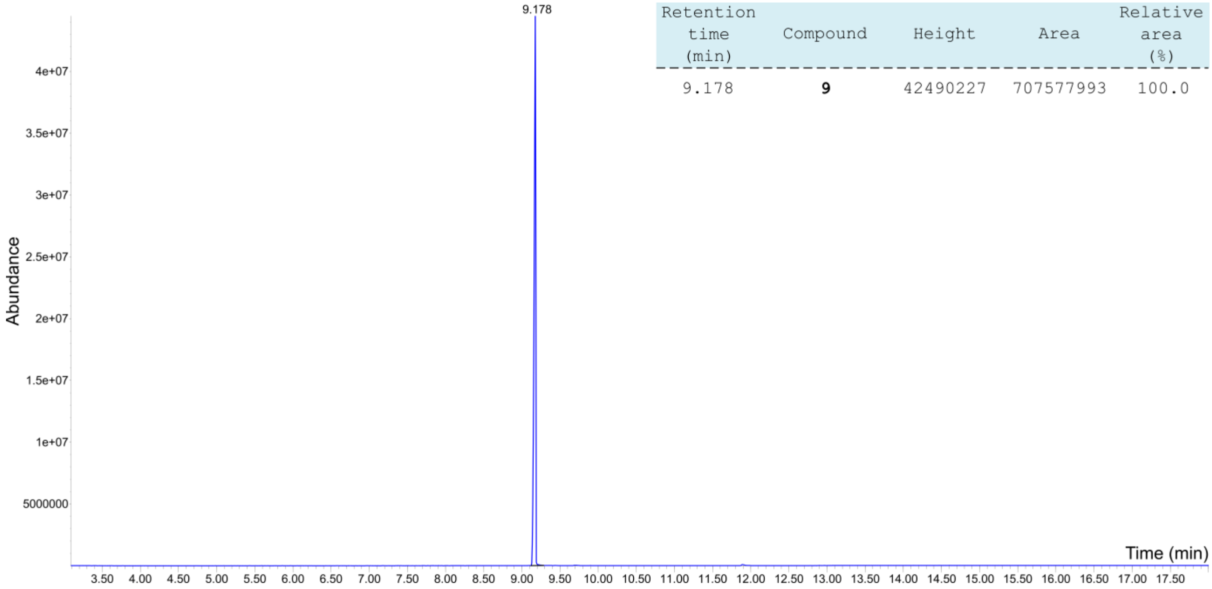

Retention time (min)	Compound	Height	Area	Relative area (%)
9.178	**9**	42490227	707577993	100.0

Fig. S38 GC-MS chromatogram of **9** with a table of components in insert. MS spectrum corresponding to the individual compound can be found in section 12.

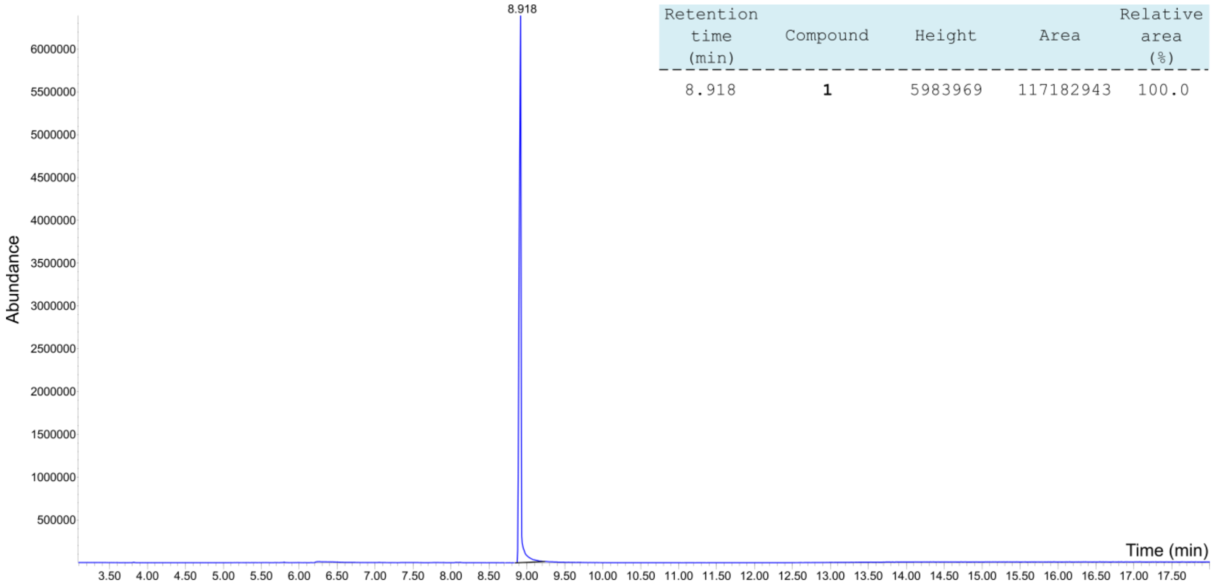

Retention time (min)	Compound	Height	Area	Relative area (%)
8.918	**1**	5983969	117182943	100.0

Fig. S39 GC-MS chromatogram of **1C** recovered after S_NAR reaction by vacuum distillation.

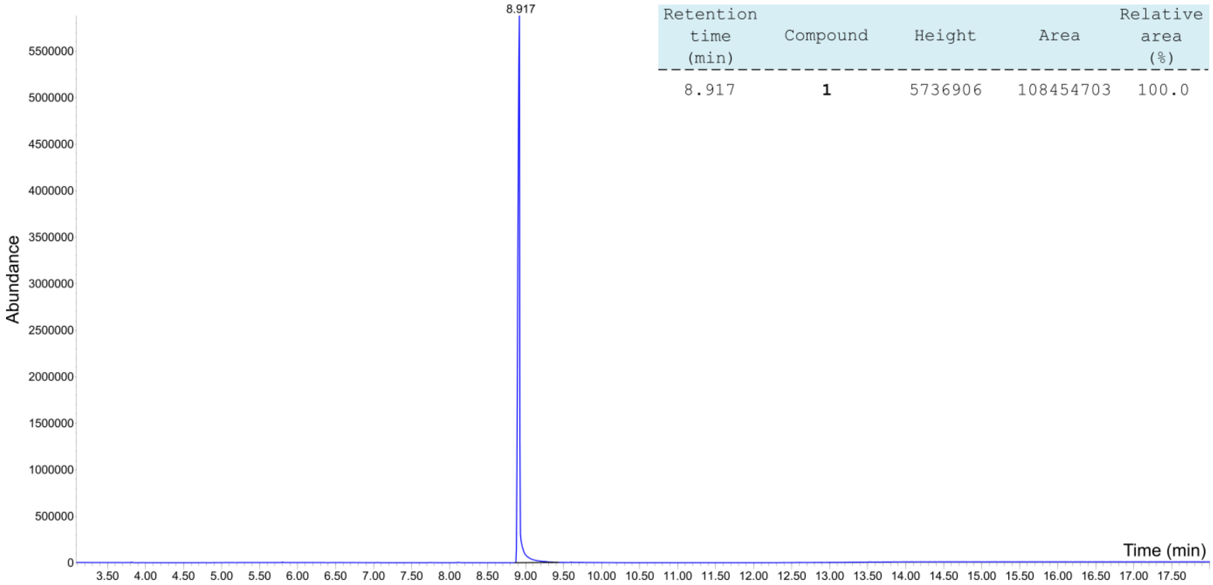

Retention time (min)	Compound	Height	Area	Relative area (%)
8.917	**1**	5736906	108454703	100.0

Fig. S40 GC-MS chromatogram of **1C** recovered after S_NAR reaction by vacuum distillation.

12. Mass spectrometry

The GS-MS methodology is described in section 11. High resolution mass measurements were performed on a Thermo Exactive plus EMR Orbitrap mass spectrometer, used with a Thermo Ultimate 3000 UHPLC using 100% methanol as mobile phase. The electrospray ionisation technique was used in positive mode.

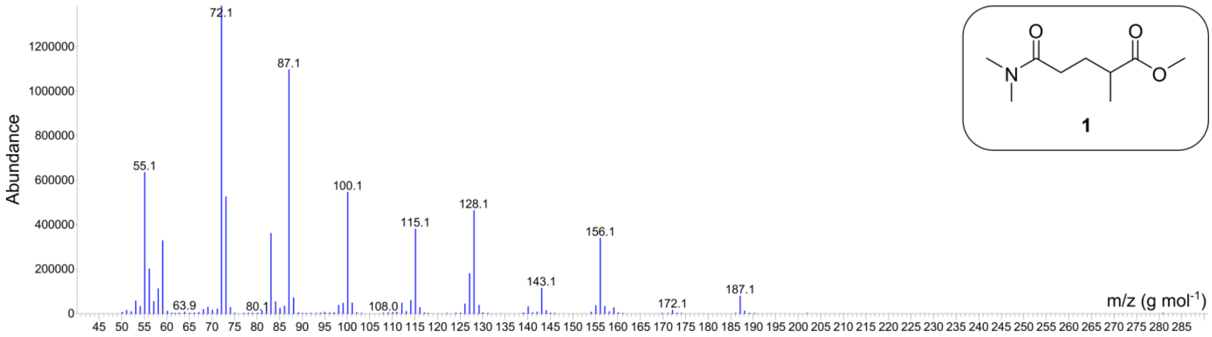

Fig. S41 Mass spectrum of **1** with the structure in insert obtained from the peak with 9.001 min retention time in the GC-MS chromatogram of PolarCleanY. Peaks with retention times between 8.986–9.023 min in the GC-MS chromatograms of PolarCleanX, **1B** and **1C** exhibited identical mass spectra.

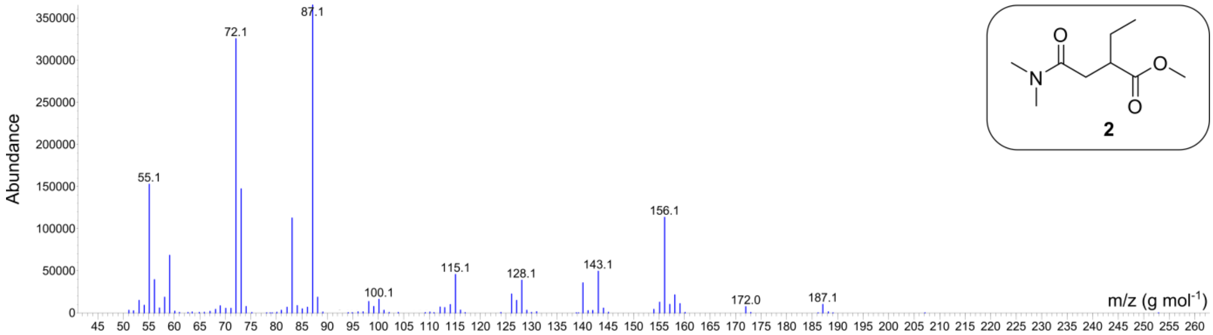

Fig. S42 Mass spectrum of **2** with the structure in insert obtained from the peak with 8.832 min retention time in the GC-MS chromatogram of PolarCleanY. Peak with retention time of 8.829 min in the GC-MS chromatogram of PolarCleanX exhibited identical mass spectrum.

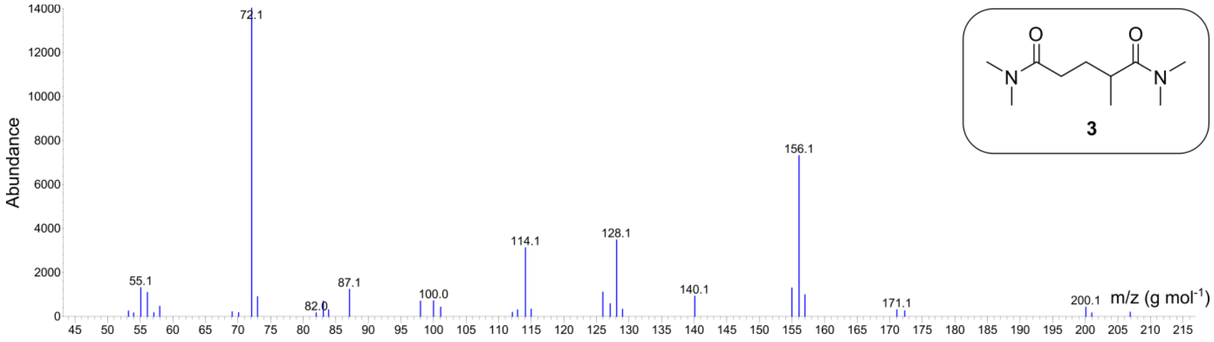

Fig. S43 Mass spectrum of **3** with the structure in insert obtained from the peak with 10.026 min retention time in the GC-MS chromatogram of PolarCleanY. Peak with retention time of 10.029 min in the GC-MS chromatogram of PolarCleanX exhibited identical mass spectrum.

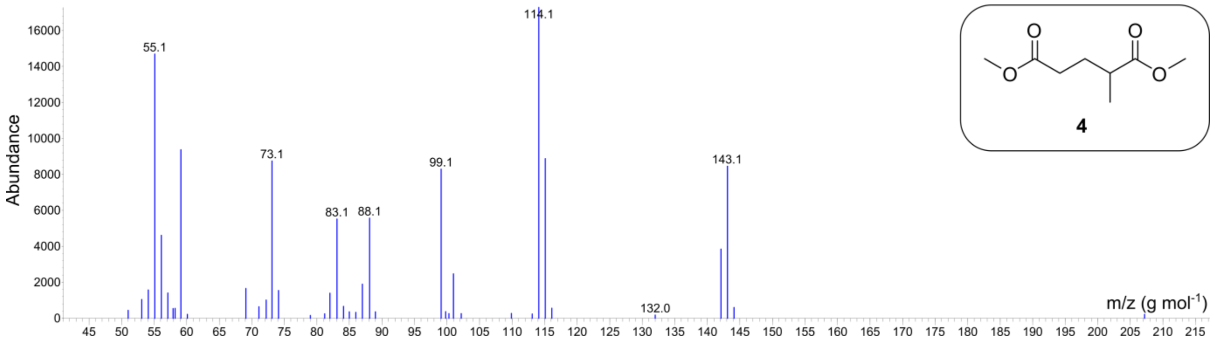

Fig. S44 Mass spectrum of **4** with the structure in insert obtained from the peak with 7.297 min retention time in the GC-MS chromatogram of PolarCleanY. Peak with retention time of 7.303 min in the GC-MS chromatogram of PolarCleanX exhibited identical mass spectrum. Although the molecular ion (174.1 g mol^{-1}) was not observed due to the low concentration, the rest of the mass spectrum showed perfect match with the literature.[23]

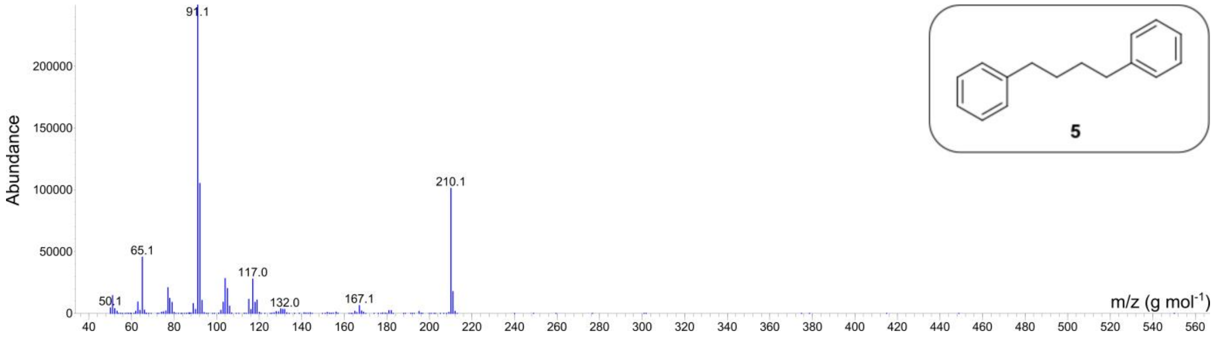

Fig. S45 Mass spectrum of **5** with the structure in insert obtained from the peak with 10.500 min retention time in the GC-MS chromatogram of **1B**.

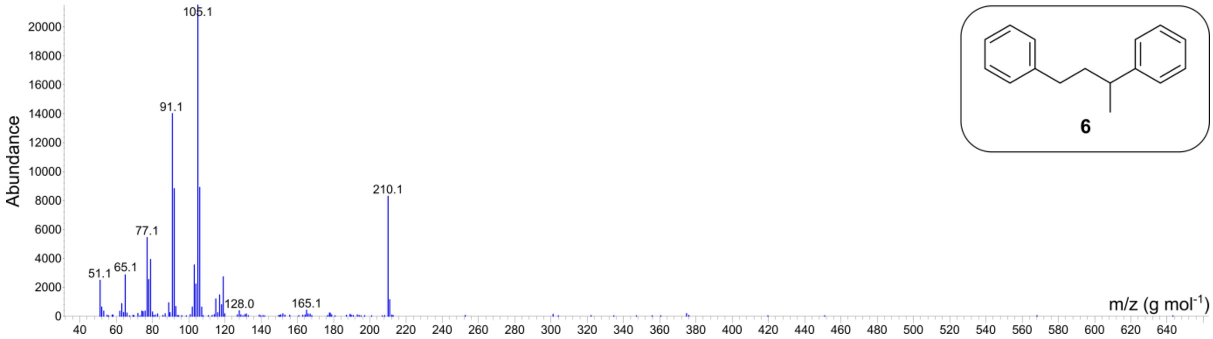

Fig. S46 Mass spectrum of **6** with the structure in insert obtained from the peak with 10.179 min retention time in the GC-MS chromatogram of **1B**.

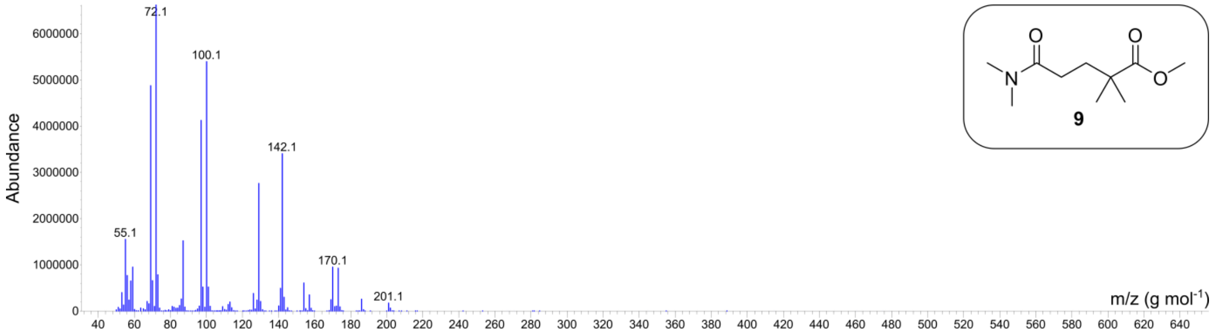

Fig. S47 Mass spectrum of **9** with the structure in insert obtained from the peak with 9.178 min retention time in the GC-MS chromatogram.

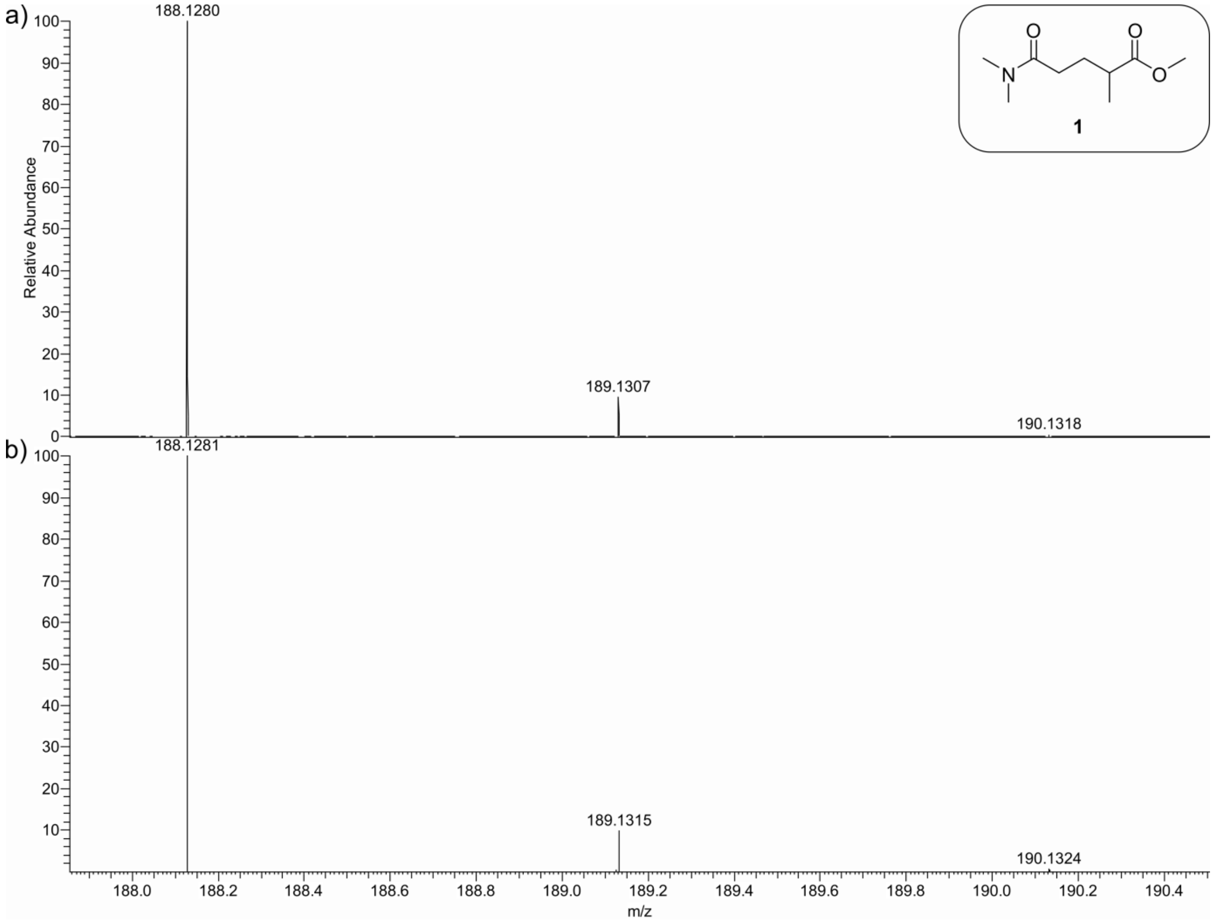

Fig. S48 (a) Observed ESI+ high resolution mass spectrum of **1C** and (b) calculated isotopic distribution of the $[M+H]^+$ ion with the structure of **1** in insert.

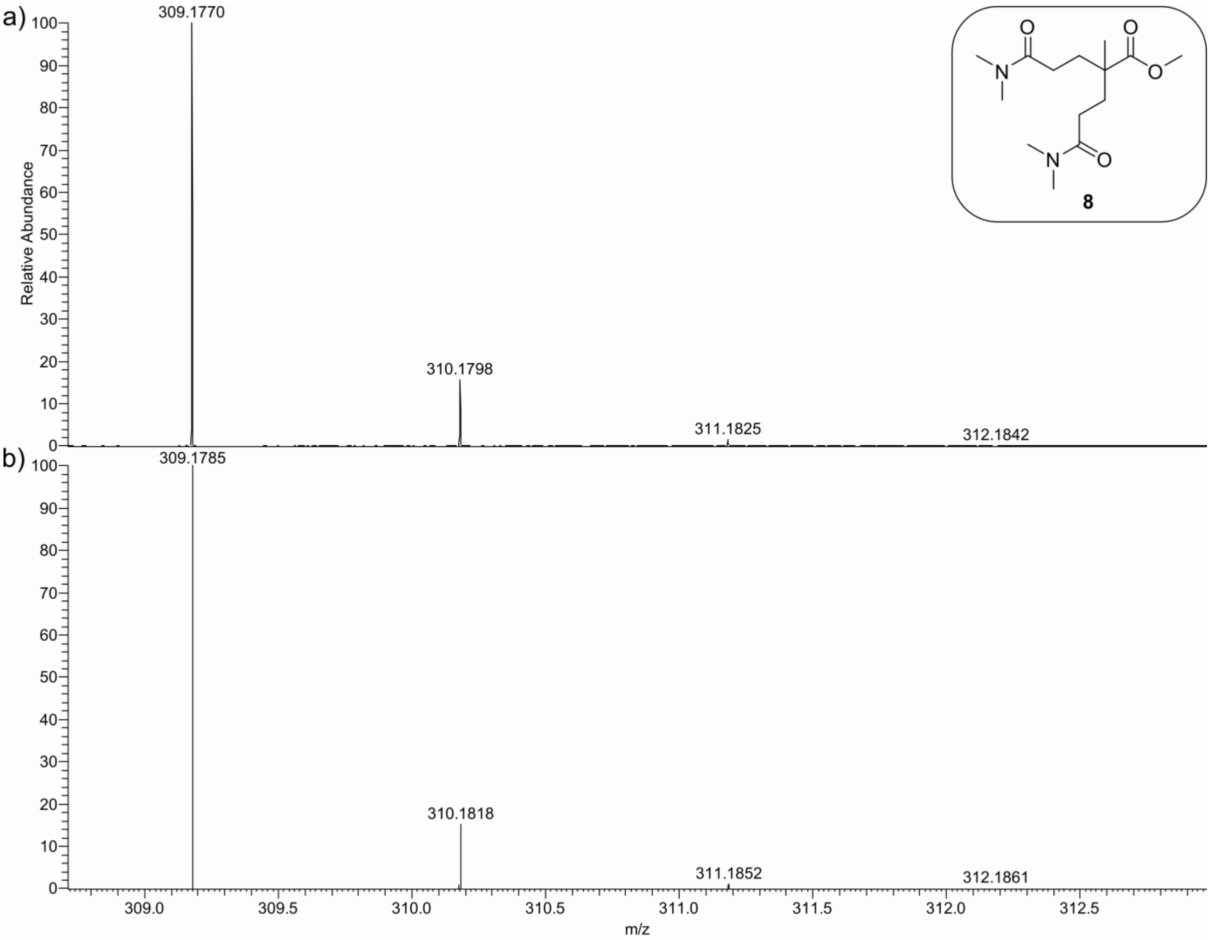

Fig. S49 (a) Observed ESI+ high resolution mass spectrum of **8** and (b) calculated isotopic distribution of the $[M+Na]^+$ ion with the structure in insert.

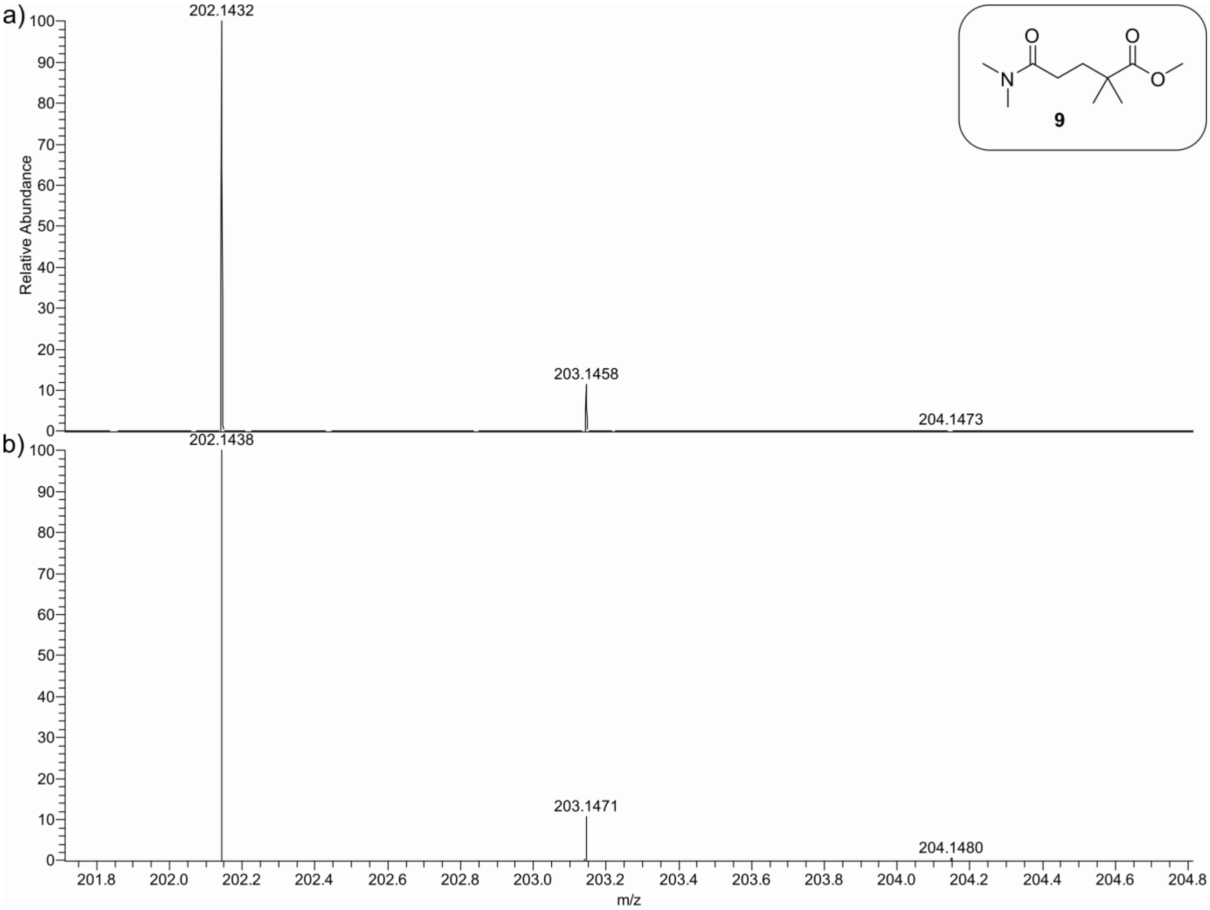

Fig. S50 (a) Observed ESI+ high resolution mass spectrum of **9** and (b) calculated isotopic distribution of the $[M+H]^+$ ion with the structure in insert.

13. IR spectroscopy

IR spectra were recorded from neat samples using a Thermo Fisher Nicolet iS5 iD5 ATR-FTIR spectrometer.

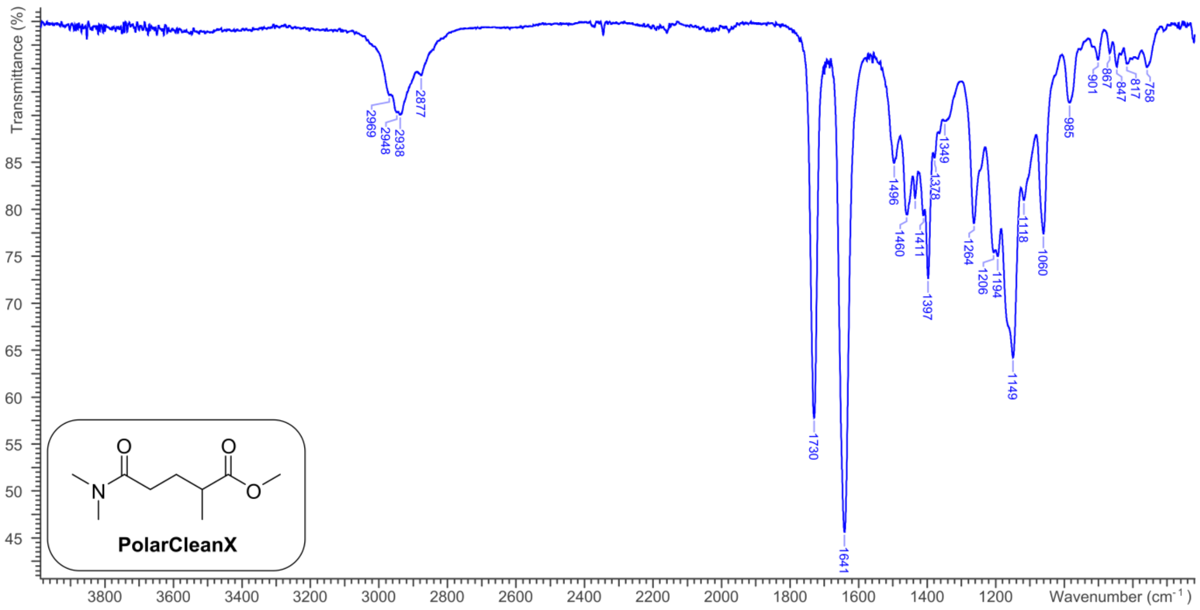

No	cm^{-1}	%T	Intensity
1	758.49	95.148	VW
2	816.83	95.512	VW
3	846.72	95.204	VW
4	867.09	96.634	VW
5	901.44	95.959	VW
6	984.72	91.351	W
7	1060.42	77.416	M
8	1117.79	80.970	M
9	1149.37	64.208	S
10	1193.96	75.011	M
11	1205.89	75.392	M
12	1263.63	78.503	M
13	1348.84	89.403	W
14	1378.37	85.507	W
15	1397.17	72.670	M
16	1411.16	79.339	M
17	1435.26	81.202	M
18	1459.61	79.419	M
19	1496.49	84.954	W
20	1641.00	45.619	VS
21	1729.83	57.777	S
22	2876.91	94.274	W
23	2938.02	90.079	W
24	2947.90	90.318	W
25	2969.36	92.161	W

Fig. S51 IR spectrum of PolarCleanY with the structure of the main component and table of peaks in insert.

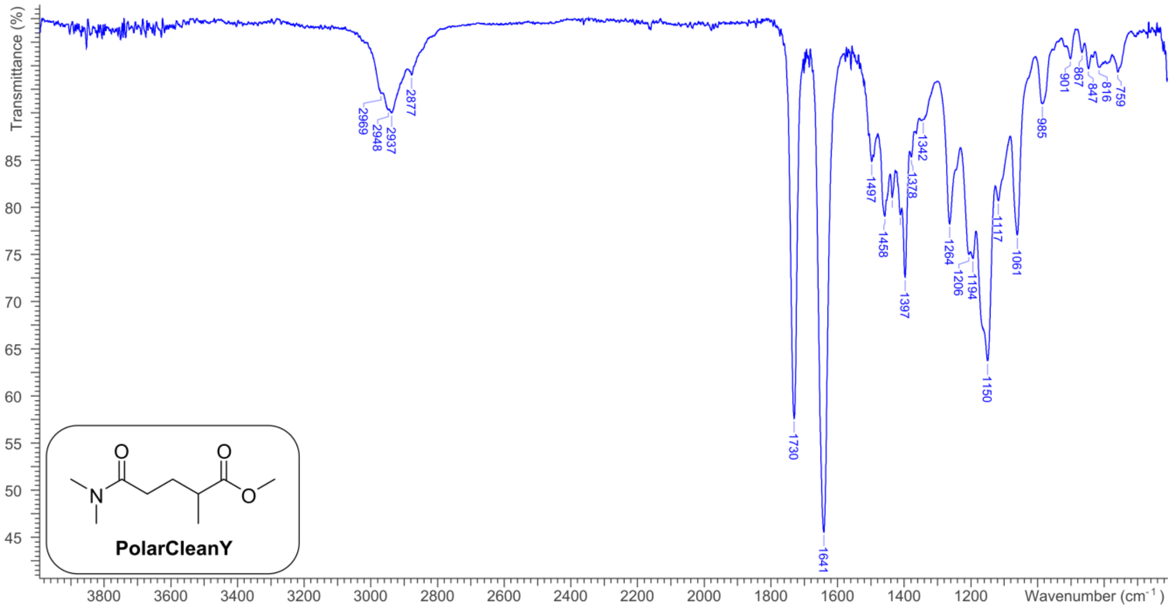

No	cm⁻¹	%T	Intensity
1	758.73	94.355	W
2	815.62	94.850	VW
3	846.96	94.705	VW
4	866.60	96.424	VW
5	901.32	95.752	VW
6	985.45	90.996	W
7	1060.90	77.056	M
8	1117.43	80.697	M
9	1149.61	63.711	S
10	1193.96	74.575	M
11	1205.89	75.008	M
12	1263.75	78.247	M
13	1342.45	89.315	W
14	1378.37	85.331	W
15	1397.42	72.605	M
16	1411.28	79.205	M
17	1435.98	81.063	M
18	1457.92	79.049	M
19	1497.09	84.867	W
20	1641.13	45.562	VS
21	1729.71	57.614	S
22	2877.39	94.041	W
23	2937.18	90.013	W
24	2947.54	90.312	W
25	2969.24	92.074	W

Fig. S52 IR spectrum of PolarCleanY with the structure of the main component and table of peaks in insert.

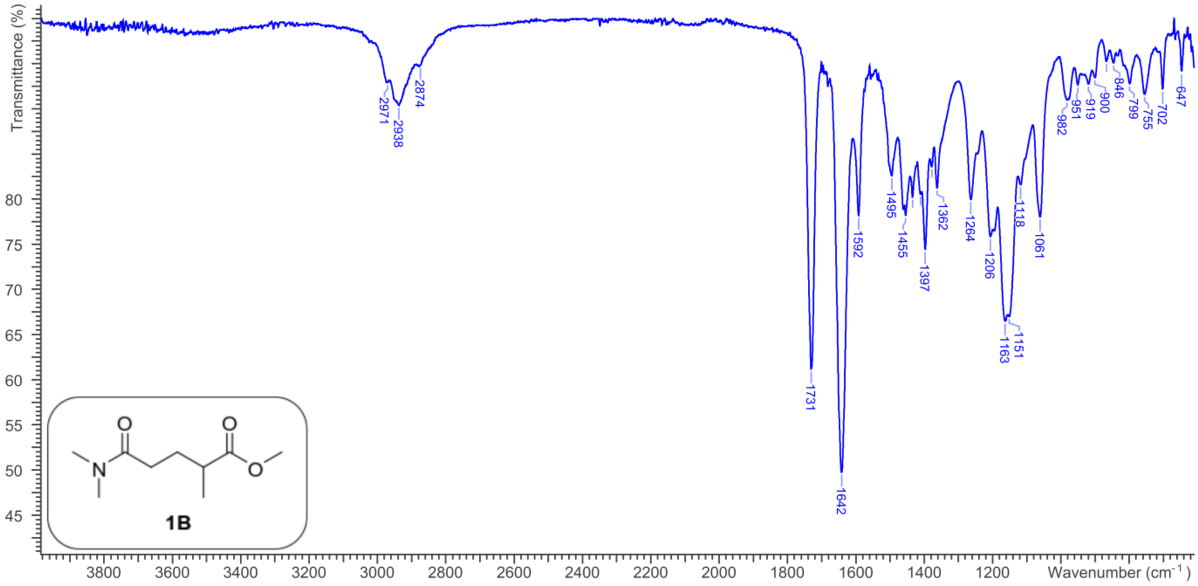

No	cm⁻¹	%T	Intensity
1	646.88	94.127	W
2	702.32	92.186	W
3	754.99	91.611	W
4	798.75	92.787	W
5	845.99	95.083	VW
6	866.97	95.269	VW
7	900.23	93.480	W
8	919.03	92.753	W
9	950.85	92.686	W
10	982.19	90.995	W
11	1060.90	78.041	M
12	1118.15	81.602	M
13	1151.17	67.002	S
14	1162.99	66.513	S
15	1206.14	75.881	M
16	1263.51	79.952	M
17	1362.34	81.244	M
18	1378.13	83.584	M
19	1397.29	74.434	M
20	1410.67	80.543	M
21	1434.30	80.199	M
22	1454.55	78.208	M
23	1494.92	82.588	M
24	1592.07	78.203	M
25	1641.97	49.757	VS
26	1730.56	61.201	S
27	2874.02	94.831	W
28	2937.66	90.428	W
29	2970.56	92.904	W

Fig. S53 IR spectrum of **1B** with the structure of the main component and table of peaks in insert.

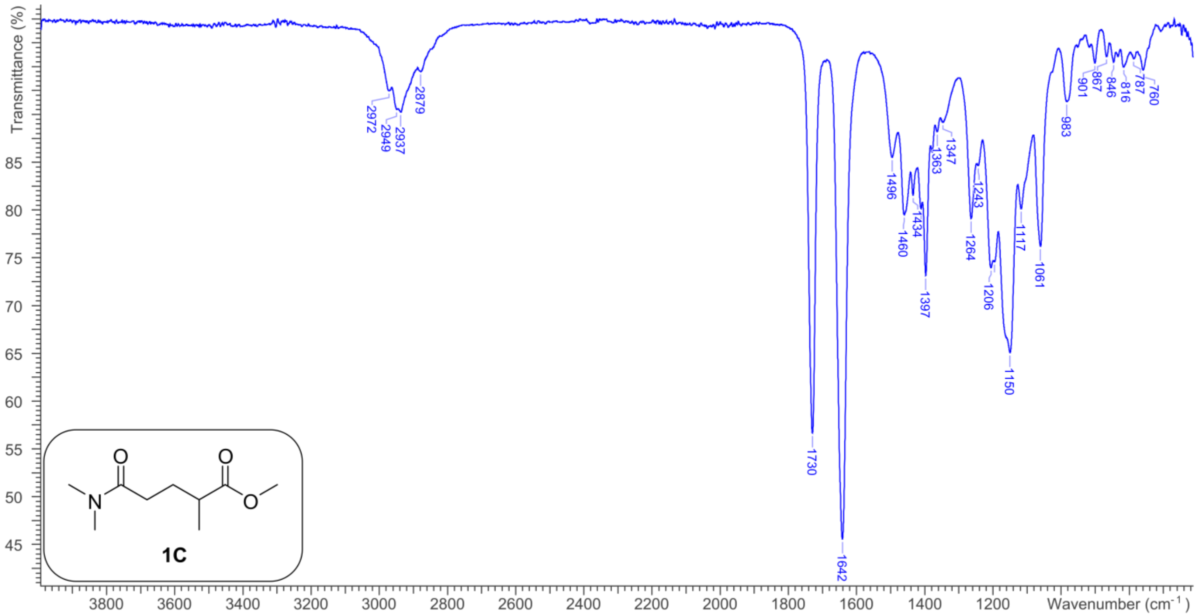

No	cm⁻¹	%T	Intensity	No	cm⁻¹	%T	Intensity	No	cm⁻¹	%T	Intensity
1	759.70	94.641	VW	10	1149.85	65.075	S	19	1434.42	81.540	M
2	786.93	95.809	VW	11	1195.29	74.592	M	20	1460.45	79.505	M
3	816.46	94.960	VW	12	1206.01	73.943	M	21	1495.77	85.506	W
4	845.75	95.480	VW	13	1243.26	84.658	W	22	1641.73	45.544	VS
5	866.73	96.054	VW	14	1263.87	79.098	M	23	1729.59	56.656	S
6	901.08	95.374	VW	15	1346.67	89.178	W	24	2879.32	94.505	W
7	983.40	91.356	W	16	1363.43	88.181	W	25	2936.93	90.226	W
8	1060.66	76.193	M	17	1397.05	73.136	M	26	2949.23	90.524	W
9	1117.18	80.113	M	18	1411.16	80.149	M	27	2972.13	92.481	W

Fig. S54 IR spectrum of **1C** with table of peaks and the structure in insert.

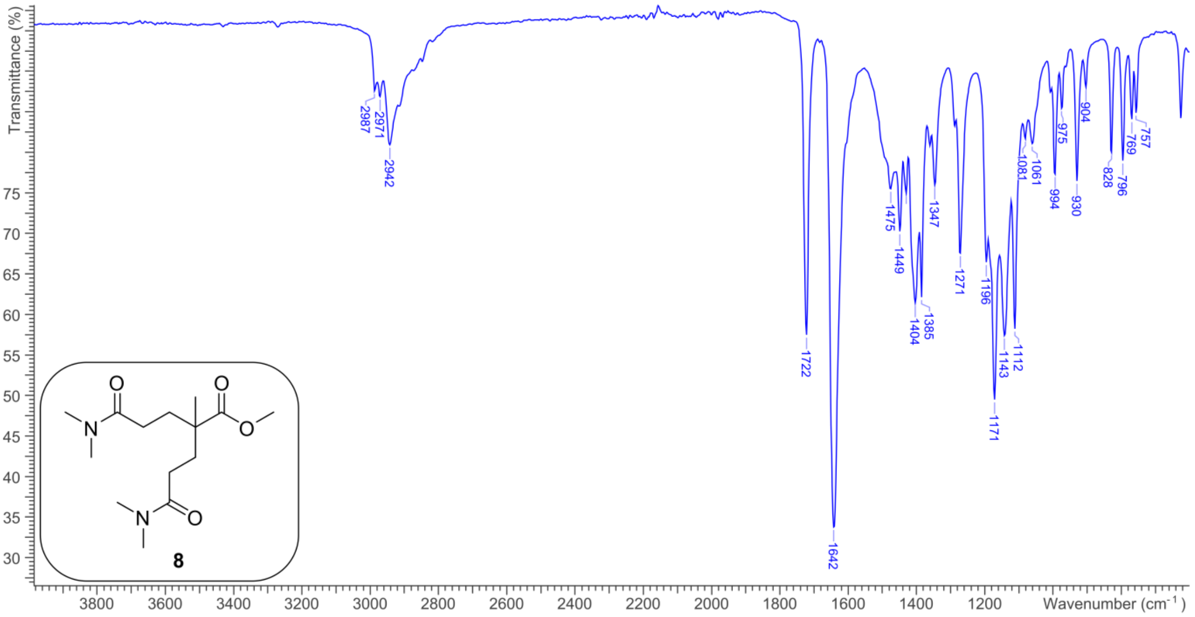

No	cm⁻¹	%T	Intensity	No	cm⁻¹	%T	Intensity	No	cm⁻¹	%T	Intensity
1	756.96	84.865	W	10	1081.38	81.664	W	19	1430.28	74.933	M
2	769.21	84.094	W	11	1111.98	58.236	S	20	1448.64	70.226	M
3	795.73	78.949	W	12	1142.59	57.361	S	21	1475.16	75.478	M
4	828.38	79.985	W	13	1171.15	49.502	S	22	1642.47	33.727	VS
5	903.87	88.011	W	14	1195.64	66.413	M	23	1722.04	57.484	S
6	930.39	76.467	M	15	1271.13	67.538	M	24	2942.17	80.918	W
7	975.28	85.415	W	16	1346.62	75.974	M	25	2970.73	86.861	W
8	993.64	77.298	M	17	1385.39	62.130	M	26	2987.05	87.546	W
9	1060.98	81.048	W	18	1403.75	61.403	M				

Fig. S55 IR spectrum of **8** with table of peaks and the structure in insert.

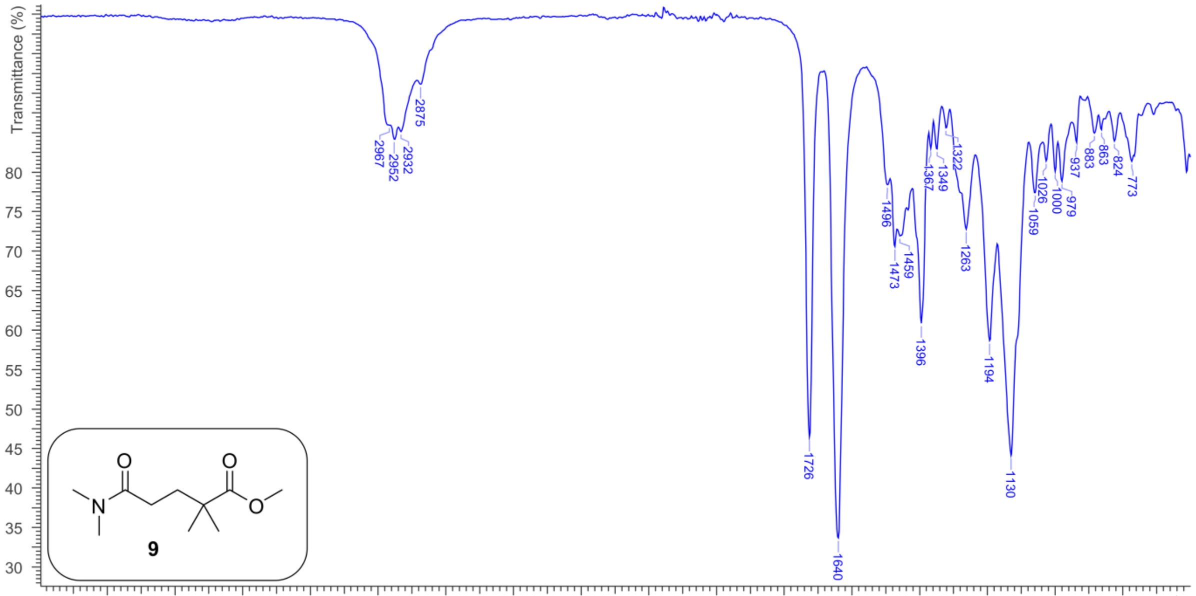

No	cm^{-1}	%T	Intensity
1	773.29	81.364	W
2	824.30	83.952	W
3	863.06	85.396	W
4	883.47	84.961	W
5	936.51	83.756	W
6	979.36	78.853	M
7	999.77	80.079	M
8	1026.29	81.396	W
9	1058.93	77.415	M
10	1130.35	44.085	S
11	1193.60	58.646	S
12	1262.97	72.799	M
13	1322.14	85.594	W
14	1348.66	82.945	W
15	1367.03	83.010	W
16	1395.59	60.850	M
17	1458.84	71.923	M
18	1473.12	70.590	M
19	1495.57	78.404	M
20	1640.43	33.653	VS
21	1726.13	46.431	S
22	2874.83	91.139	W
23	2931.96	85.149	W
24	2952.37	84.167	W
25	2966.65	85.957	W

Fig. S56 IR spectrum of **9** with table of peaks and the structure in insert.

14. HPLC analysis

When necessary, preparative HPLC was used for purification. For the preparative HPLC purification, VWR LaPrep Sigma instrument was used with preparative solvent pump (La Prep Sigma LP1200), sample injection pump (La Prep Sigma LP1000), UV detector (La Prep Sigma LP3101), Interchim, Uptisphere Strategy 100A, 10 µm, C18-3 (250 × 30 mm) column; with eluent A: water type I (18.2 MΩ) with 0.1% TFA and eluent B: methanol.

HPLC analyses were measured on a VWR Hitachi Chromaster instrument with 5160 pump, 5260 autosampler, 5310 column oven, and 5430 diode array detector (DAD). Analyses were performed on an ACE-C18, 5 µm, 100 Å, 150 × 4.6 mm column from Hichrom. The solvent system used was eluent A: water type I (18.2 MΩ) with 0.1 % TFA and eluent B: acetonitrile with 0.1% TFA. Gradient elution was selected with 1 mL min^{-1} flow rate and column temperature at 30 °C.

Method 1: B was held at 5% for 3 min, increased to 15% in 3 min and then it was eluted from 15% to 20% in 12 min. Detection at 210 nm.

Method 2: B was held at 5% for 3 min, increased to 20% in 3 min and then it was eluted from 20% to 40% in 12 min. Detection at 210 nm.

Method 3: B was held at 10% for 3 min, eluted from 10% to 98% in 10 min and then it was held at 98% for 5 min. Detection at 270 nm.

Method 4: B was held at 40% for 3 min, eluted from 40% to 98% in 10 min and then it was held at 98% for 5 min. Detection at 270 nm.

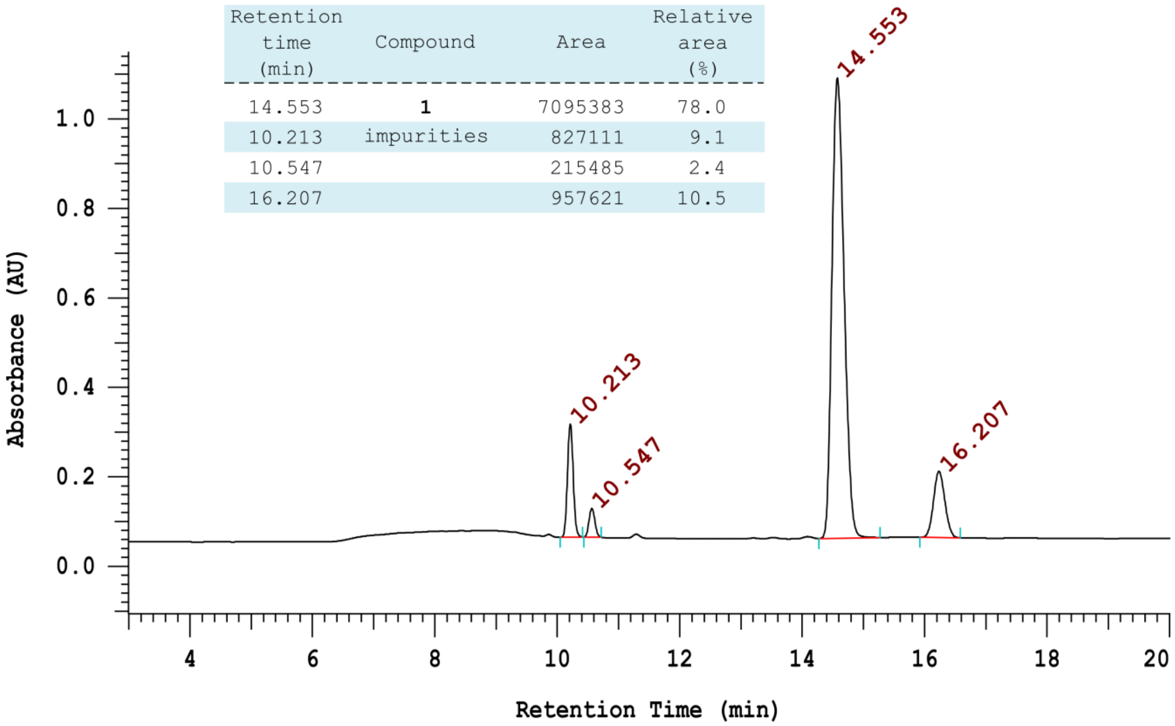

Retention time (min)	Compound	Area	Relative area (%)
14.553	**1**	7095383	78.0
10.213	impurities	827111	9.1
10.547		215485	2.4
16.207		957621	10.5

Fig. S57 HPLC chromatogram of PolarCleanX at 210 nm with the table of peaks in insert. The compound was analysed with Method 1. Impurities were identified by GC-MS analysis (sections 11–12).

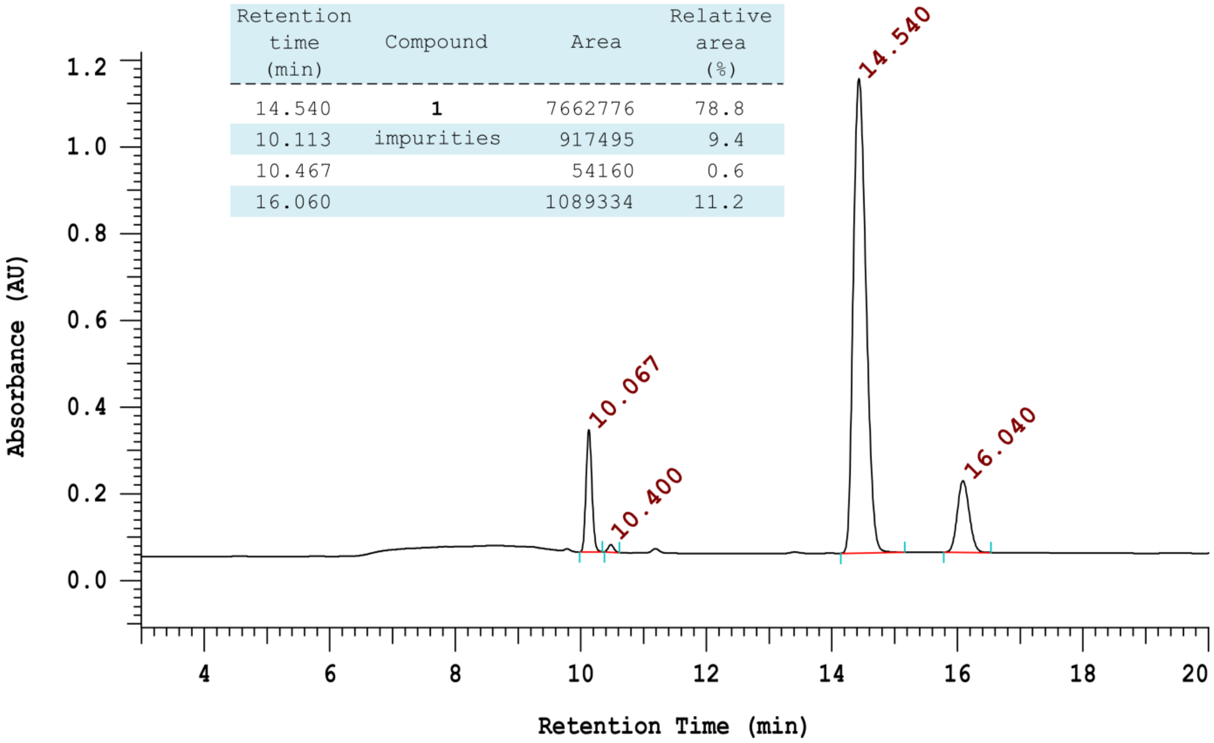

Retention time (min)	Compound	Area	Relative area (%)
14.540	**1**	7662776	78.8
10.113	impurities	917495	9.4
10.467		54160	0.6
16.060		1089334	11.2

Fig. S58 HPLC chromatogram of PolarCleanY at 210 nm with the table of peaks in insert. The compound was analysed with Method 1. Impurities were identified by GC-MS analysis (sections 11–12).

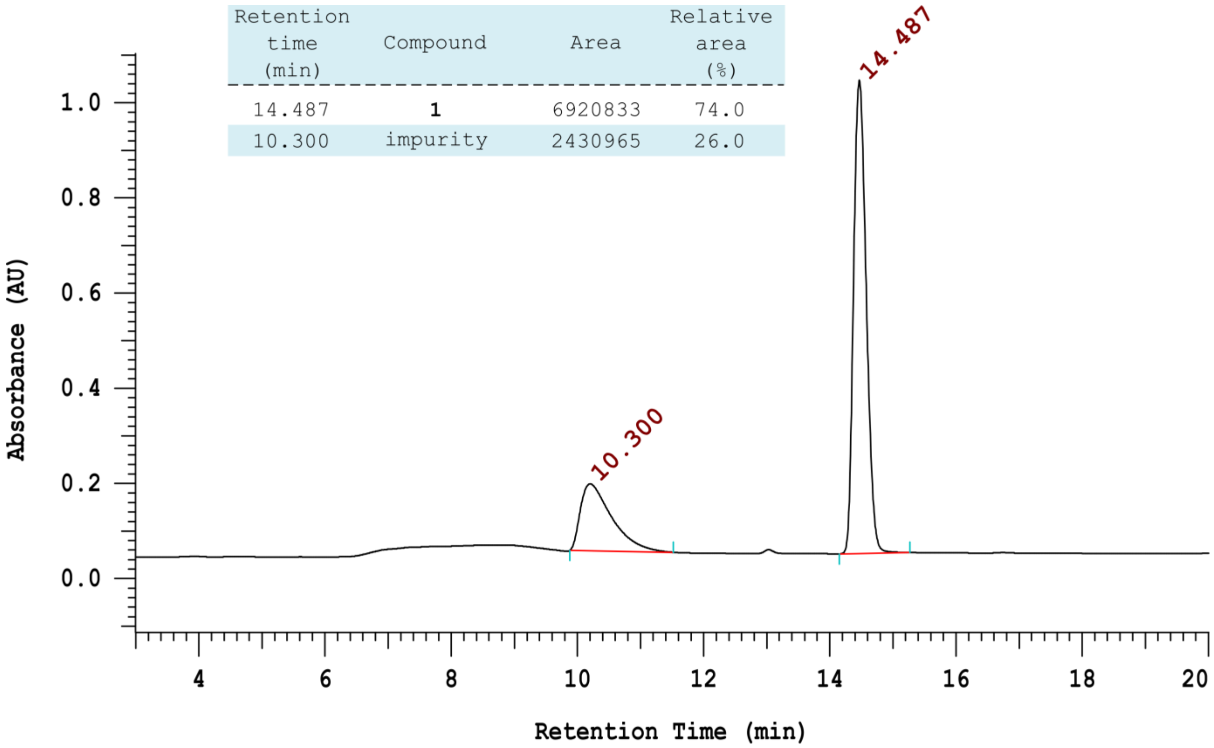

Retention time (min)	Compound	Area	Relative area (%)
14.487	**1**	6920833	74.0
10.300	impurity	2430965	26.0

Fig. S59 HPLC chromatogram of **1B** at 210 nm with the table of peaks in insert. The compound was analysed with Method 1. Impurities were identified by GC-MS analysis (sections 11–12).

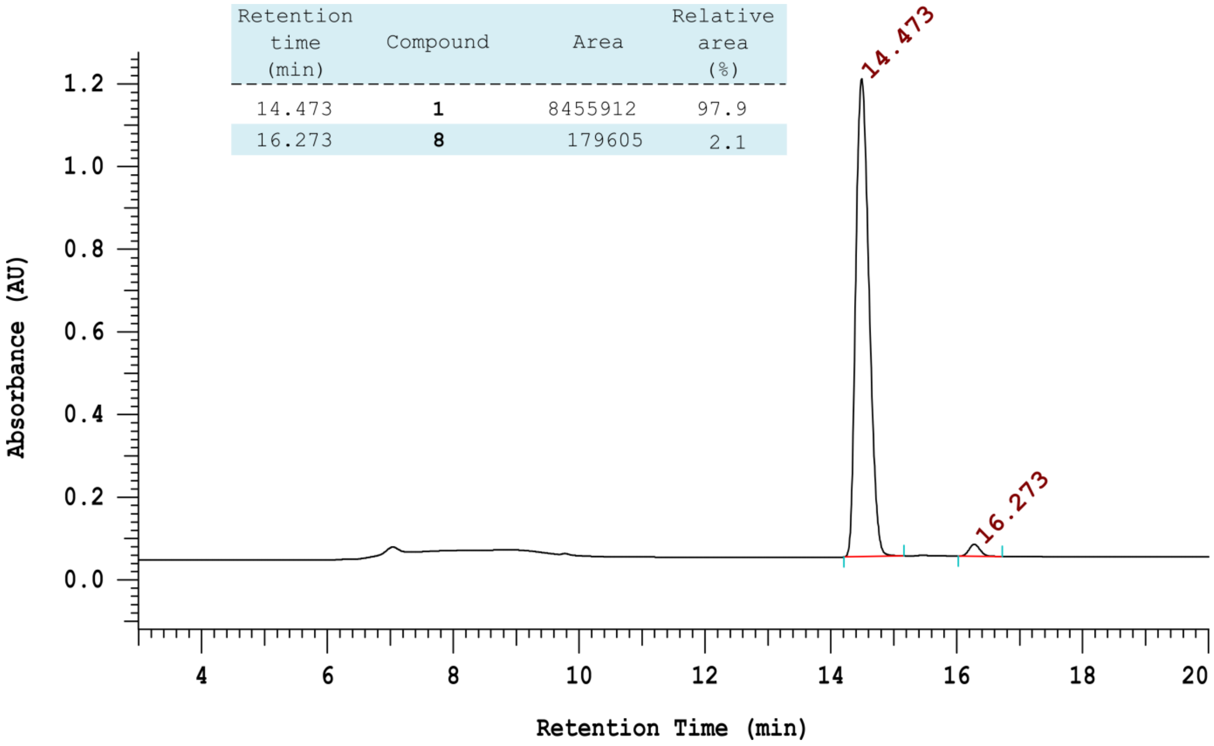

Retention time (min)	Compound	Area	Relative area (%)
14.473	**1**	8455912	97.9
16.273	**8**	179605	2.1

Fig. S60 HPLC chromatogram of **1C** at 210 nm with the table of peaks in insert. The compound was analysed with Method 1.

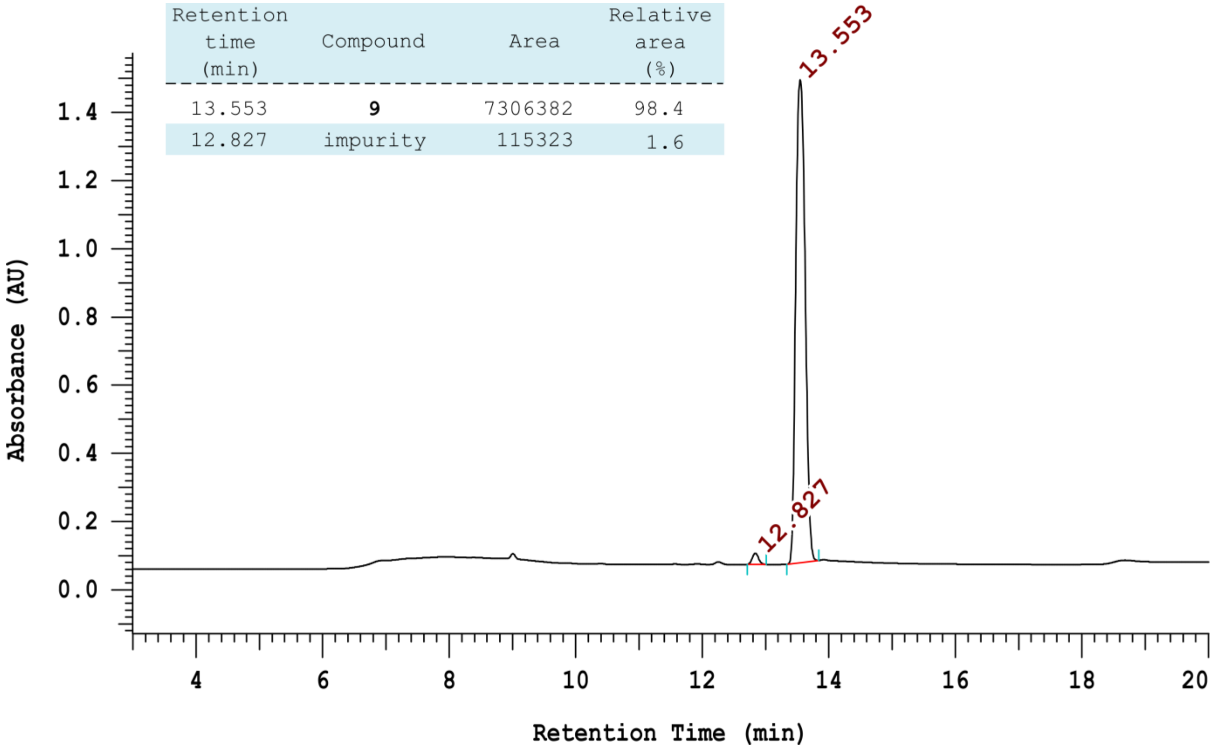

Retention time (min)	Compound	Area	Relative area (%)
13.553	**9**	7306382	98.4
12.827	impurity	115323	1.6

Fig. S61 HPLC chromatogram of **9** at 210 nm with the table of peaks in insert. The compound was analysed with Method 2.

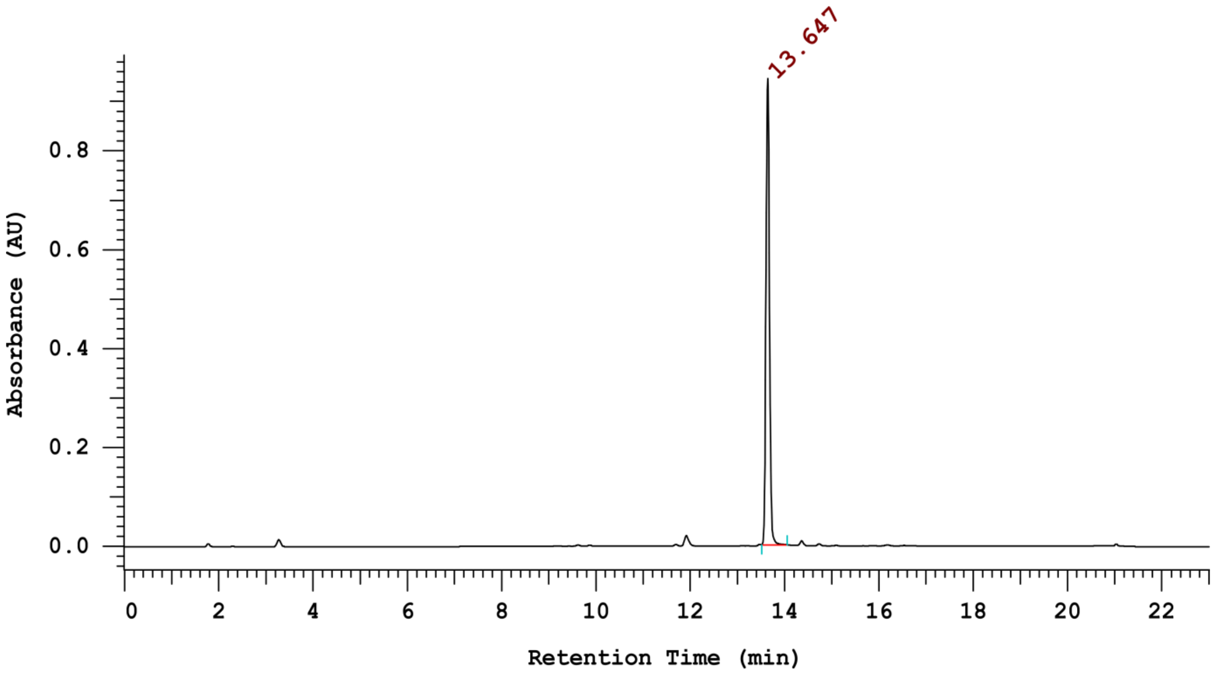

Fig. S62 HPLC chromatogram of the reaction mixture corresponding to Table 4 Entry 1 at 270 nm showing the peak of the product (**10**). The reaction was monitored with Method 4.

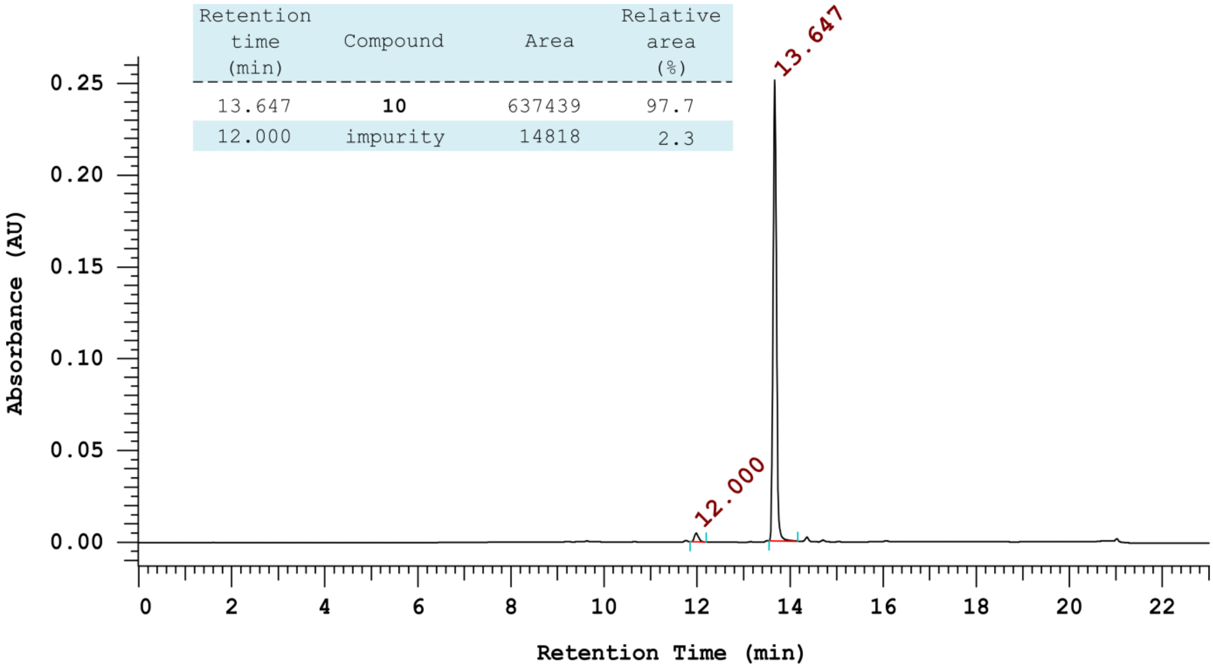

Retention time (min)	Compound	Area	Relative area (%)
13.647	**10**	637439	97.7
12.000	impurity	14818	2.3

Fig. S63 HPLC chromatogram of **10** after crystallisation at 270 nm with the table of peaks in insert obtained from the reaction corresponding to Table 4 Entry 1. The compound was analysed with Method 4.

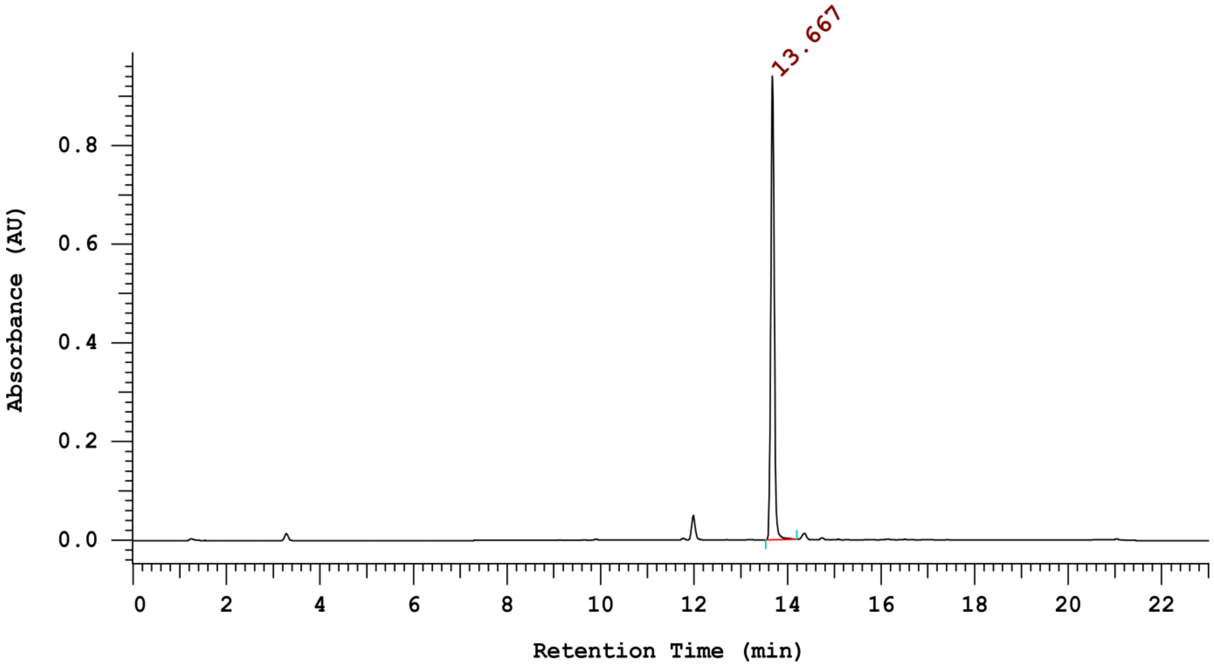

Fig. S64 HPLC chromatogram of the reaction mixture corresponding to Table 4 Entry 2 at 270 nm showing the peak of the product (**10**). The reaction was monitored with Method 4.

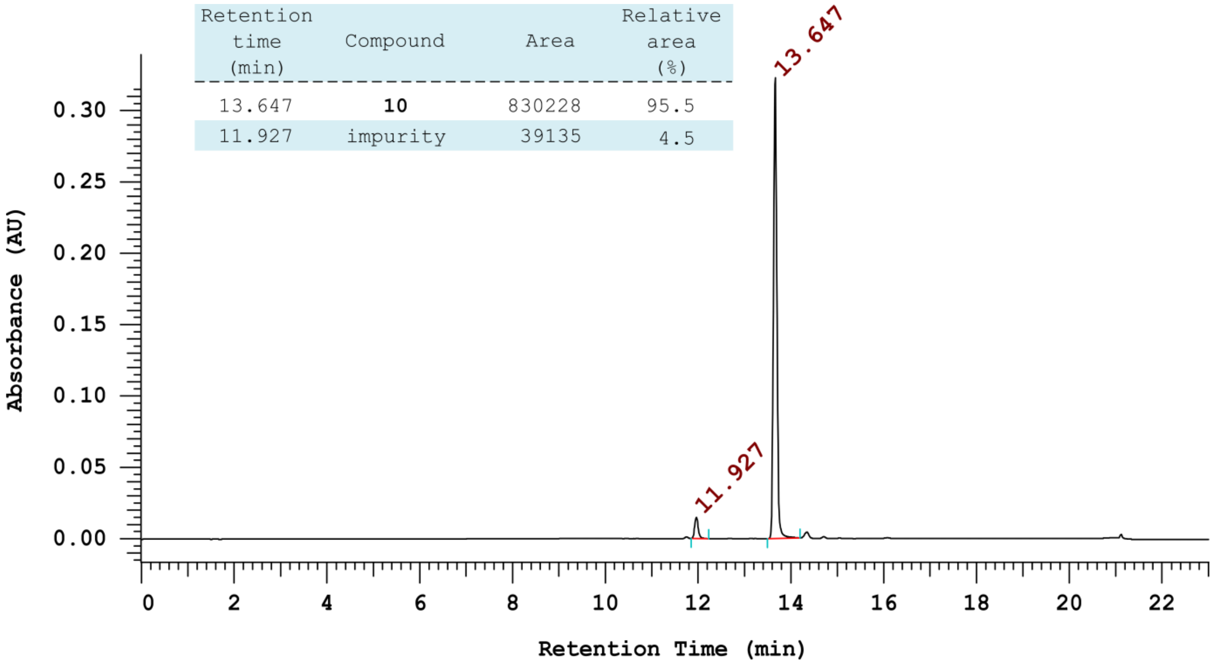

Retention time (min)	Compound	Area	Relative area (%)
13.647	**10**	830228	95.5
11.927	impurity	39135	4.5

Fig. S65 HPLC chromatogram of **10** after crystallisation at 270 nm with the table of peaks in insert obtained from the reaction corresponding to Table 4 Entry 2. The compound was analysed with Method 4.

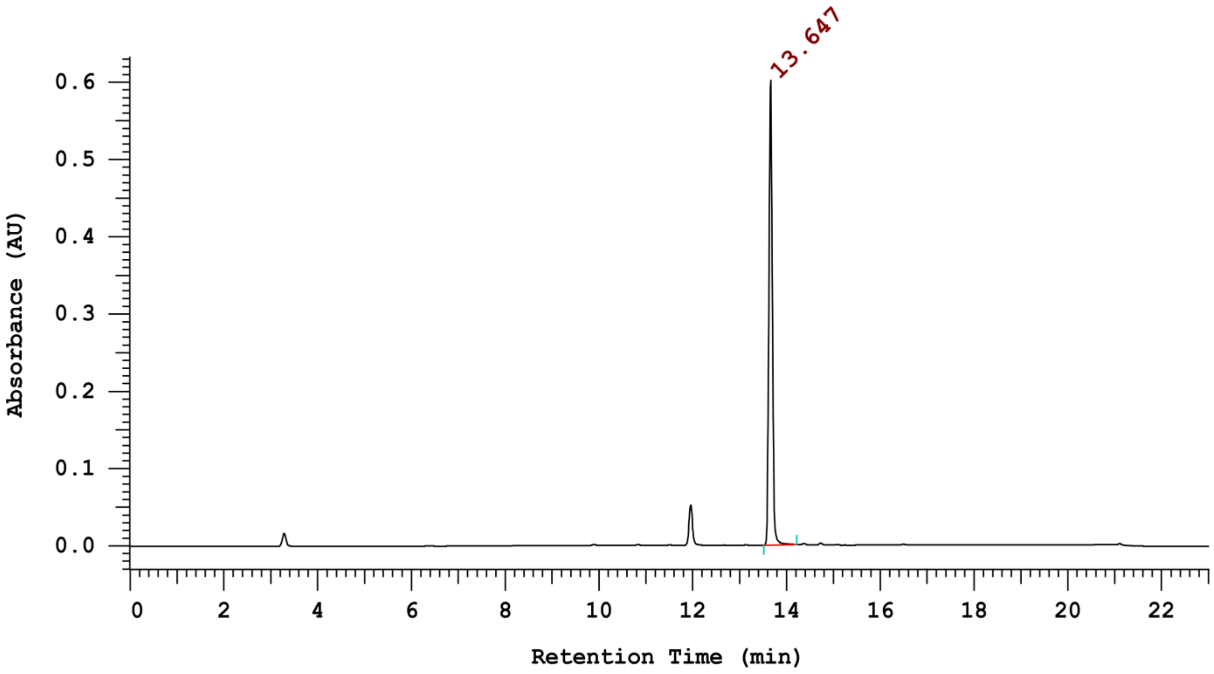

Fig. S66 HPLC chromatogram of the reaction mixture corresponding to Table 4 Entry 3 at 270 nm showing the peak of the product (**10**). The reaction was monitored with Method 4.

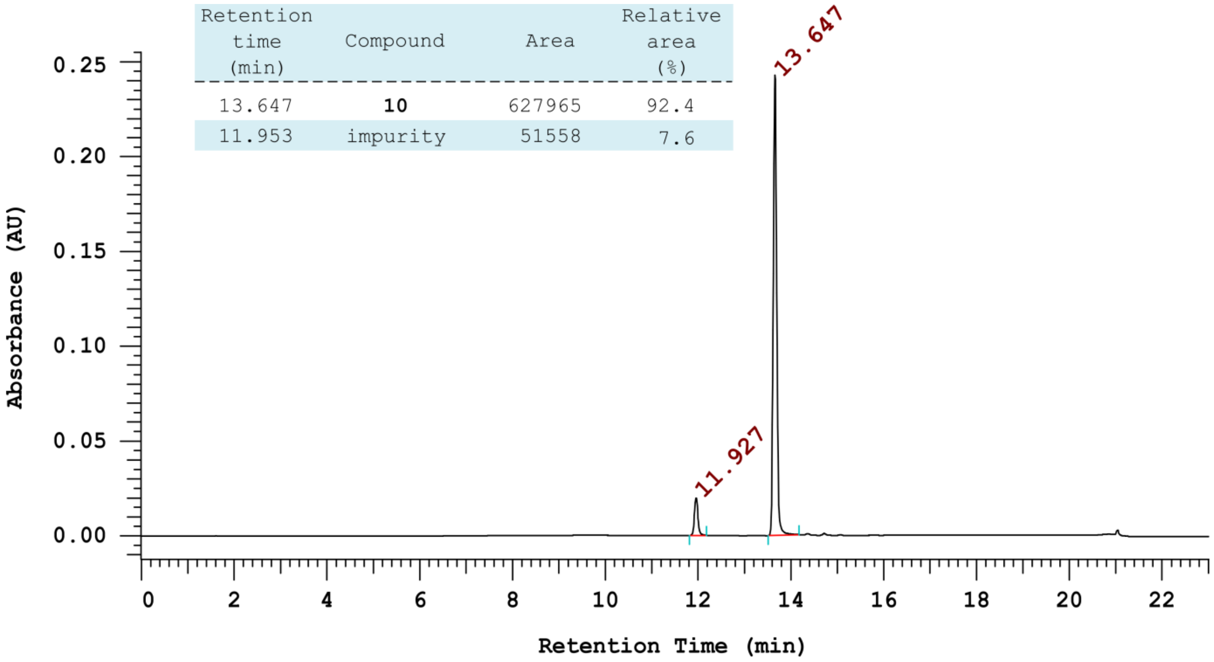

Retention time (min)	Compound	Area	Relative area (%)
13.647	**10**	627965	92.4
11.953	impurity	51558	7.6

Fig. S67 HPLC chromatogram of **10** after crystallisation at 270 nm with the table of peaks in insert obtained from the reaction corresponding to Table 4 Entry 3. The compound was analysed with Method 4.

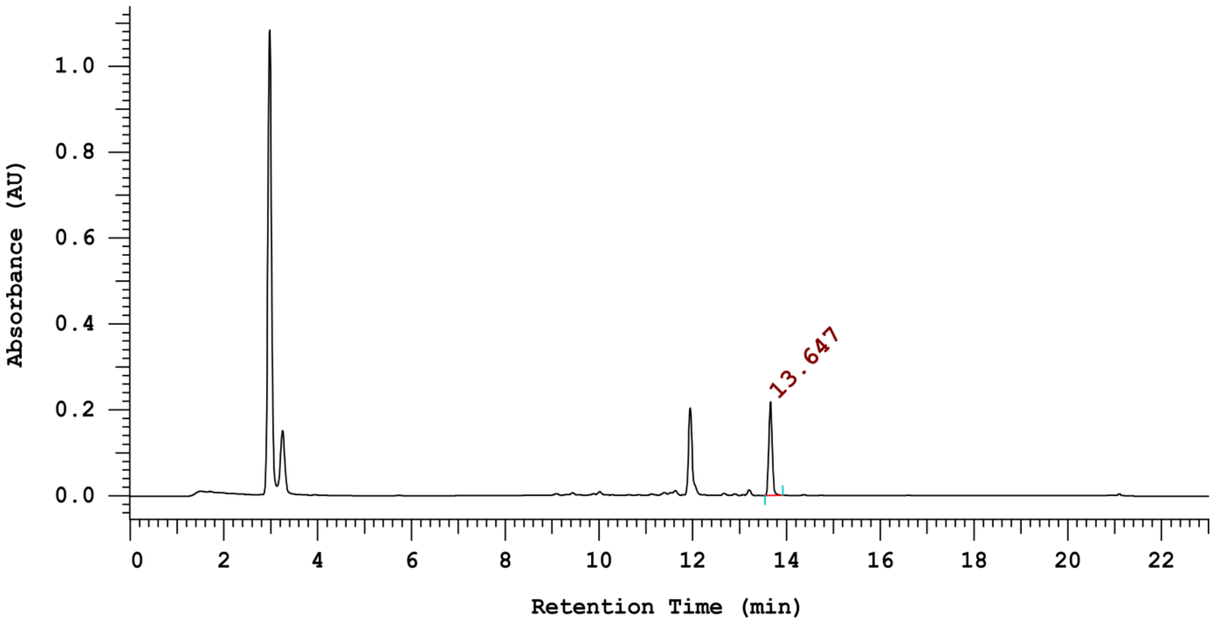

Fig. S68 HPLC chromatogram of the reaction mixture corresponding to Table 4 Entry 4 at 270 nm showing the peak of the product (**10**). The reaction was monitored with Method 4.

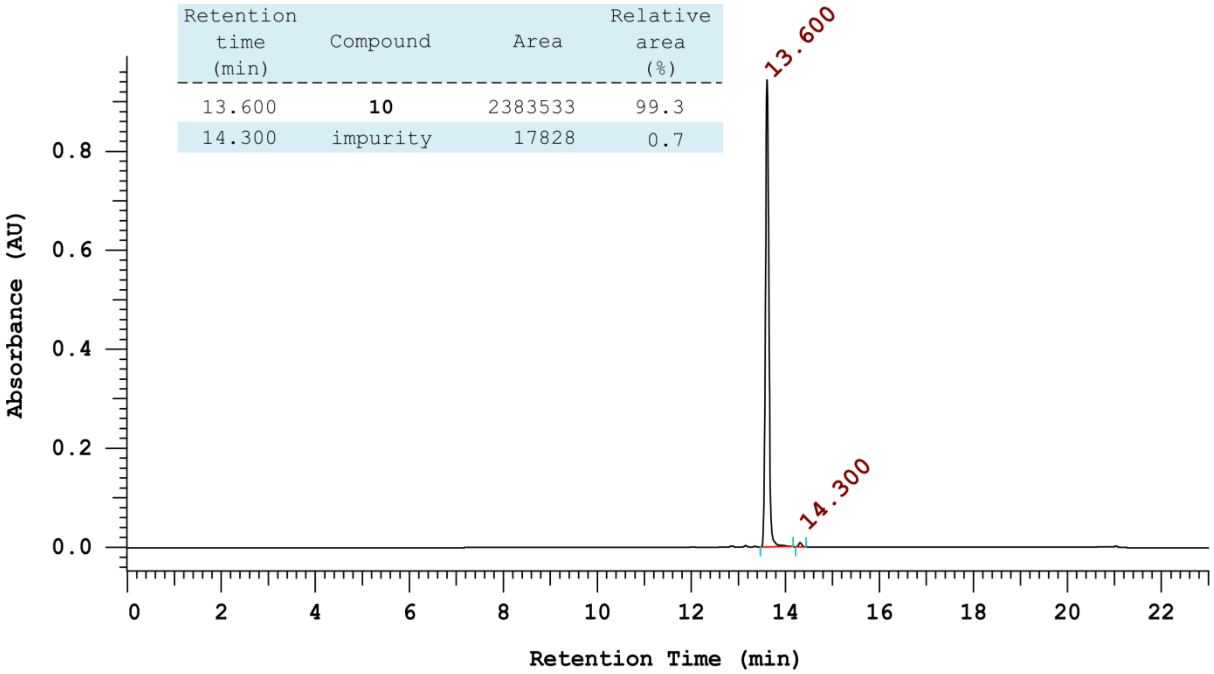

Retention time (min)	Compound	Area	Relative area (%)
13.600	**10**	2383533	99.3
14.300	impurity	17828	0.7

Fig. S69 HPLC chromatogram of **10** after preparative HPLC at 270 nm with the table of peaks in insert obtained from the reaction corresponding to Table 4 Entry 4. The compound was analysed with Method 4.

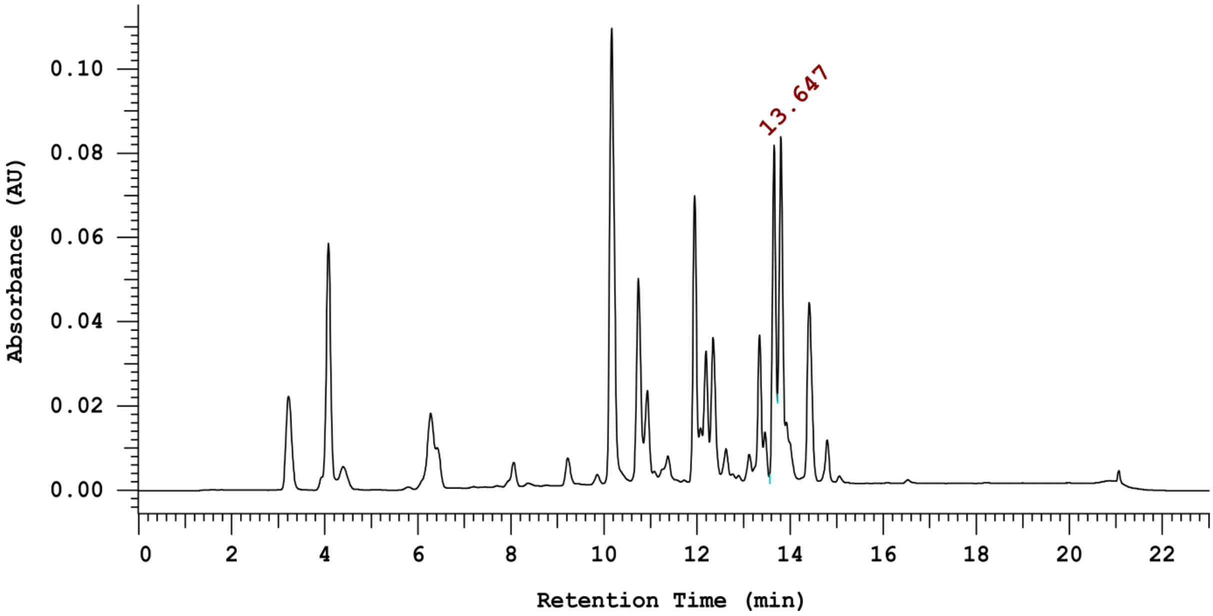

Fig. S70 HPLC chromatogram of the reaction mixture corresponding to Table 4 Entry 5 at 270 nm showing the peak of the product (**10**). The reaction was monitored with Method 4.

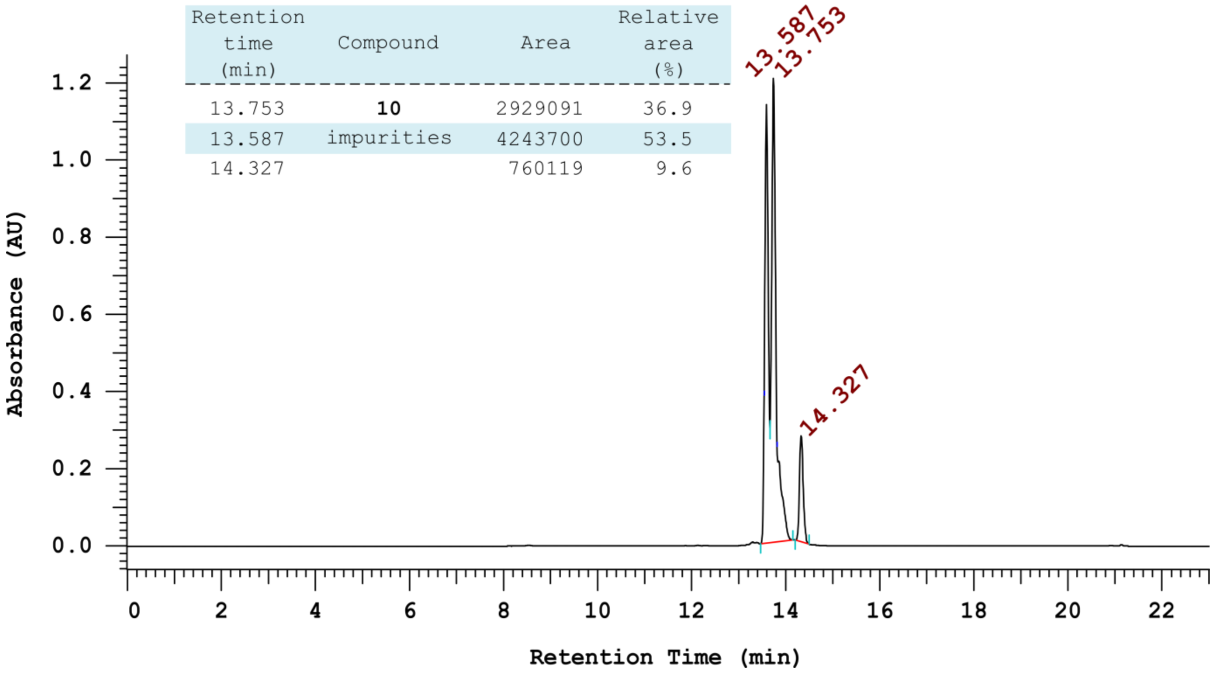

Retention time (min)	Compound	Area	Relative area (%)
13.753	**10**	2929091	36.9
13.587	impurities	4243700	53.5
14.327		760119	9.6

Fig. S71 HPLC chromatogram of **10** after preparative HPLC at 270 nm with the table of peaks in insert obtained from the reaction corresponding to Table 4 Entry 5. The compound was analysed with Method 4.

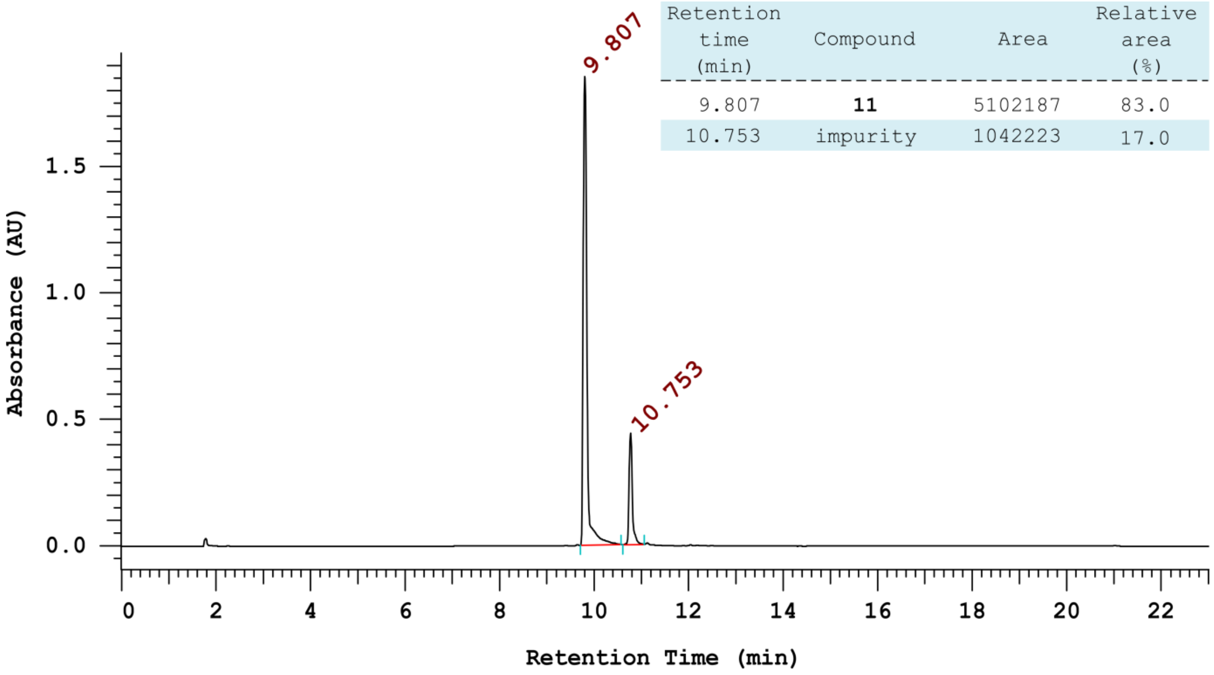

Retention time (min)	Compound	Area	Relative area (%)
9.807	**11**	5102187	83.0
10.753	impurity	1042223	17.0

Fig. S72 HPLC chromatogram of **11** after crystallisation at 270 nm with the table of peaks in insert obtained from the reaction corresponding to Table 5 Entry 1. The compound was analysed with Method 3.

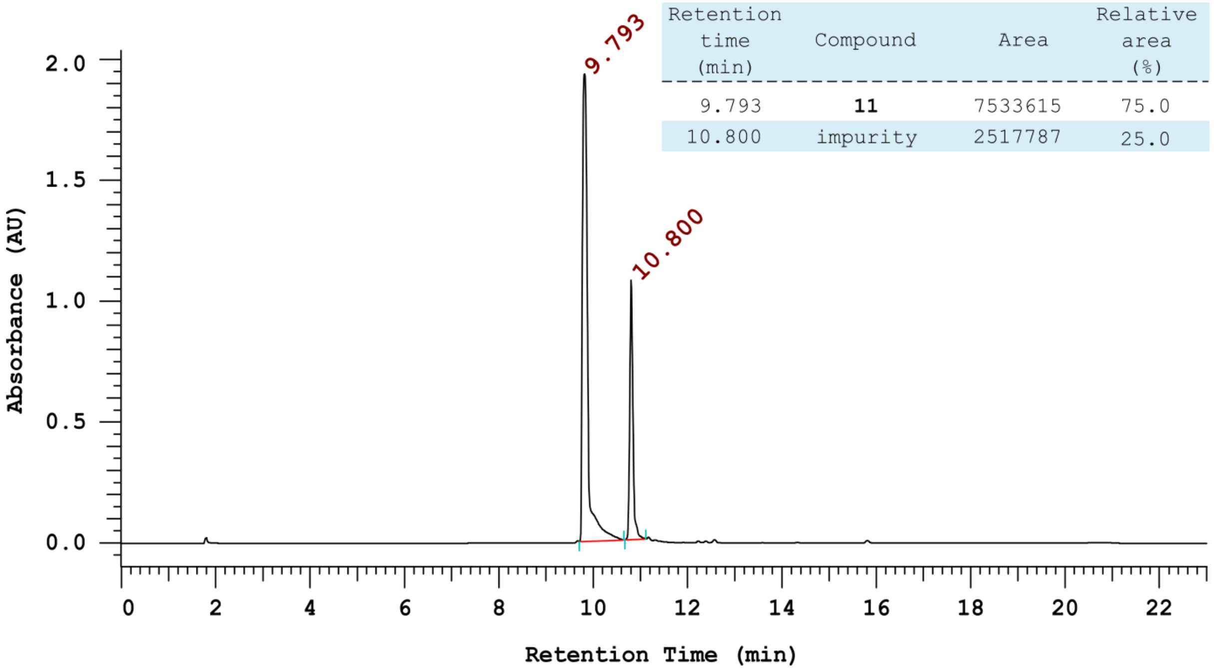

Retention time (min)	Compound	Area	Relative area (%)
9.793	**11**	7533615	75.0
10.800	impurity	2517787	25.0

Fig. S73 HPLC chromatogram of **11** after crystallisation at 270 nm with the table of peaks in insert obtained from the reaction corresponding to Table 5 Entry 2. The compound was analysed with Method 3.

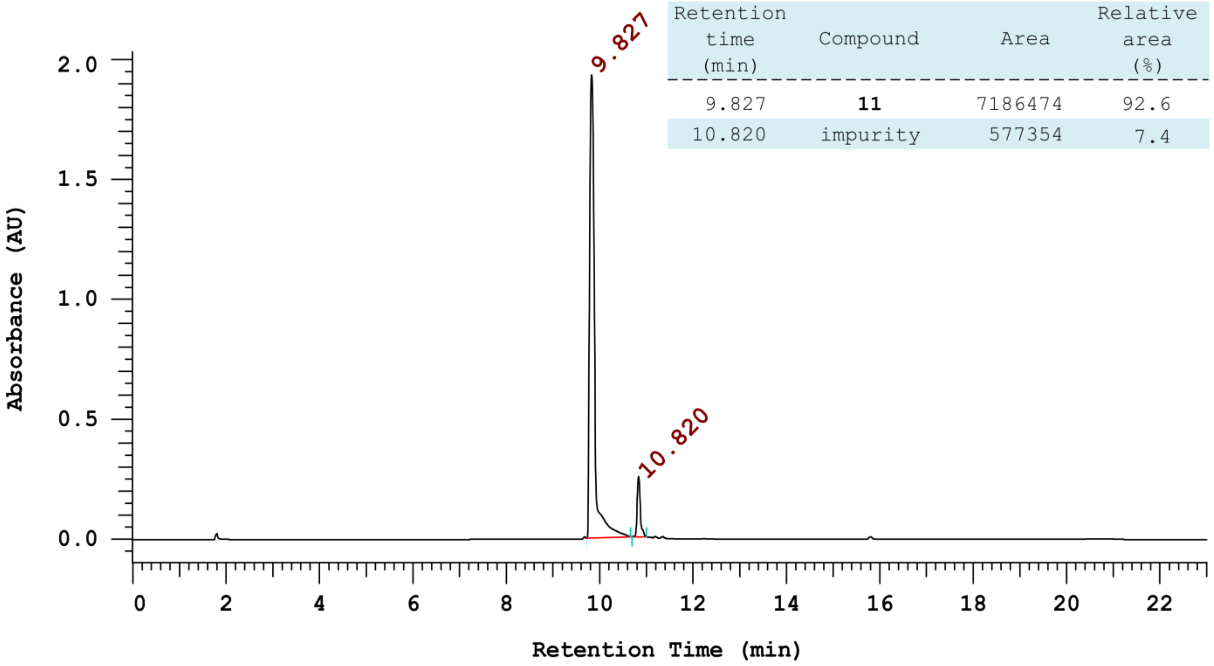

Retention time (min)	Compound	Area	Relative area (%)
9.827	**11**	7186474	92.6
10.820	impurity	577354	7.4

Fig. S74 HPLC chromatogram of **11** after crystallisation at 270 nm with the table of peaks in insert obtained from the reaction corresponding to Table 5 Entry 3. The compound was analysed with Method 3.

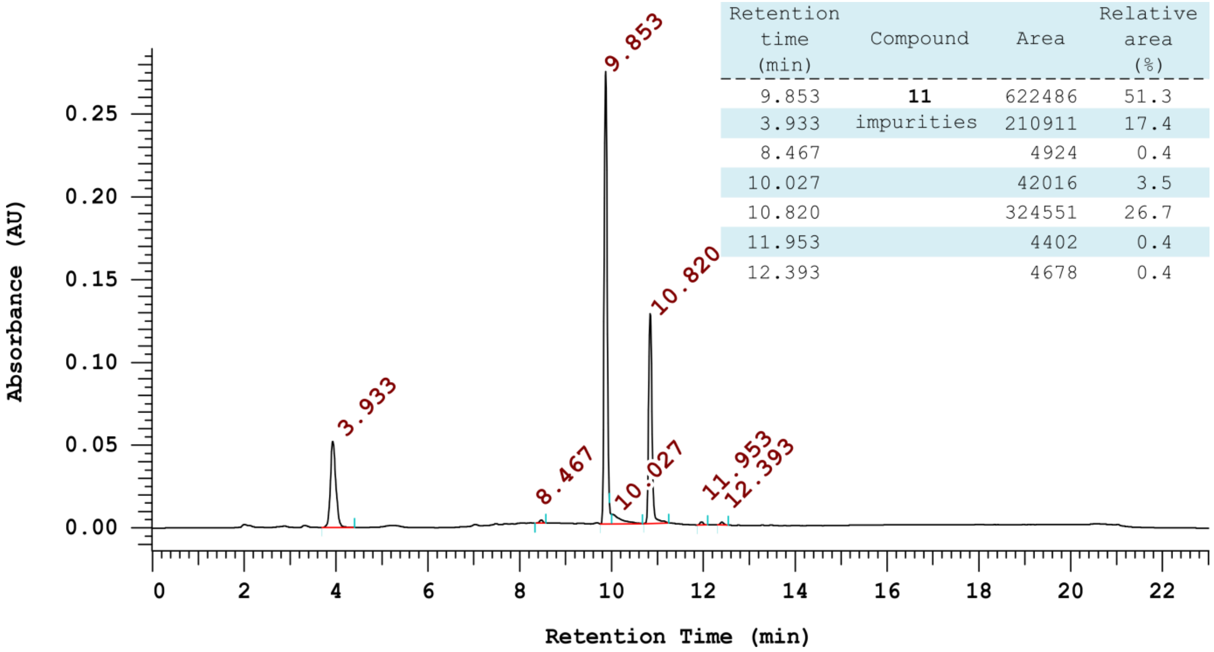

Retention time (min)	Compound	Area	Relative area (%)
9.853	**11**	622486	51.3
3.933	impurities	210911	17.4
8.467		4924	0.4
10.027		42016	3.5
10.820		324551	26.7
11.953		4402	0.4
12.393		4678	0.4

Fig. S75 HPLC chromatogram of the reaction mixture corresponding to Table 5 Entry 4 at 270 nm with the table of peaks in insert. The reaction was monitored with Method 3.

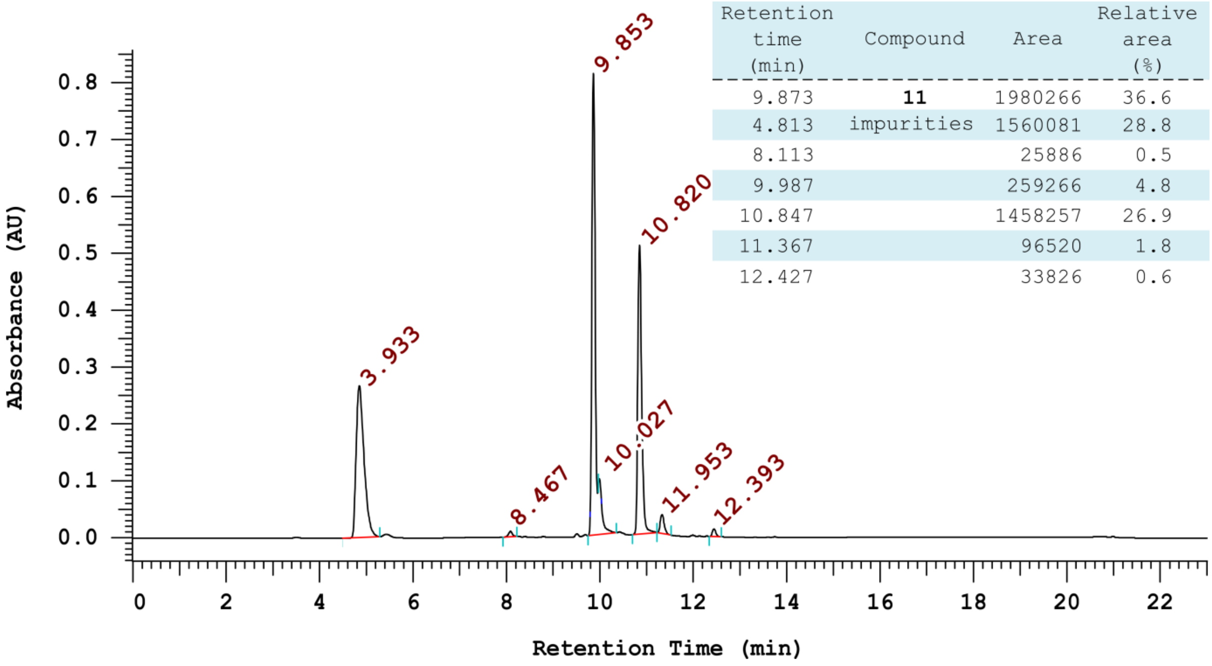

Retention time (min)	Compound	Area	Relative area (%)
9.873	**11**	1980266	36.6
4.813	impurities	1560081	28.8
8.113		25886	0.5
9.987		259266	4.8
10.847		1458257	26.9
11.367		96520	1.8
12.427		33826	0.6

Fig. S76 HPLC chromatogram of the reaction mixture corresponding to Table 5 Entry 5 at 270 nm with the table of peaks in insert. The reaction was monitored with Method 3.

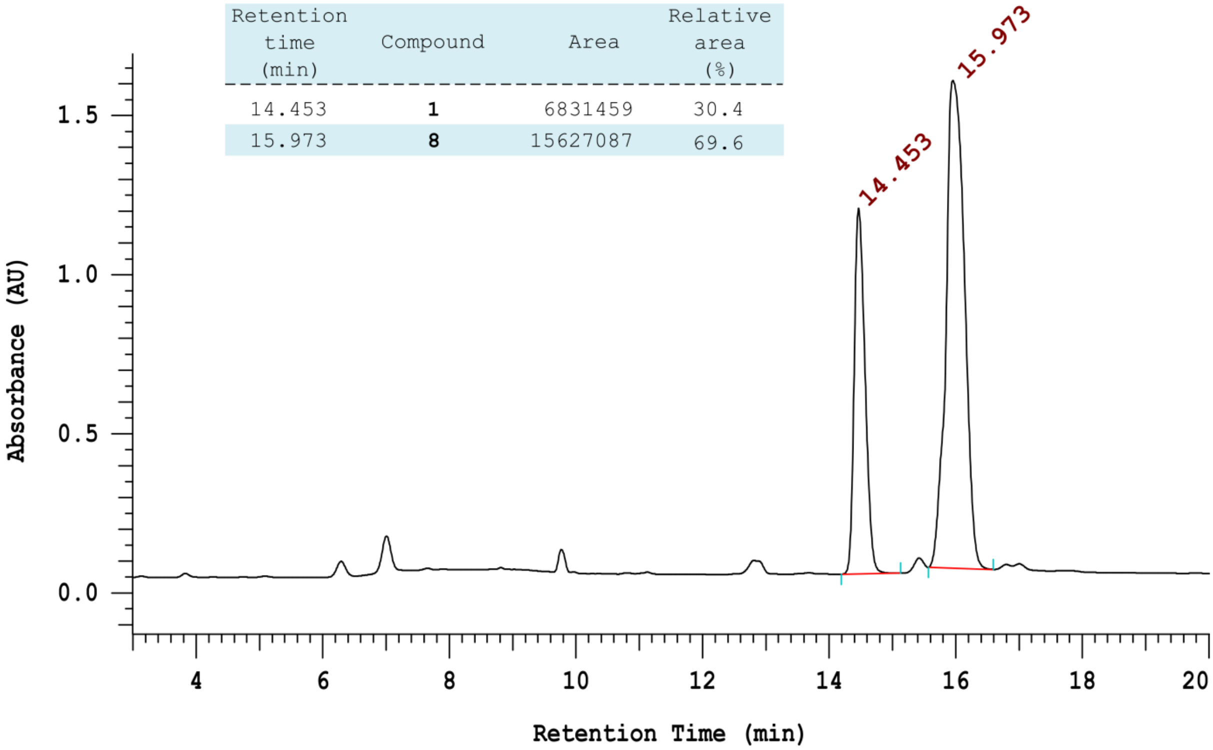

Retention time (min)	Compound	Area	Relative area (%)
14.453	**1**	6831459	30.4
15.973	**8**	15627087	69.6

Fig. S77 HPLC chromatogram of the reaction mixture corresponding to Table 3 Entry 1 at 210 nm showing the relative amounts of the product **1** and by-product **8**. The reaction was monitored with Method 1.

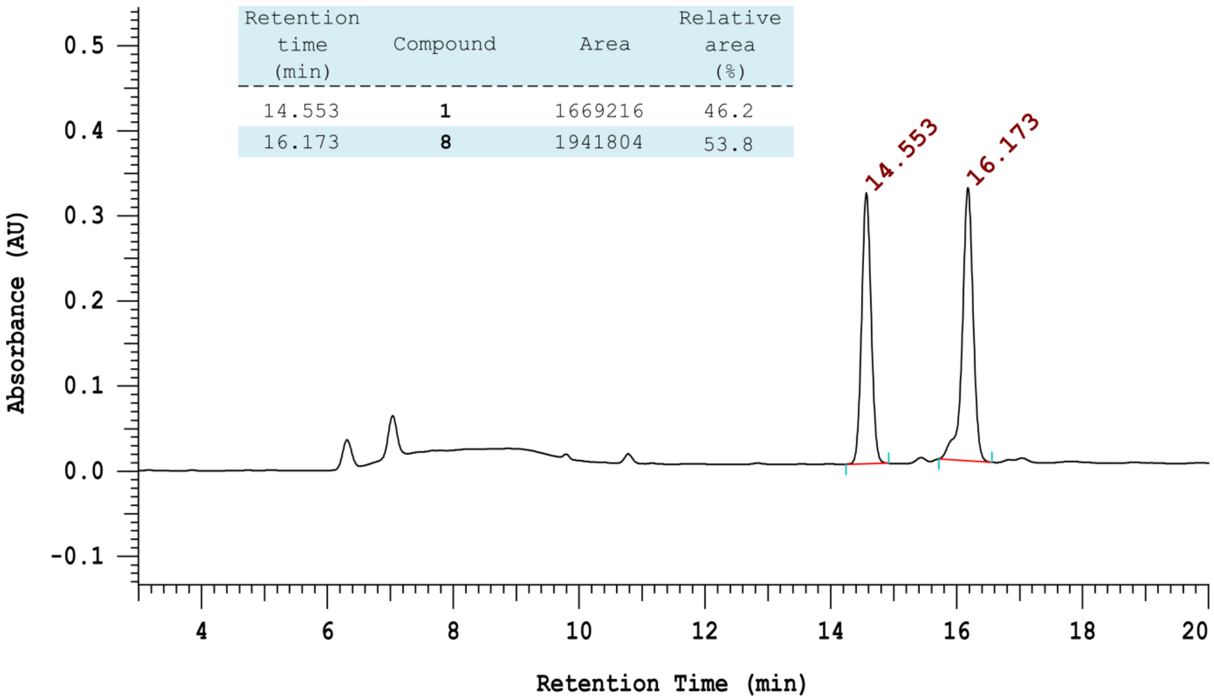

Retention time (min)	Compound	Area	Relative area (%)
14.553	**1**	1669216	46.2
16.173	**8**	1941804	53.8

Fig. S78 HPLC chromatogram of the reaction mixture corresponding to Table 3 Entry 2 at 210 nm showing the relative amounts of the product **1** and by-product **8**. The reaction was monitored with Method 1.

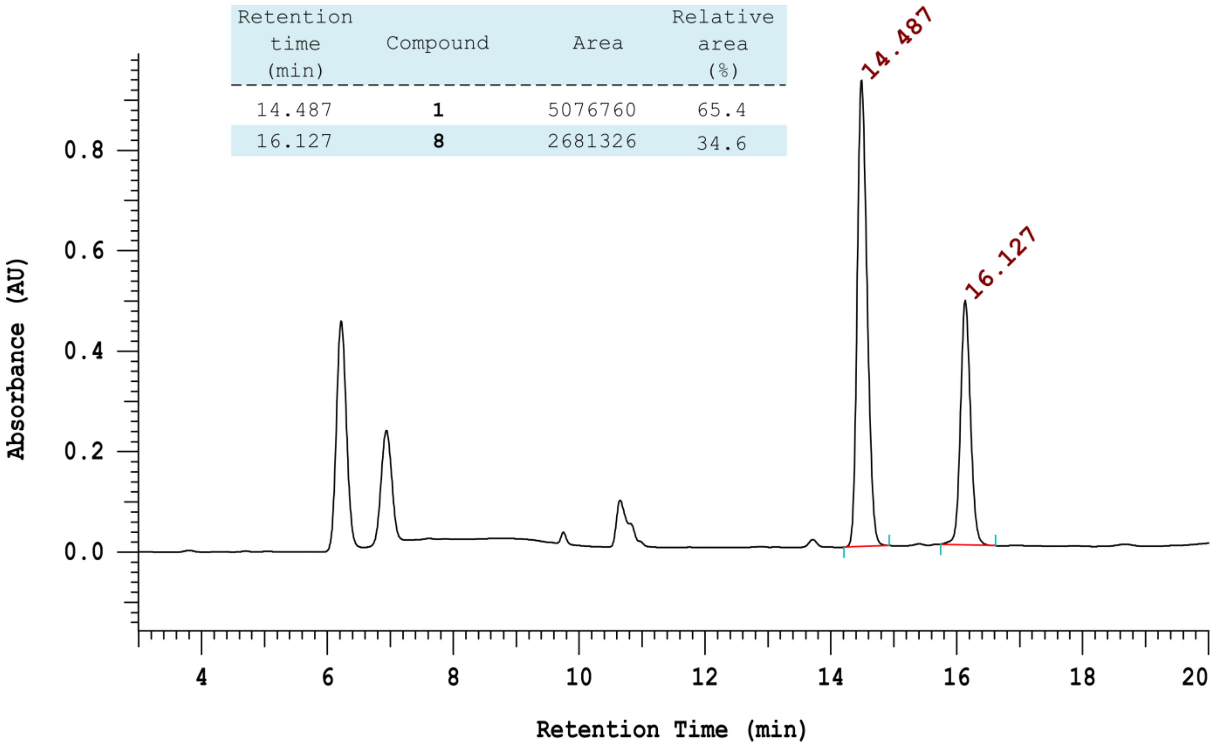

Retention time (min)	Compound	Area	Relative area (%)
14.487	**1**	5076760	65.4
16.127	**8**	2681326	34.6

Fig. S79 HPLC chromatogram of the reaction mixture corresponding to Table 3 Entry 3 at 210 nm showing the relative amounts of the product **1** and by-product **8**. The reaction was monitored with Method 1.

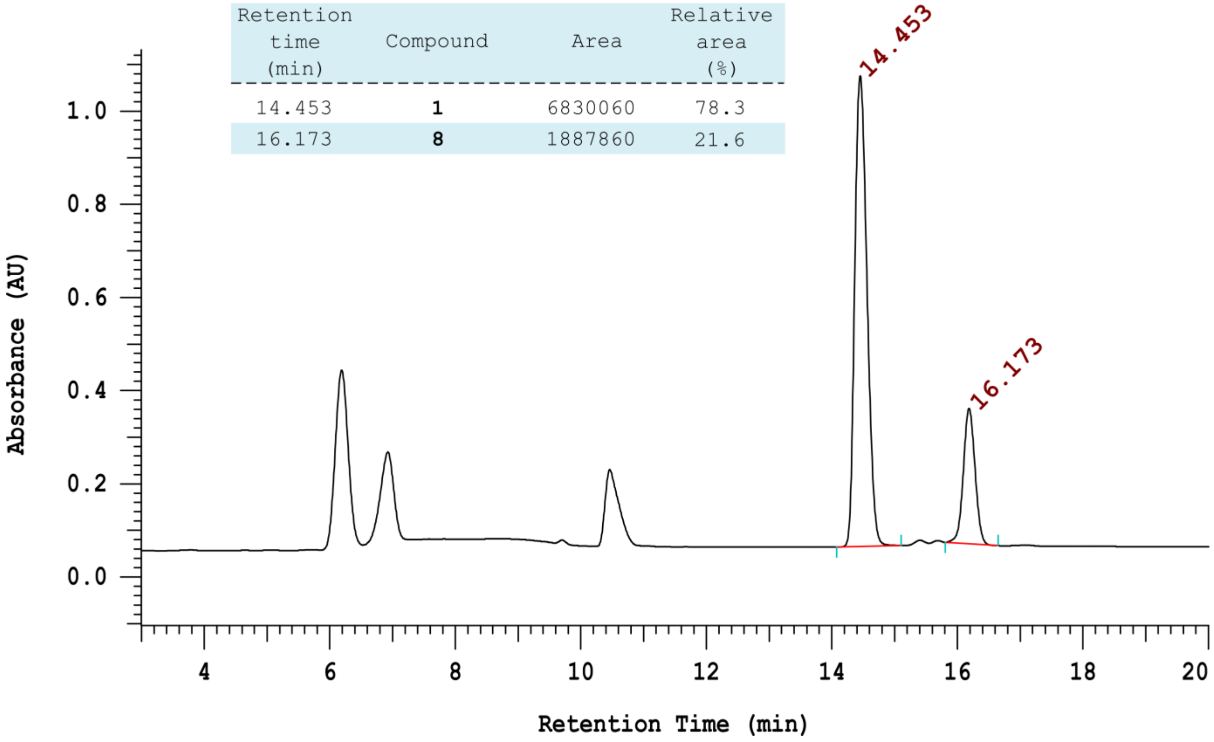

Retention time (min)	Compound	Area	Relative area (%)
14.453	**1**	6830060	78.3
16.173	**8**	1887860	21.6

Fig. S80 HPLC chromatogram of the reaction mixture corresponding to Table 3 Entry 4 at 210 nm showing the relative amounts of the product **1** and by-product **8**. The reaction was monitored with Method 1.

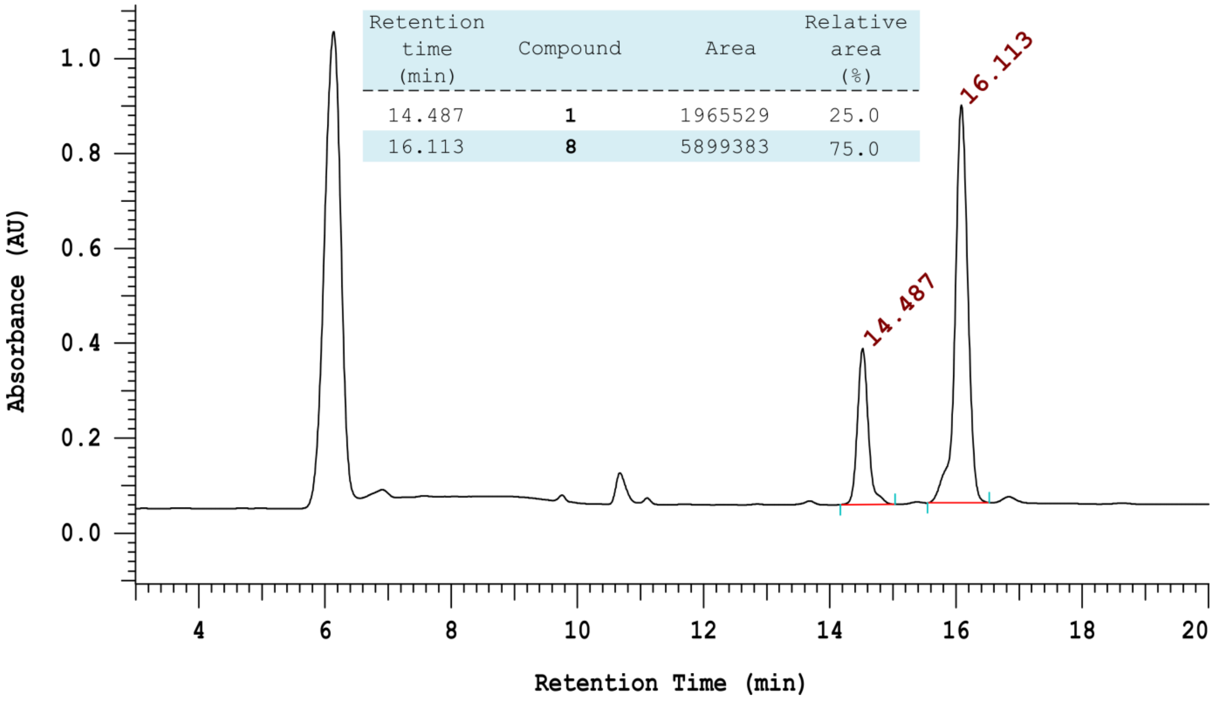

Retention time (min)	Compound	Area	Relative area (%)
14.487	**1**	1965529	25.0
16.113	**8**	5899383	75.0

Fig. S81 HPLC chromatogram of the reaction mixture corresponding to Table 3 Entry 5 at 210 nm showing the relative amounts of the product **1** and by-product **8**. The reaction was monitored with Method 1.

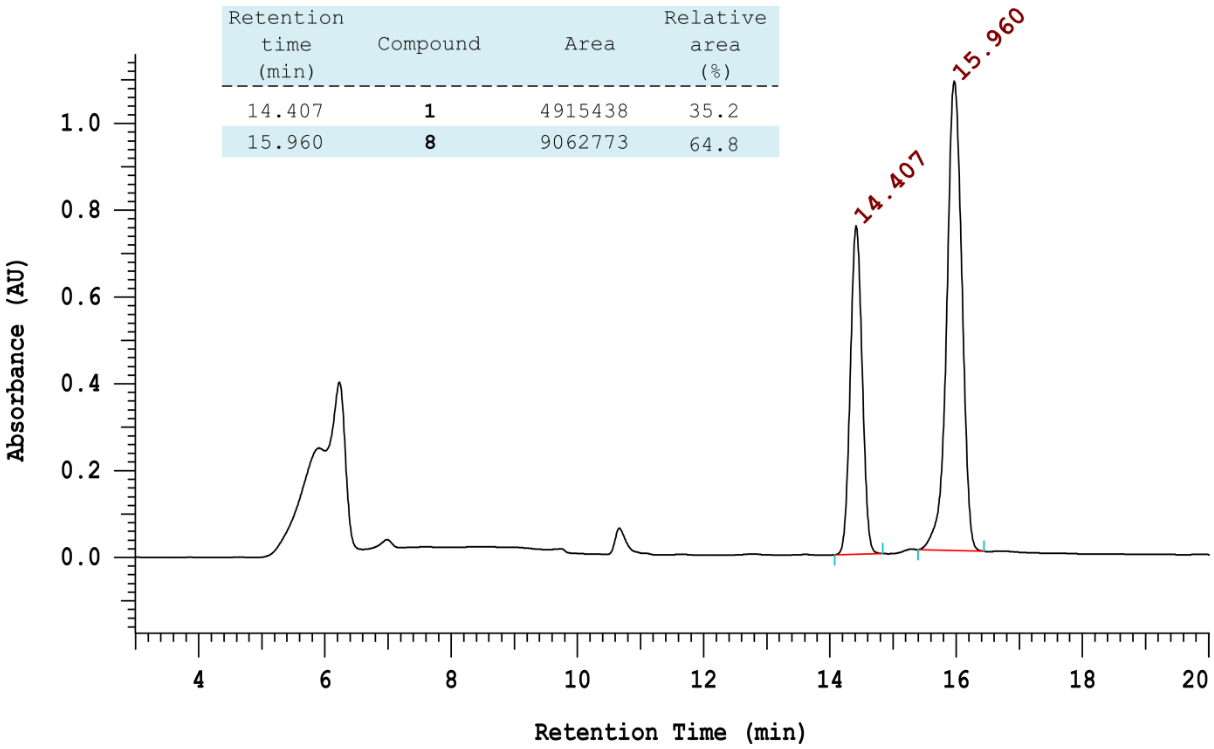

Retention time (min)	Compound	Area	Relative area (%)
14.407	**1**	4915438	35.2
15.960	**8**	9062773	64.8

Fig. S82 HPLC chromatogram of the reaction mixture corresponding to Table 3 Entry 6 at 210 nm showing the relative amounts of the product **1** and by-product **8**. The reaction was monitored with Method 1.

15. References

---

[1] G. Ignacz, F. Fei and G. Szekely, *ACS Appl. Nano Mater.*, 2018, **1**, 6349–6356.
DOI: 10.1021/acsanm.8b01563

[2] X. Weng, J. E. Baez, M. Khiterer, M. Y. Hoe, Z. Bao and K. J. Shea, *Angew. Chem. Int. Ed.*, 2015, **54**, 11214–11218.
DOI: 10.1002/anie.201504934

[3] F. Fei, L. Cseri, G. Szekely and C. F. Blanford, *ACS Appl. Mater. Interfaces*, 2018, **10**, 16140–16147.
DOI: 10.1021/acsami.8b03591

[4] Solvay Specialty Polymers USA LLC, US Pat. App., 20170240723 2017.

[5] I. I. Ponomarev, I. I. Ponomarev, Y. A. Volkova, M. Yu. Zharinova and D. Yu. Razorenov, *Mendeleev Commun.*, 2012, **22**, 162–163.
DOI: 10.1016/j.mencom.2012.05.018

[6] F. Roschangar, Y. Zhou, D. J. C. Constable, J. Colberg, D. P. Dickson, P. J. Dunn, M. D. Eastgate, F. Gallou, J. D. Hayler, S. G. Koenig, M. E. Kopach, D. K. Leahy, I. Mergelsberg, U. Scholz, A. G. Smith, M. Henry, J. Mulder, J. Brandenburg, J. R. Dehli, D. R. Fandrick, K. R. Fandrick, F. Gnad-Badouin, G. Zerban, K. Groll, P. T. Anastas, R. A. Sheldon and C. H. Senanayake, *Green Chem.*, 2018, **20**, 2206–2211.
DOI: 10.1039/C8GC00616D

[7] R. A. Sheldon, *Green Chem.*, 2017, **19**, 18–43.
DOI: 10.1039/c6gc02157c

[8] Rhodia Operations, US Pat., 9392785 2016.

[9] Rhodia Operations, US Pat., 8119838 2012.

[10] D. Zimmerli, *myRoche*, 2015, **4**.
(https://www.igz.ch/downloads/17919/myRoche_1504_CH_05_en_Findenser.pdf, Last accessed: 12/06/2019)

[11] UK Government Conversion Factors for greenhouse gas (GHG) reporting, 2018.
(https://www.gov.uk/government/collections/government-conversion-factors-for-company-reporting, Last accessed: 12/06/2019)

[12] T. Astrup, J. Møller and T. Fruergaard, *Waste Manage. Res.*, 2009, 27, 789–799.
DOI: 10.1177/0734242X09343774

[13] G.-J. Lee, J. H. McCain and M. M. Bhasin, Synthetic Organic Chemicals, in *Riegel's Handbook of Industrial Chemistry*, ed. J.A. Kent, Springer, Boston, MA, 2003.

[14] F. Cavani, S. Albonetti, F. Basile and A. Gandini, *Chemicals and Fuels from Bio-Based Building Blocks*, Wiley-VCH, Weinheim, Germany, 2016.

[15] Brian S. Furniss, Antony J. Hannaford, Peter W.G. Smith and Austin R. Tatchell, *Vogel's Textbook of Practical Organic Chemistry*, Longman Group UK Limited, England, 1989.

[16] J. K. H. Ma and B. Hadzija, *Basic Physical Pharmacy*, Jones & Bartlett Publishers, Burlington, MA, 2013.

[17] Y. Chernyak, *J. Chem. Eng. Data*, 2006, **51**, 416–418.
DOI: 10.1021/je050341y

[18] C. Wohlfarth, Dielectric constant of γ-valerolactone (Supplement to IV/6), in *Landolt-Börnstein - Group IV Physical Chemistry*, ed. M. D. Lechner, Springer-Verlag, Berlin, Heidelberg, 2008.
DOI: 10.1007/978-3-540-75506-7_143

[19] ASTM Standard D1209, 2005 (2011), "Color of Clear Liquids (Platinum-Cobalt Scale)," ASTM International, West Conshohocken, PA, 2011, DOI: 10.1520/D1209-05R11, www.astm.org.

[20] ASTM Standard E313, 1967 (2015), "Calculating Yellowness and Whiteness Indices from Instrumentally Measured Color Coordinates", ASTM International, West Conshohocken, PA, 2015, DOI: 10.1520/E0313-15E01, www.astm.org.

[21] E.M. Barrall, *Thermochim. Acta*, 1973, **5**, 377–389.
DOI: 10.1016/0040-6031(73)80016-4.

[22] Solvay Specialty Polymers USA LLC, US Pat. App., 20170240723 2017.

[23] National Institute of Advanced Industrial Science and Technology, Spectral Database System (SDBS), 19856, (https://sdbs.db.aist.go.jp/sdbs/cgi-bin/landingpage?sdbsno=19856, Last accessed: 12/06/2019)